

Influence of Stellar Multiplicity On Planet Formation. I. Evidence of Suppressed Planet Formation Due to Stellar Companions Within 20 AU and Validation of Four Planets From the *Kepler* Multiple Planet Candidates

Ji Wang¹, Ji-Wei Xie^{2,3}, Thomas Barclay^{4,5}, Debra A. Fischer¹

ji.wang@yale.edu

ABSTRACT

The planet occurrence rate for multiple stars is important in two aspects. First, almost half of stellar systems in the solar neighborhood are multiple systems. Second, the comparison of the planet occurrence rate for multiple stars to that for single stars sheds light on the influence of stellar multiplicity on planet formation and evolution. We developed a method of distinguishing planet occurrence rates for single and multiple stars. From a sample of 138 bright ($K_P < 13.5$) *Kepler* multi-planet candidate systems, we compared the stellar multiplicity rate of these planet host stars to that of field stars. Using dynamical stability analyses and archival Doppler measurements, we find that the stellar multiplicity rate of planet host stars is significantly lower than field stars for semi-major axes less than 20 AU, suggesting that planet formation and evolution are suppressed by the presence of a close-in companion star at these separations. The influence of stellar multiplicity at larger separations is uncertain because of search incompleteness due to a limited Doppler observation time baseline and a lack of high resolution imaging observation. We calculated the planet confidence for the sample of multi-planet candidates, and find that the planet confidences for KOI 82.01, KOI 115.01, KOI 282.01 and KOI 1781.02 are higher than 99.7% and thus validate the planetary nature of these four planet candidates. This sample of bright *Kepler* multi-planet candidates with refined stellar and orbital parameters, planet confidence estimation, and nearby stellar companion identification offers a well-characterized sample for future theoretical and observational study.

Subject headings: Planets and satellites: detection - surveys

¹Department of Astronomy, Yale University, New Haven, CT 06511 USA

²Department of Astronomy and Astrophysics, University of Toronto, Toronto, ON M5S 3H4, Canada

³Department of Astronomy & Key Laboratory of Modern Astronomy and Astrophysics in Ministry of Education, Nanjing University, 210093, China

⁴NASA Ames Research Center, M/S 244-30, Moffett Field, CA 94035, USA

⁵Bay Area Environmental Research Institute, Inc., 560 Third Street West, Sonoma, CA 95476, USA

1. Introduction

The occurrence rate of planets in multiple stellar systems is an important factor when calculating the overall planet occurrence rate because almost half of the stellar systems in the solar neighborhood are multiple systems (Duquennoy & Mayor 1991; Fischer & Marcy 1992; Raghavan et al. 2010). By comparing the planet occurrence rate of multiple stars and that of single stars, the influence of stellar multiplicity on planet formation, migration and evolution can be understood. In order to study the planet occurrence rate of multiple stars, there are two approaches: a dedicated survey for planets in multiple stellar systems can be carried out; or, the stellar multiplicity rate of stars with known planets can be determined and compared to a control sample. Adopting the first approach, surveys for planets in spectroscopic binaries were launched (Eggenberger et al. 2003; Eggenberger & Udry 2007; Konacki 2005; Konacki et al. 2009). Using the second approach, the stellar multiplicity rate has been studied with imaging techniques, mostly with the Lucky Imaging and the adaptive optic (AO) techniques.

Table 1 summarizes previous works in the latter approach. The stellar multiplicity rate for planet host stars is less than or comparable to that of field stars in the solar neighborhood from previous works, but there are still a few issues that need to be addressed. Most of previous work focused on giant planets due to planet detection limit and the sample size was small. Studies of planets detected by the radial velocity (RV) technique suffer from the selection bias that close-in binaries are avoided in Doppler planet surveys. In addition, planet formation and evolution is most likely to be affected when stars have small separations (Desidera & Barbieri 2007; Bonavita & Desidera 2007), but stellar companions at small separations pose challenges for imaging techniques. The Doppler technique measuring stellar RV may be a more effective way of searching for stellar companions with small separations.

The *Kepler* mission has revolutionized the search for exoplanets and allows us to overcome several limitations. Since its launch in 2009, more than 5000 planet candidates have been discovered¹ (Borucki et al. 2010, 2011; Batalha et al. 2013; Burke et al. 2013). Since the target selection process is not strongly discriminative to close-in binaries (Brown et al. 2011), several circumbinary planets have been detected around binary stars with periods ranging from ~ 10 -40 days (e.g., Doyle et al. 2011; Orosz et al. 2012; Schwamb et al. 2013). Therefore, the *Kepler* mission provides us with a large sample of planet candidates without the severe selection bias against binary stars.

Since the *Kepler* era, planet occurrence rates have been addressed by many groups (Catanzarite & Shao 2011; Youdin 2011; Traub 2012; Howard et al. 2012; Mann et al. 2012; Fressin et al. 2013; Dressing & Charbonneau 2013; Swift et al. 2013; Petigura et al. 2013; Gaidos 2013; Kopparapu 2013; Morton & Swift 2013; Dong & Zhu 2013). However, these works focused on an overall planet occurrence rate without distinguishing single stars and multiple stars. These two populations account for 54% (single stars) and 46% (multiple stars) of all stellar systems according to Raghavan et al. (2010). Comparing

¹<http://exoplanetarchive.ipac.caltech.edu/>

planet occurrence rates for these two populations sheds light on how stellar multiplicity affects planet formation and evolution.

In this paper, we will compare the stellar multiplicity rate for a sample of bright stars with multi-planet candidates to the stellar multiplicity rate for field stars. We will also provide a method of distinguishing between planet occurrence rates for single and multiple stars. In §2, we will discuss the methods and analyses that are necessary for calculating the stellar multiplicity rate and estimating the planet confidence. We present an algorithm for obtaining a self consistent solution for stellar and orbital parameters that iterates between stellar evolution model and transiting light curve measurement in §2.2. We conduct a search for stellar companions around planet host stars using the imaging technique in §2.3. We calculate the likelihood of a planet candidate being a bona fide planet in §2.4. The calculation leads to the validation of 4 planet candidates with planet confidence higher than 99.7%. We conduct a search for stellar companions using the Doppler technique based on archival data in §2.5. We present a dynamical analysis to constrain possible stellar companions based on co-planarity of transiting multi-planet systems in §2.6. The results of the stellar multiplicity rate calculation and the planet occurrence rate calculation are given in §3. Discussion and summary will be given in §4.

2. Method and Analysis

2.1. Target Sample: Bright Multiple Planet Candidates From *Kepler*

Our sample consists of bright host stars with multi-planet transiting systems from *Kepler*. Bright stars provide a higher signal to noise ratio (S/N) for photometric measurements, which helps to better determine stellar and orbital properties. Follow-up observations will be relatively easier for brighter stars. Multi-planet systems have lower false positive rates; they are more likely to be bona fide exoplanet systems. The presence of a second planet transit signal increases the likelihood of a bona fide planet by a factor of at least 25, and additional planet transit signals around one star provide an even larger boost of this likelihood (Lissauer et al. 2012). Out of 5779 *Kepler* Objects of Interest (KOIs)² (Borucki et al. 2010; Batalha et al. 2013), we selected all the systems with a *Kepler* magnitude (K_P) brighter than 13.5 mag and with at least two planet candidates (not with false positive disposition). Most of these are FGK stars with $3700 \text{ K} \leq T_{\text{eff}} \leq 7500 \text{ K}$ and $\log g$ higher than 4.0. The sample includes 343 planet candidates in 138 systems. For this sample, we have refined their stellar and orbital solutions, searched for stellar companions, and calculated the planet confidence levels. These analyses allow us to compare the stellar multiplicity rate with field stars and infer the planet occurrence rate for single and multiple star systems.

²<http://exoplanetarchive.ipac.caltech.edu/>

2.2. An Iterative Algorithm For Stellar and Orbital Parameters

Stellar and orbital parameters from the KOI table are obtained independently from stellar evolution modeling and transit light curve analysis (Batalha et al. 2013). Occasionally the calculations of some parameters are not consistent between stellar evolution modeling and transit light curve analysis. For example, a/R_S , the ratio of the planet orbital semi-major axis and the stellar radius, is sometimes different from these two analysis techniques. a/R_S can be directly obtained from the transit light curve analysis based on a model described in Mandel & Agol (2002). We note that in their paper the notation d/R_S , the ratio of star-planet separation during transit and the stellar radius, is used and only circular orbits are considered. We used a/R_S instead of d/R_S and considered eccentric orbits in this paper. Alternatively, a/R_S can be calculated from the Kepler’s Third Law when the stellar mass and radius are known from a stellar evolution model and the orbital period is known from transit observations. Fig. 1 (left panel) shows the comparison of a/R_S from these two calculations based on KOI values. The values for a/R_S are not always consistent with each other, and can be off by a factor of 3-4, which is much larger than the predicted error bar. An algorithm that iterates between stellar evolution modeling and transit light curve analysis is needed to alleviate this discrepancy.

We therefore developed an iterative algorithm that uses a/R_S to link the results from the stellar evolution modeling and transit light curve analysis. A similar approach can also be found in Torres et al. (2012); Dawson & Johnson (2012). For stellar parameters, we used the Yonsei-Yale interpreter (Demarque et al. 2004) to calculate stellar mass, radius and luminosity based on the observation results reported in KOI table, such as effective temperature (T_{eff}), surface gravity ($\log g$), and metallicity ($[\text{Fe}/\text{H}]$). In a Monte-Carlo simulation, we generated a large sample of inputs (including T_{eff} , $\log g$, $[\text{Fe}/\text{H}]$, α elements abundance, and age) for the Yonsei-Yale interpreter. The values for T_{eff} , $\log g$ and $[\text{Fe}/\text{H}]$ follow a Gaussian distribution centered at the reported value from the KOI table and with a standard deviation equal to the reported error bar. For α elements abundance and age, we assumed uniform distribution with a range of [0.0 dex, 0.2 dex] and [0.08 Gyr, 15 Gyr], respectively. We estimated the median values and the 68% credible interval for stellar mass, radius, and luminosity based on their distributions from the outputs of the interpreter. With the orbital period, which is usually the most precisely determined parameter in a transit observation, the value and uncertainty of a/R_S are calculated based on stellar evolution modeling.

Once the distribution of a/R_S is obtained from the stellar evolution modeling, it can be used as a prior for the estimation of orbital parameters in the transit light curve analysis. Instead of searching for a/R_S values based purely on the light curves fitting, we considered only a/R_S values that are consistent with the prior distribution. In the light curve fitting process, we used the model described in Mandel & Agol (2002). We adopted a boot-strapping algorithm to estimate the uncertainties of orbital parameters, in which we ran a larger number of trials in analyzing light curves that are perturbed based on the reported photometric measurement uncertainty. To avoid the dependence of results on the initial guess, we also perturbed the initial guess based on distributions of orbital parameters from previous runs. Initial guesses within $5\text{-}\sigma$ dispersion were

tried in order to avoid the sensitivity of the initial guess, and to explore a large parameter space. Orbital parameters are determined based on the distribution of the fitting results. The best fit values and their 68% credible intervals are reported. A distribution of a/R_S will be given at the end of the transit light curve analysis. The a/R_S distribution will be fed into the Yonsei-Yale interpreter as a sampler. Only the outputs of the interpreter will be selected for a/R_S distribution for the next round of iteration.

Fig. 1 (right panel) shows two examples of an a/R_S distribution from stellar evolution modeling (blue dashed line) and transit light curve analysis (green dotted line) and the converged a/R_S distribution from the iterative algorithm (red solid line). For KOI 94.02, because the stellar parameters (such as T_{eff} , $\log g$, and $[\text{Fe}/\text{H}]$) are determined by the SME analysis (Valenti & Fischer 2005), the uncertainties for these parameters are smaller. Therefore, the constraint on a/R_S from the stellar evolution modeling is tighter than that from the transit light curve analysis. Thus, the converged a/R_S distribution is mainly determined by the a/R_S distribution from the stellar evolution modeling. Conversely, for KOI 289.02, since T_{eff} , $\log g$, and $[\text{Fe}/\text{H}]$ are determined by J - K color, the constraint on a/R_S from the stellar evolution modeling is weak, and the converged distribution of a/R_S is mainly determined by the transiting light curve analysis.

The iterative algorithm unifies the stellar evolution modeling and the transit light curve analysis, resulting in a consistent set of stellar and orbital parameters. The results of stellar and orbital parameters for the systems in our sample are presented in Table 2 and Table 3. Fig. 2 compares the results of the iterative algorithm with the values from the KOI table. The iterative results generally agree well with the KOI values, as the data points are mostly located along the 1:1 line within the error bars. However, for cases when independent stellar evolution modeling and the transit light curve analysis show discrepancies, the iterative algorithm will give a different result from the KOI value because it considers measurement errors of both methods and thus gives a more consistent result. As a general trend, we found that stellar radii from KOI values are underestimated, which is in agreement with previous studies (Brown et al. 2011; Verner et al. 2011; Plavchan et al. 2012). Everett et al. (2013) suggested that 87% of the KOIs’ radii need an upward correction and 26% of the KOIs’ radii are underestimated by more than a factor of 1.35. In our case, we find that 86% have radii larger than KOI values and 17% are at least 1.35 larger than KOI values. Fig. 3 shows the distribution of revised planet radii for the sample of bright *Kepler* multiple planet candidates. The sample is dominated by smaller planet candidates. There are 233 planet candidates with radii smaller than 2.5 earth radii, 68 with radii between 2.5 and 5.0 earth radii, and 42 larger than 5.0 earth radii.

2.3. Search For Stellar Companions Using UKIRT Archival Images

The UKIRT data archive in Edinburgh provides positions and magnitudes for J band sources within the *Kepler* field. Archive tools generate high resolution cut-out images on the fly and allow source cross matches around user-specified lists of coordinates. The current UKIRT dataset

covers 99.5% of the field and was observed and supplied by Phil Lucas. The images have a typical spatial resolution of 0.8-0.9 arcsec. They are therefore useful for separating blended stellar pairs and spatially resolving external galaxies.

We used UKIRT images to calculate brightness contrast curves and to detect stellar companions around planet candidate host stars. For each star in our sample, we downloaded a UKIRT image from the WFCAM Science Archive³. We calculated the median and the standard deviation of brightness (with outlier rejection) for many concentric annuli centering at the planet host star. The brightness ratio of $5\text{-}\sigma$ above the median and the central star is defined as contrast. A contrast curve plots contrast as a function of the radii of concentric annuli, or the distance to the central star in arcsec. The contrast curve defines a brightness limit above which a visual companion can be detected. If there was a source with a brightness of at least 5σ brighter than the median brightness, then we recorded a detection of a visual companion to the central star.

Within a 20 arcsec radius centered on the central star, we detected 177 visual companions around 99 planet host stars. The other 39 stars in our sample have no visual companions down to the contrast limit. Table 4 presents the results of visual companions detected with the UKIRT images. The average contrast curve and its $3\text{-}\sigma$ variation are plotted in Fig 4. The detections are also plotted in Fig. 4 as asterisks, which agree well with the average contrast curve. In this sample of 138 stars, we do not find any stars with a visual companion within 2 arcsec. We note that KOI 119 and KOI 2311 have elongated PSFs; however, the possible stellar companions failed the $5\text{-}\sigma$ detection criteria. About 7% (10/138) have a visual companion within 6 arcsec. The numbers are much lower than those numbers from Adams et al. (2012) by a factor of 9. This result implies the incompleteness of visual companion searches using the UKIRT archival images, and the strength of AO observations in spatial resolution and contrast limit. However, the UKIRT images provide a contrast curve for each star and will be used to constrain parameter space in planet confidence estimation in §2.4. There are 177, 82, 32, and 5 stars with companion star separations less than 20, 15, 10, and 5 arcsec, respectively. These numbers are roughly proportional to the sky area around the central star, implying that they are likely to be background stars rather than physically bound companions.

2.4. Planet Confidence

The likelihood of a planet candidate being a bona fide exoplanet can be estimated by calculating the probability of false positives and the probability of a true planet transiting event. The BLENDER technique has been used to validate *Kepler* planet candidates (e.g., Torres et al. 2011; Fressin et al. 2011). A similar approach was later developed for planet candidate validation (Wang et al. 2013; Barclay et al. 2013b). In order to perform planet confidence calculation,

³<http://surveys.roe.ac.uk/wsa/>

several observational constraints should be taken into consideration to exclude unlikely regions in a ΔK_P -separation parameter space. ΔK_P is the differential magnitude of a possible contaminating object, and separation is its projected distance from the central star. These observational constraints include pixel centroid offset, transit depth, and UKIRT contrast curve.

The *Kepler* light curve files contain information on both the position of the star at a given time (flux-weighted centroids, called MOM_CENTR1 and MOM_CENTR2) and the predicted position of the star based on the position of reference stars (called POS_CORR1 and POS_CORR2). By subtracting one from the other we can find the centroid position of a star. We measured the centroid position during the prospective transit, and immediately before and after transit to search for centroid shifts. If the transit occurs on a star other than the target star, the centroid position should move away from that star by an amount proportional to the transit depth (Bryson et al. 2013). The magnitude of the shift can be used to calculate how far away this source is from the target. Even if no obvious shift is detected, we can still calculate a confusion region around the star. In our planet confidence calculations, we used the $3\text{-}\sigma$ confusion radius as the outer limit on the separation between the target and a false positive source.

The KOI table gives results of pixel centroid offset measurement. We used values from the flux-weighted method because this method is similar to our independent analysis. Out of 343 planet candidates in our sample, there are 240 with measured pixel centroid offset values from the KOI table, 34 of them show significant (above $3\text{-}\sigma$) pixel centroid offsets. In comparison, for these 240 planet candidates, our independent pixel centroid offset analysis found 20 candidates with significant offsets, 14 of them are overlapped with systems characterized by significant offsets in the KOI table. The difference between our independent analysis and the measured offsets from the KOI table may be attributed to a different window size and de-trending functional form selected for analysis. For the polynomial functional form that we used for de-trending the centroid measurements, the optimal polynomial order depends on the variability of the measurement results, and the window sizes for both in- and out-of-transit measurement. However, we chose a second-order polynomial function and fixed window sizes to serve the purpose of a streamline the data reduction. These choices are empirical and may be responsible for the differences from the values from the KOI table. For the 103 planet candidates without measured pixel centroid offset values from KOI table, we found 7 with significant offsets. In the column of pixel centroid offset significance in Table 3, we marked values larger than $3\text{-}\sigma$ in bold text.

Transit depth places a lower brightness limit to a possible contaminating object. The contrast curve of each star is calculated as described in §2.3. Once the observational constraints are put on the parameter space, the planet confidence will be calculated based on a galactic stellar population model (Robin et al. 2003). The details of planet confidence calculations can be found in (Wang et al. 2013; Barclay et al. 2013b). Table 3 gives the planet confidences for each of the KOIs in our sample. Two sets of planet confidences are given. The p1 column in Table 3 contains the planet confidences before considering the existence of other candidates in the same system. The p2 column contains the augmented planet confidences for a multi-planet system (Lissauer et al. 2012;

Barclay et al. 2013b).

There are 14 planet candidates with p_2 higher than 0.997, a value high enough to promote a planet candidate to a validated planet. KOI 70.01 (Fressin et al. 2012), KOI 72.01 (Batalha et al. 2011), KOI 85.01 (Chaplin et al. 2013), KOI 94.01 (Weiss et al. 2013), KOI 244.01, KOI 244.02 (Steffen et al. 2012), KOI 245.01 (Barclay et al. 2013a), and KOI 246.01 (Gilliland et al. 2013) are planet candidates that were previously validated or confirmed. For these KOIs, we note that all but KOI 70.01 have pixel centroid offsets larger than 3σ . KOI 72, KOI 85, KOI 244, KOI 245 and KOI 246 are bright stars in the *Kepler* field that cause pixel saturation, resulting in an imprecise pixel centroid offset measurement. KOI 94 is in a crowded field with 4 visual companions detected within 20 arcsec. We therefore caution that the flux-weighted pixel centroid offset measurement may not be precise for stars brighter than $K_P=11$, or for stars in a crowded field. There are 10 stars (7.2%) in the sample that are brighter than 11th *Kepler* magnitude and 9 stars (6.5%) with more than 3 detected stellar companions within 22 arcsec. In addition to previously confirmed KOIs, we find 6 other KOIs with higher than 0.997 planet confidence: KOI 5.01, KOI 82.01, KOI 115.01, KOI 282.01, KOI 1781.01 and KOI 1781.02. However, KOI 5.01 and KOI 1781.01 have a significant pixel centroid offset, and their K_P s are 11.6 mag and 12.2 mag, which raises concerns about their planet nature. Therefore, our planet confidence calculation results in 4 newly validated KOIs: KOI 82.01, KOI 115.01, KOI 282.01 and KOI 1781.02. The validation plots for them are shown in Fig. 5, Fig.6, Fig. 7, and Fig. 8. We note that KOI 115, KOI 282 and KOI 1781 all have one visual stellar companion within 8.5 arcsec. Although the possibility of the transit signal originating from the companion is excluded, flux contamination may affect the determination of the planet radius. However, given the relatively large magnitude difference between the companion and the center star ($\Delta K_P \geq 3.0$), the major contribution to the uncertainty of the planet radius is the stellar radius estimation rather than the flux contamination. We note that the planet confidence considers only scenarios in which a planet is physically associated with the primary. There is a chance that it orbits an undetected physical companion. This chance is likely low but is not accounted for.

2.5. Doppler Measurements and Incompleteness

There are 23 KOIs in our sample with more than 2 epochs of RV measurement results. They are available through the *Kepler* Community Follow-up Observing Program (CFOP). The purpose of the website is to facilitate collaboration on follow-up observing projects of KOIs and optimize the use of available facilities. Most of the RV measurements were conducted using the Keck HIRES or SAO TRES spectrographs. Table 5 summarizes the RV data for 23 KOIs. The median measurement precision is 7.3 m s^{-1} and the median observation baseline is 447.8 day. Among 23 KOIs, one non-transiting gas giant planet (Kepler-68d) was revealed by the RV technique (Gilliland et al. 2013), and two (KOI 5 and KOI 148) exhibit a long-term RV trend. KOI 148 (*Kepler*-48, Steffen et al. 2013; Xie 2012) shows a RV slope of $\sim 80 \text{ m s}^{-1} \text{ yr}^{-1}$, but this slope is caused by a ~ 2 Jupiter-mass planet with an orbital period of ~ 1000 days (Howard Isaacson, private communication). KOI 5

shows a RV slope of $\sim 100 \text{ m s}^{-1} \text{ yr}^{-1}$. If the mass of this companion is in the stellar regime, it must be more than 9.5 AU away from the central star in an edge-on orbit with respect to an observer. An edge-on orbit for a potential stellar companion is a probable configuration for stars with multiple transiting planets (see detailed discussions in §3.1). We therefore flag KOI 5 as a possible multiple stellar system. However, close-in ($a \leq \sim 10 \text{ AU}$) stellar companions are excluded.

We studied the completeness of Doppler measurements based on the reported RV precision and observation cadence. We defined a parameter space of orbital separation and companion inclination. For each point in the parameter space, we generated a set of simulated RV signals at the reported observation epochs, but with random mass and argument of periastron (ω). The mass ratio follows a distribution of stellar companion mass ratios from Duquennoy & Mayor (1991) with a median of 0.23 and a standard deviation of 0.46. The distribution of ω is uniform between 0 and 2π . Eccentricity is assumed to be 0.4 for all simulations. This value roughly corresponds to the median eccentricity determined in studies of stellar companions around solar-type stars (Duquennoy & Mayor 1991; Raghavan et al. 2010). If the simulated RV set has a RMS scatter 3 times larger than the reported RV measurement error, then a stellar companion in a certain range of parameter space can be detected. One hundred simulations were run at each point in a grid of orbital separation and inclination space. The fraction of detectable trials is reported in Fig. 9. Completeness decreases with increasing separation and decreasing inclination. This information will be used in assessing the probability of multiple stars in calculations of the stellar multiplicity rate and the planet occurrence rate in §3.

2.6. Dynamical Analysis

A companion star can affect the stability of a planetary orbit. Given the semimajor axis of the outmost planet’s orbit (a_p), we have a critical (lower limit) semimajor axis of the companion (Holman & Wiegert 1999),

$$a_{c1} = a_p / (0.464 - 0.380\mu - 0.631e_B + 0.586\mu e_B + 0.150e_B^2 - 0.198\mu e_B^2), \quad (1)$$

where e_B is the orbital eccentricity of the stellar companion and $\mu = m_B / (m_A + m_B)$ is the ratio between the mass of the companion and the total mass of the stellar system. Note that a_{c1} is only an empirical estimate based on the test particle simulation. Considering the mutual perturbation of planets, the real lower limit should be larger than a_{c1} . In any case, a_{c1} can be treated as a lower limit.

Besides stability, a stellar companion can affect the coplanarity of a multiple planet system if the companion is on an inclined orbit with respect to the planets’ orbits. This occurs when the planet’s orbital node precession is dominated by stellar-planet interaction rather than the planets’ mutual interaction. For a two-planet system, the node precession timescale of the outer planet due to the stellar companion t_{Bp} can be estimated as twice the Kozai time-scale (Kiseleva et al. 1998),

i.e.,

$$t_{\text{BP}} \sim \frac{4}{3\pi} \frac{P_{\text{B}}^2}{P_2} (1 - e_{\text{B}}^2)^{3/2} \frac{m_{\text{A}} + m_{\text{B}}}{m_{\text{B}}} \quad (2)$$

where P_{B} and P_2 are the orbital period of the stellar companion and the outer planet, respectively. The precession timescale due to planet-planet interaction can be estimated using the second order Laplace-Lagrange secular theory (Murray & Dermott 1999), i.e.,

$$t_{\text{PP}} \sim \frac{4P_2}{b_{3/2}^{(1)}(\alpha)} \frac{m_{\text{A}}}{\alpha m_1 + \alpha^{1/2} m_2}, \quad (3)$$

where m_1 and m_2 are the masses of the two planets, $\alpha = a_1/a_2$ is the ratio of their semimajor axes, and $b_{3/2}^{(1)}(\alpha)$ is the Laplace coefficient. Equating the above two timescales for precession due to stellar-planet interaction and planet-planet interaction, we obtain a critical orbital period for the companion, i.e.,

$$P_{\text{B}} = P_2 \left(\frac{3\pi}{b_{3/2}^{(1)}(\alpha)} \right)^{1/2} \left(\frac{m_{\text{A}}}{\alpha m_1 + \alpha^{1/2} m_2} \right)^{1/2} \left(\frac{m_{\text{B}}}{m_{\text{A}} + m_{\text{B}}} \right)^{1/2} (1 - e_{\text{B}}^2)^{-3/4}, \quad (4)$$

corresponding to a critical semimajor axis, i.e.,

$$a_{c2} = a_2 \left(\frac{3\pi}{b_{3/2}^{(1)}(\alpha)} \right)^{1/3} \left(\frac{m_{\text{B}}}{\alpha m_1 + \alpha^{1/2} m_2} \right)^{1/3} (1 - e_{\text{B}}^2)^{-1/2}. \quad (5)$$

For a system with more than two planets, we calculate equation 5 for each pair of planets and adopt the minimum value as the a_{c2} of the system. Below this critical semi-major axis, planetary coplanarity would be significantly affected by the companion’s perturbation. Generally, $a_{c2} > a_{c1}$ for a typical planet system, and thus coplanarity puts a stronger constraint on the companion’s orbit.

Our analysis gives a qualitative estimate of how planetary stability and coplanarity would be affected by a stellar companion. To quantitatively measure such effects, we perform the following an N-body simulation. For each multiple KOI system, we add a test stellar companion and use the N-body simulation package MERCURY (Chambers & Migliorini 1997) to integrate the orbits of the system up to a timescale of $10t_{\text{BP}}$. In each integration, we monitor the relative orbital inclinations of all the planets and calculate the fraction of time during which their relative inclinations are all less than 5° . This time fraction is then treated as the probability⁴(P_{DA}) at which the proposed stellar companion can not be ruled out. Here, the proposed stellar companion is drawn from a range of semimajor axes of $0.5a_{c2} < a_{\text{B}} < 2a_{c2}$ and a range of inclinations of $0 < i_{\text{B}} < 90^\circ$. The companion’s mass and orbital eccentricity are set to: $m_{\text{B}} = 0.1M_{\odot}$ and $e_{\text{B}} = 0.1$, to get a conservative estimate

⁴We set $P_{\text{DA}} = 1$ if there was any instability event, e.g., ejection or collision.

of P_{DA} . The relative inclination cut-off at 5° is chosen because *Kepler* planets are believed to be highly coplanar with a relative inclination within $1^\circ - 2^\circ$ (Lissauer et al. 2011; Fang & Margot 2012; Tremaine & Dong 2012; Fabrycky et al. 2012; Figueira et al. 2012; Johansen et al. 2012). In all simulations, the planet mass is set to a nominal value, $m_p = (R_p/R_\oplus)^{2.06} M_\oplus$ (Lissauer et al. 2011), and the planets are started with circular and coplanar orbits. As an example, Fig. 10 plots the result for KOI 275.

3. Planet Occurrence Rate and Stellar Multiplicity

Planet host stars with detected physical companions are categorized as multiple stars. Those with non-detections are assigned a probability of being a multiple star. The probability is calculated based on the overall search completeness for the star and the stellar multiplicity rate for solar-type stars. For example, if the overall completeness for a companion detection is 80% and the stellar multiplicity rate is 46% (Raghavan et al. 2010), then the probability of the star without a detected companion is $(100\% - 80\%) \times 46\% = 0.092$. Following this procedure, we calculate the number of multiple stars N_M and the number of single stars N_S . N_M and N_S are the sums of probabilities, so they will not necessarily be integers:

$$N_M = \sum_{i=1}^n p_M(i), \quad N_S = \sum_{i=1}^n [1 - p_M(i)], \quad (6)$$

where $p_M(i)$ is the probability of the i_{th} star being a multiple star.

The ratio of planet occurrence rate for multiple stars (f_M) and single stars (f_S) can be calculated with the ratio of N_{PM}/N_{PS} and the stellar multiplicity rate for the field stars:

$$\frac{f_S}{f_M} = \left(\frac{N_{PS}}{0.54} \right) / \left(\frac{N_{PM}}{0.46} \right), \quad (7)$$

where N_{PM} and N_{PS} are the numbers of planets around multiple stars and single stars in the sample:

$$N_{PM} = \sum_{i=1}^n \sum_{j=1}^m p_M(i) \cdot p_{PL}(i, j), \quad N_{PS} = \sum_{i=1}^n \sum_{j=1}^m [1 - p_M(i)] \cdot p_{PL}(i, j), \quad (8)$$

where $p_{PL}(i, j)$ is the planet confidence of the j_{th} planet candidate in the i_{th} star with a total of m planet candidates in the system. The planet confidence is a measure of the relative probability of a bona-fide planet to false positives after a series of false positive tests (see §2.4 for details). The overall planet occurrence rate (in the unit of number of planet per system) can be calculated by the following equation:

$$f = 0.54 \times f_S + 0.46 \times f_M, \quad (9)$$

where f is overall planet occurrence rate. With both the stellar multiplicity rate and f_S/f_M in

hand, the planet occurrence rate for multiple stars and single stars can be calculated:

$$f_M = \frac{f \cdot (\frac{0.54}{0.46} + 1)}{\frac{0.54}{0.46} \cdot \frac{f_S}{f_M} + 1}, \quad f_S = f_M \cdot \frac{f_S}{f_M}. \quad (10)$$

The planet occurrence rate for single stars and multiple stars can therefore be distinguished and compared. With Equation 10, the comparison of f_S and f_M will lead to the understanding of the influence of stellar multiplicity on planet formation.

3.1. Combining Doppler and Dynamical Results

The Doppler technique and the dynamical stability analysis are two complementary methods, with the former sensitive to edge-on companions and the latter sensitive to face-on companions. The difference between these two methods is that the Doppler technique sets constraints from observation while the constraints from the dynamical analysis come from numerical simulations.

At each point in the a - i parameter space for a possible stellar companion in a planetary system, two constraining numbers are given. One is from the Doppler analysis and the other one is from the dynamical analysis. For example, the completeness of the Doppler technique at $[a, i] = [10 \text{ AU}, 50^\circ]$ is 60%, and the dynamical analysis predicts that 10% of simulations do not meet coplanarity condition. The probability of an undetected companion is therefore $40\% \times 90\% \times p(a, i)$, where 40% is the incompleteness of Doppler observations, 90% is the probability of coplanar configuration from the dynamical analysis, and $p(a, i)$ is the probability of a stellar companion at a given a and i . We note that the results from Doppler observation and the dynamical analysis may be correlated. For example, the 10% rejected orbits in the previous example may be partially detected by Doppler observations. The correlation will result in an underestimation of the probability of an undetected companion. However, the correlation should be small because they are sensitive to different phase spaces and the results are thus nearly orthogonal. Most face-on companions missed by Doppler observations will be excluded by the dynamical analysis, and vice versa. Highly eccentric orbits that are occasionally missed by Doppler observations due to limited phase coverage can also be excluded by the dynamical analysis.

We treat the probability $p(a, i)$ as a product of $p(a)$ and $p(i)$. We used the Gaussian distribution of stellar companion periods of solar type stars (Raghavan et al. 2010), and converted periods to separations to describe $p(a)$. For $p(i)$, the distribution of inclinations for stellar companions, we adopted the result from Hale (1994). All systems in our sample are multi-planet systems, and there is evidence of alignment of stellar spin and planet orbital planes for multi-planet systems (Hirano et al. 2012; Albrecht et al. 2013). Hale (1994) suggested that the spin-orbit alignment is likely for binaries with separations less than $\sim 15 \text{ AU}$ and the spin-orbit angle becomes random when separations exceed $\sim 30 \text{ AU}$. Therefore, if there is a stellar companion within 15 AU around a star in our sample, its orbital plane should align approximately with the orbital plane of the planets. This alignment probability becomes smaller and randomized as the separation grows

larger than 30 AU. We used different functions of $p(i)$ for different separations. For separations less than 15 AU, we adopted a Gaussian form with a median of 80° and a standard deviation of 5° ; for $15\text{AU} \leq a \leq 30\text{AU}$, we used a combination of the Gaussian form and a uniform distribution between 0° to 90° with equal probability; for separations larger than 30 AU, we used a uniform distribution between 0° and 90° to describe $p(i)$. These functions at different separations agree well with the observations in Hale (1994). The probability of a star being in a multiple stellar system is then calculated by integrating over the a - i phase space.

3.2. Planet Host Stars Multiplicity Rate

Fig. 11 shows the average sensitivity contours after combining the Doppler observations and the dynamical analysis. When compared to Fig. 9, the Doppler observation incompleteness is complemented by the dynamical analysis at low inclinations. There are a total of 23 systems with Doppler observations among 138 systems in our sample.

Fig. 12 shows the comparison of the stellar multiplicity rate for field stars and planet host stars as a function of separation. We performed calculations for two samples. The first sample contained stars with both Doppler measurements and dynamical analysis (RV sample, $N=23$), and the second sample included all stars ($N=138$). The dashed line is the field star multiplicity rate (Raghavan et al. 2010). The blue region is the calculated stellar multiplicity rate, i.e., N_M/N , for the RV sample, where the vertical height of the region at a given separation indicates the $1\text{-}\sigma$ error bar. The error bar of N_M is estimated based on Poisson statistics. The square root of the closest integer to N_M is used to estimate the error of N_M unless the closest integer is 0, in which case, we used 1 for the error of N_M . At $a = 20.8$ AU, the blue hatched area crosses over the dashed line, suggesting that the stellar multiplicity rates for field stars and for the RV sample become indistinguishable beyond ~ 20 AU. The lower stellar multiplicity rate for planet host stars suggests that the presence of a close-in stellar companion may have a suppressive effect on planet formation and evolution. From the completeness contours in Fig. 11, the completeness is $\sim 50\%$ around 20 AU. At this completeness level, the majority of stellar companions within 20 AU would be detected or excluded due to orbit stability concern, leading to a conclusion of suppressive influence of a close-in stellar companion within 20 AU.

The red hatched area is the stellar multiplicity rate for the entire sample of multi-planet host stars. The error bar is smaller due to a larger sample. The crossover with the dashed line takes place at 85 AU. However, the significant incompleteness beyond 20 AU (see Fig. 11) prevents us from determining whether the crossover is due to an indistinguishable stellar multiplicity rate between planet host stars and field stars, or merely an incomplete survey. If it is the former case, then the large sample helps to reduce the statistical error and push the effective separation of a stellar companion from 20 AU to 85 AU. If it is the latter case, a longer RV measurement baseline or AO imaging would detect more stellar companions, pushing the red hatched area upward and the effective separation closer than 85 AU. Nonetheless, the suppressive influence of a close-in stellar

companion is shown. It is the effective separation that is currently lacking a satisfactory constraint due to statistical error and survey incompleteness.

3.3. Planet Occurrence Rate For Single and Multiple Stars

§3 provides a method of calculating the planet occurrence rate for single and multiple stars respectively. The result depends on f , the overall planet occurrence rate. Since f is still an issue of debate (Cumming et al. 2008; Howard et al. 2010; Mayor et al. 2011; Catanzarite & Shao 2011; Youdin 2011; Traub 2012; Howard et al. 2012; Mann et al. 2012; Gaidos 2013; Swift et al. 2013; Kopparapu 2013; Bonfils et al. 2013; Fressin et al. 2013; Dressing & Charbonneau 2013; Parker & Quanz 2013; Petigura et al. 2013; Petigura et al. 2013), we will leave it in the equation as a variable to be determined. Planet occurrence rate calculations need to cover a wide range of separations to avoid omitting any possible companions. The distribution of separations for stellar companions approaches zero when a gets to more than 10^5 AU, therefore we truncate the a range at 10^5 AU. We get the ratio of f_S and f_M very close to 1, indicating that a planet is equally probable to appear around a single star or around a multiple star system. This result is not surprising due to the incompleteness of Doppler observations and the dynamical analysis. There is a large unexplored phase space as the calculation covers a wider separation range. The prior information, e.g., the stellar multiplicity rate for the field star, outweighs the observations and analysis, naturally leading to a conclusion purely based on priors of the calculation.

We could potentially reduce the separation range and therefore reduce the impact of priors. However, this would also reduce the value of this analysis. Followup observations that address the unexplored phase space are the only way to reach a sensible planet occurrence rate estimation for both single and multiple stars. It requires a longer time baseline of Doppler observations for detection of close-in companions and imaging techniques with higher spatial resolutions (e.g., AO, speckle imaging and HST snapshot program⁵) to probe for companions at wide orbits with deeper contrast.

4. Summary and Discussion

4.1. Summary

We selected a total of 138 multi-planet candidate systems from the *Kepler* mission and studied the influence of a nearby stellar companion on planet formation. For these systems, we used archival data from *Kepler* to characterize their stellar and orbital properties. We developed an iterative algorithm that combines the *Kepler* photometric data with a stellar evolution interpolator. This

⁵<http://www.stsci.edu/cgi-bin/get-proposal-info?id=12893&submit=Go&observatory=HST>

algorithm uses a/R_S as a bridge to obtain a self-consistent stellar and orbital solution. We used this algorithm to refine stellar and orbital solutions for the 138 systems in our sample. The results are reported in Table 2 and Table 3. The majority of the planet candidates are in compact systems: 90%(310/343) of them have semi-major axes less than 0.28 AU. We used the archival data from UKIRT to study the stellar environment of these planet host stars, and found 177 visual companions within 20 arcsec, but we argued that these are likely to be background stars according to a statistical test.

We calculated the planet confidence for these multi-planet candidate systems (Table 3). The calculation involves pixel centroid offset analysis, transit depth analysis, and contrast curve calculations. A total of 14 planet candidates have a planet confidence higher than 0.997, indicating a high likelihood of being a bona fide planet. Eight of them are previously confirmed or validated planets. The other 6 planet candidates are validated for the first time, but two of them have a significant pixel centroid offset. Thus, KOI 82.01, KOI 115.01, KOI 282.01 and KOI 1781.02 become 4 newly validated planets from *Kepler* data. Future AO observations will further reduce the parameter space for a possible contaminating stellar companions, and increase the planet confidences for other unvalidated planet candidates.

The majority of previous work on stellar multiplicity made use of imaging techniques, such as AO and Lucky imaging, and searched for stellar companions at wide separations. In comparison, we used a unique combination of the Doppler technique and dynamical stability analysis to evaluate stellar companions out to ~ 100 AU. This approach demonstrates the influence of a close-in stellar companion on planet formation. We presented a statistical method for calculating the stellar multiplicity rate and the planet occurrence rate for both single stars and multiple stars. We found that the stellar multiplicity within 20.8 AU for planet host stars is significantly lower than that of field stars, indicating a strong suppressive effect of a stellar companion on planet occurrence. The influence of a stellar companion at larger separations is uncertain because of statistical error and survey sensitivity. Doppler observations for the 23 KOIs in our sample are not optimal for a search of stellar companions at larger separations. Future followup Doppler observations with a longer time base line will help set further constraints on stellar companions.

4.2. Discussion

In our dynamical analysis, we used several conservative assumptions. First, we assumed a moderate eccentricity of 0.1 in the analysis. If this is replaced by 0.5, roughly the median of eccentricity for binaries (Raghavan et al. 2010), a larger fraction of orbital configurations will become non-coplanar for the same a and i . The dynamical analysis thus becomes even more effective with a higher eccentricity assumption. Second, we assumed a mutual inclination limit to be 5° , which is a weaker constraint compared to the highly coplanar orbits found by *Kepler* with a mutual inclination of less than 2° (Lissauer et al. 2011; Fang & Margot 2012; Tremaine & Dong 2012; Fabrycky et al. 2012; Figueira et al. 2012; Johansen et al. 2012). A decreasing limit of mutual in-

clination will result in more rejections in dynamical analysis and thus increase the constraint on undetected stellar companions. However, we must note some limitations of the dynamical analysis. For example, we do see several cases in which a possible planet candidate is found in a region predicted to be unstable by the dynamical analysis, e.g., KOI 191 and 204 (Lissauer et al. 2011), and ν Octantis (Goździewski et al. 2013).

The stellar multiplicity rate for field stars in the solar neighborhood has been calculated by Raghavan et al. (2010) for solar-type stars within 25 pc of the Sun. The majority of the stars in our sample are within 550 pc of the Sun based on the magnitude cut at 13.5 *Kepler* mag and the assumption that most of them are main sequence stars. The caveat of extrapolating the measurement to a larger volume must be noted. If the stellar multiplicity rate of the *Kepler* field is different from the solar neighborhood, the ratio (0.54/0.46) in §3 should be replaced with a different (but unknown) value. In addition, we compared the stellar multiplicity rate for field stars and planet host stars, but we do not know the fraction of field stars hosting planets. If all field stars have planets, then the comparison provides information about the difference of stellar companions in terms of separation distribution and the stellar multiplicity rate, because we would have compared two groups of planet hosting stars in two environments. One is the solar neighborhood, the other is the *Kepler* field. However, if (1) not all field stars have a planet; and (2) the statistics of multiple stars (multiplicity, separation distribution, etc.) is similar for the nearby solar-type stars and the stars in our sample, then the difference in Fig. 12 indeed suggests the impact of a close-in stellar companion on planet occurrence. In this case, the field stars are a sample contaminated by planet host stars. If a difference is seen when compared to a sample of planet host stars, then the difference would have been more distinct when comparing a planet host sample and a non-planet host sample. The latter is difficult to obtain because of current detection precision limitation. However, a planet mass or radius limit can be set in investigations of a certain type of planet, e.g., comparing the stellar multiplicity rate for the giant planet host stars and stars without a gas giant. For future studies, the combination of the Doppler technique, AO observation and dynamical stability analysis will contribute an almost complete survey for stellar companions around planet host stars, and will ultimately reveal how stellar multiplicity influences on planet formation.

REFERENCES

- Adams, E. R., Ciardi, D. R., Dupree, A. K., Gautier, III, T. N., Kulesa, C., & McCarthy, D. 2012, *AJ*, 144, 42
- Adams, E. R., Dupree, A. K., Kulesa, C., & McCarthy, D. 2013, *AJ*, 146, 9
- Albrecht, S., Winn, J. N., Marcy, G. W., Howard, A. W., Isaacson, H., & Johnson, J. A. 2013, *ApJ*, 771, 11
- Ammons, S. M., Robinson, S. E., Strader, J., Laughlin, G., Fischer, D., & Wolf, A. 2006, *ApJ*, 638, 1004

- Barclay, T., et al. 2013a, *Nature*, 494, 452
- . 2013b, *ApJ*, 768, 101
- Batalha, N. M., et al. 2011, *ApJ*, 729, 27
- . 2013, *ApJS*, 204, 24
- Bergfors, C., et al. 2013, *MNRAS*, 428, 182
- Bonavita, M., & Desidera, S. 2007, *A&A*, 468, 721
- Bonfils, X., et al. 2013, *A&A*, 549, A109
- Borucki, W. J., et al. 2010, *Science*, 327, 977
- . 2011, *ApJ*, 736, 19
- Brown, T. M., Latham, D. W., Everett, M. E., & Esquerdo, G. A. 2011, *AJ*, 142, 112
- Bryson et al. 2013, *PASP*, submitted
- Burke, C. J., Bryson, S., Christiansen, J., Mullally, F., Rowe, J., Science Office, K., & Kepler Science Team. 2013, in *American Astronomical Society Meeting Abstracts*, Vol. 221, *American Astronomical Society Meeting Abstracts*, 216.02
- Catanzarite, J., & Shao, M. 2011, *ApJ*, 738, 151
- Chambers, J. E., & Migliorini, F. 1997, in *Bulletin of the American Astronomical Society*, Vol. 29, *AAS/Division for Planetary Sciences Meeting Abstracts #29*, 1024
- Chaplin, W. J., et al. 2013, *ApJ*, 766, 101
- Cumming, A., Butler, R. P., Marcy, G. W., Vogt, S. S., Wright, J. T., & Fischer, D. A. 2008, *PASP*, 120, 531
- Daemgen, S., Hormuth, F., Brandner, W., Bergfors, C., Janson, M., Hippler, S., & Henning, T. 2009, *A&A*, 498, 567
- Dawson, R. I., & Johnson, J. A. 2012, *ApJ*, 756, 122
- Demarque, P., Woo, J.-H., Kim, Y.-C., & Yi, S. K. 2004, *ApJS*, 155, 667
- Desidera, S., & Barbieri, M. 2007, *A&A*, 462, 345
- Dong, S., & Zhu, Z. 2013, *ApJ*, 778, 53
- Doyle, L. R., et al. 2011, *Science*, 333, 1602
- Dressing, C. D., & Charbonneau, D. 2013, *ApJ*, 767, 95

- Duquennoy, A., & Mayor, M. 1991, *A&A*, 248, 485
- Eggenberger, A., & Udry, S. 2007, ArXiv e-prints
- Eggenberger, A., Udry, S., Chauvin, G., Beuzit, J.-L., Lagrange, A.-M., Ségransan, D., & Mayor, M. 2007, *A&A*, 474, 273
- Eggenberger, A., Udry, S., Chauvin, G., Forveille, T., Beuzit, J.-L., Lagrange, A.-M., & Mayor, M. 2011, in *IAU Symposium*, Vol. 276, *IAU Symposium*, ed. A. Sozzetti, M. G. Lattanzi, & A. P. Boss, 409–410
- Eggenberger, A., Udry, S., & Mayor, M. 2003, in *Astronomical Society of the Pacific Conference Series*, Vol. 294, *Scientific Frontiers in Research on Extrasolar Planets*, ed. D. Deming & S. Seager, 43–46
- Everett, M. E., Howell, S. B., Silva, D. R., & Szkody, P. 2013, *ApJ*, 771, 107
- Fabrycky, D. C., et al. 2012, ArXiv e-prints
- Fang, J., & Margot, J.-L. 2012, *ApJ*, 761, 92
- Figueira, P., et al. 2012, *A&A*, 541, A139
- Fischer, D. A., & Marcy, G. W. 1992, *ApJ*, 396, 178
- Fressin, F., et al. 2011, *ApJS*, 197, 5
- . 2012, *Nature*, 482, 195
- . 2013, *ApJ*, 766, 81
- Gaidos, E. 2013, *ApJ*, 770, 90
- Gilliland, R. L., et al. 2013, *ApJ*, 766, 40
- Ginski, C., Mugrauer, M., Seeliger, M., & Eisenbeiss, T. 2012, *MNRAS*, 421, 2498
- Goździewski, K., Słonina, M., Migaszewski, C., & Rozenkiewicz, A. 2013, *MNRAS*, 430, 533
- Hale, A. 1994, *AJ*, 107, 306
- Hirano, T., et al. 2012, *ApJ*, 759, L36
- Holman, M. J., & Wiegert, P. A. 1999, *AJ*, 117, 621
- Howard, A. W., et al. 2010, *Science*, 330, 653
- . 2012, *ApJS*, 201, 15
- Johansen, A., Davies, M. B., Church, R. P., & Holmelin, V. 2012, *ApJ*, 758, 39

- Kiseleva, L. G., Eggleton, P. P., & Mikkola, S. 1998, *MNRAS*, 300, 292
- Konacki, M. 2005, *ApJ*, 626, 431
- Konacki, M., Muterspaugh, M. W., Kulkarni, S. R., & Helminiak, K. G. 2009, *ApJ*, 704, 513
- Kopparapu, R. K. 2013, *ApJ*, 767, L8
- Lillo-Box, J., Barrado, D., & Bouy, H. 2012, *A&A*, 546, A10
- Lissauer, J. J., et al. 2011, *ApJS*, 197, 8
- . 2012, *ApJ*, 750, 112
- Luhman, K. L., & Jayawardhana, R. 2002, *ApJ*, 566, 1132
- Mandel, K., & Agol, E. 2002, *ApJ*, 580, L171
- Mann, A. W., Gaidos, E., Lépine, S., & Hilton, E. J. 2012, *ApJ*, 753, 90
- Mayor, M., et al. 2011, *ArXiv e-prints*
- Morton, T. D., & Swift, J. J. 2013, *ArXiv e-prints*
- Mugrauer, M., & Neuhäuser, R. 2009, *A&A*, 494, 373
- Murray, C. D., & Dermott, S. F. 1999, *Solar system dynamics*
- Orosz, J. A., et al. 2012, *Science*, 337, 1511
- Parker, R. J., & Quanz, S. P. 2013, *MNRAS*, 436, 650
- Patience, J., et al. 2002, *ApJ*, 581, 654
- Petigura, E. A., Howard, A. W., & Marcy, G. W. 2013, *Proceedings of the National Academy of Sciences*
- Petigura, E. A., Marcy, G. W., & Howard, A. W. 2013, *ApJ*, 770, 69
- Pinsonneault, M. H., An, D., Molenda-Żakowicz, J., Chaplin, W. J., Metcalfe, T. S., & Bruntt, H. 2012, *ApJS*, 199, 30
- Plavchan, P., Bilinski, C., & Currie, T. 2012, *ArXiv e-prints*
- Raghavan, D., et al. 2010, *ApJS*, 190, 1
- Robin, A. C., Reylé, C., Derrière, S., & Picaud, S. 2003, *A&A*, 409, 523
- Roell, T., Neuhäuser, R., Seifahrt, A., & Mugrauer, M. 2012, *A&A*, 542, A92

- Schwamb, M. E., et al. 2013, ApJ, 768, 127
- Steffen, J. H., et al. 2012, MNRAS, 421, 2342
- . 2013, MNRAS, 428, 1077
- Swift, J. J., Johnson, J. A., Morton, T. D., Crepp, J. R., Montet, B. T., Fabrycky, D. C., & Muirhead, P. S. 2013, ApJ, 764, 105
- Torres, G., Fischer, D. A., Sozzetti, A., Buchhave, L. A., Winn, J. N., Holman, M. J., & Carter, J. A. 2012, ApJ, 757, 161
- Torres, G., et al. 2011, ApJ, 727, 24
- Traub, W. A. 2012, ApJ, 745, 20
- Tremaine, S., & Dong, S. 2012, AJ, 143, 94
- Valenti, J. A., & Fischer, D. A. 2005, ApJS, 159, 141
- Verner, G. A., et al. 2011, ApJ, 738, L28
- Wang, J., et al. 2013, ApJ, 776, 10
- Weiss, L. M., et al. 2013, ApJ, 768, 14
- Xie, J.-W. 2012, ArXiv e-prints
- Youdin, A. N. 2011, ApJ, 742, 38
-

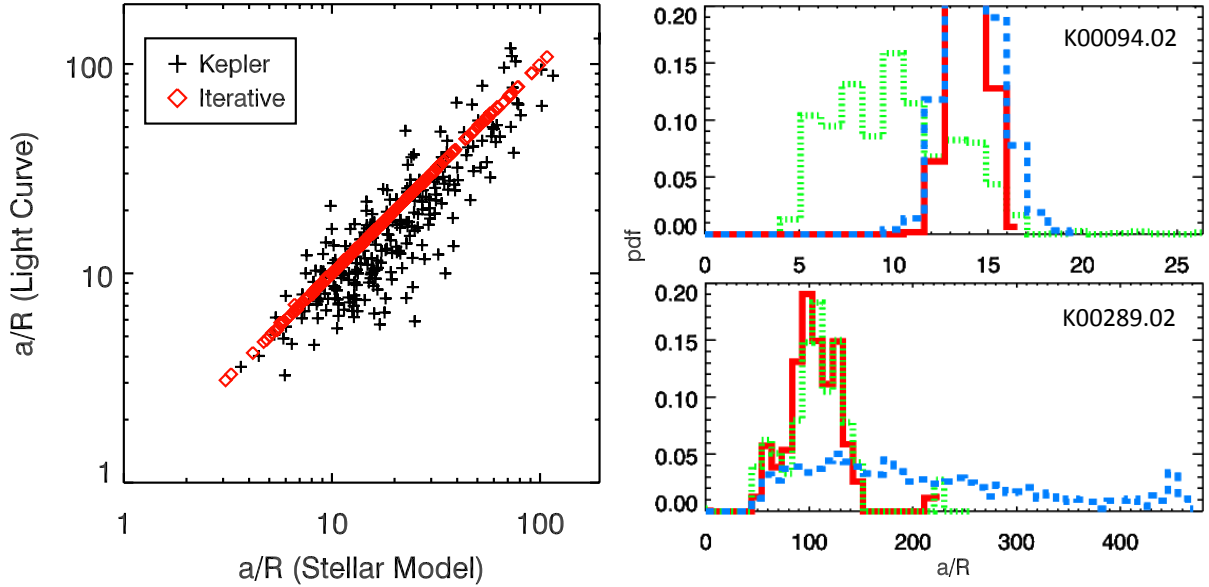


Fig. 1.— Left: comparison of a/R_S between light curve derived values and stellar evolution model derived values. Black crosses represent *Kepler* data and red diamonds represent the results of the iterative algorithm. The iterative algorithm will converge the a/R_S from two approaches: light curve fitting and stellar evolution modeling, and reach a self-consistent solution of stellar and orbital properties. Top right: example of KOI 94.02, blue dashed line is the a/R_S distribution from stellar evolution modeling, green dotted line is the a/R_S distribution from the light curve fitting, red solid line is the converged distribution using the iterative algorithm. Bottom right is the same as top right except it is for KOI 289.02.

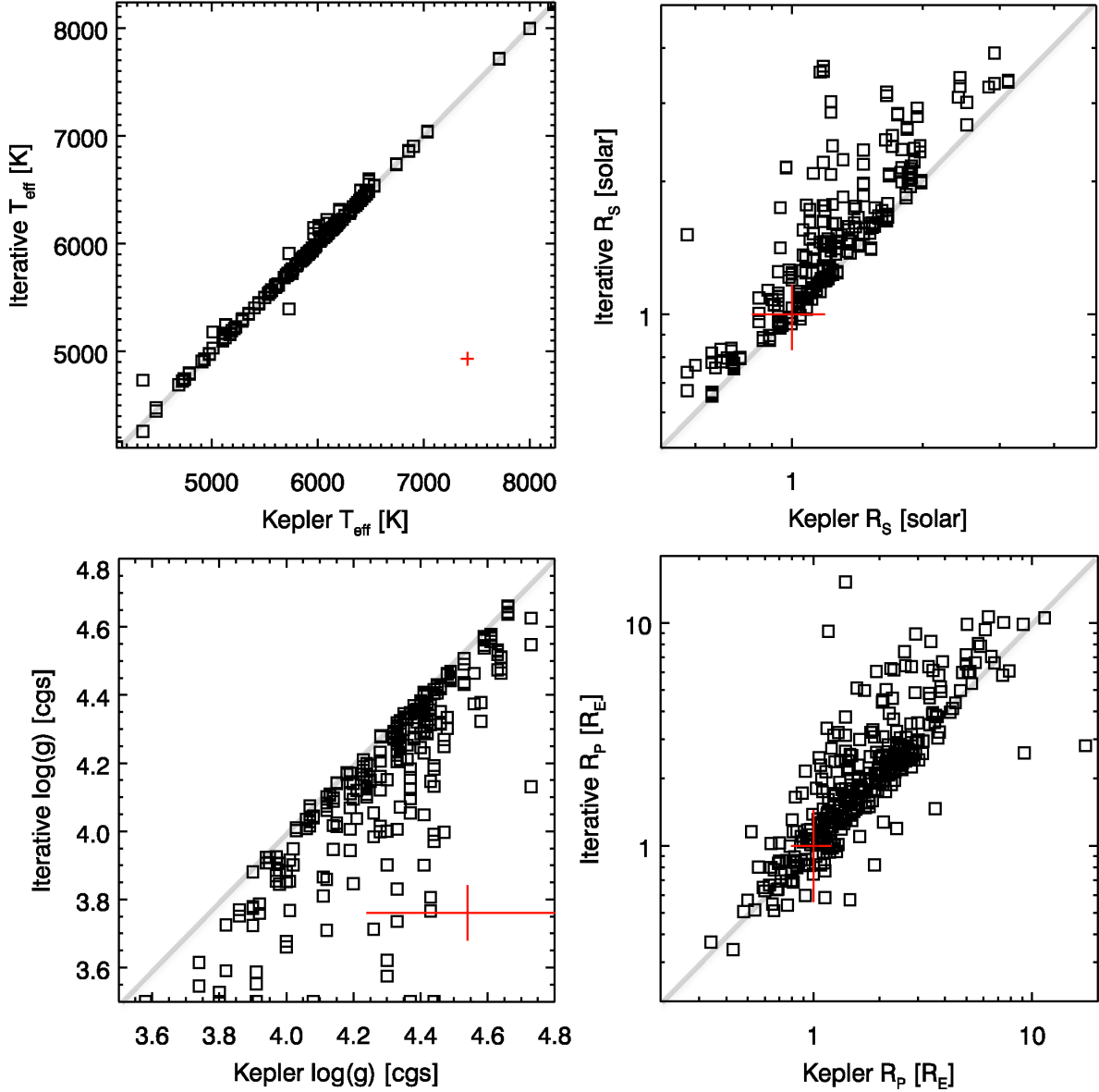


Fig. 2.— Comparison of T_{eff} , R_S , R_P and $\log(g)$ (clockwise from top left). Median error bar for each sub-plot is indicated by a red cross. The iterative algorithm results agree well with the KOI values for T_{eff} . The comparison of R_S and $\log(g)$ suggests that some of the KOI values for these two parameters are overestimated ($\log(g)$) or underestimated (R_S).

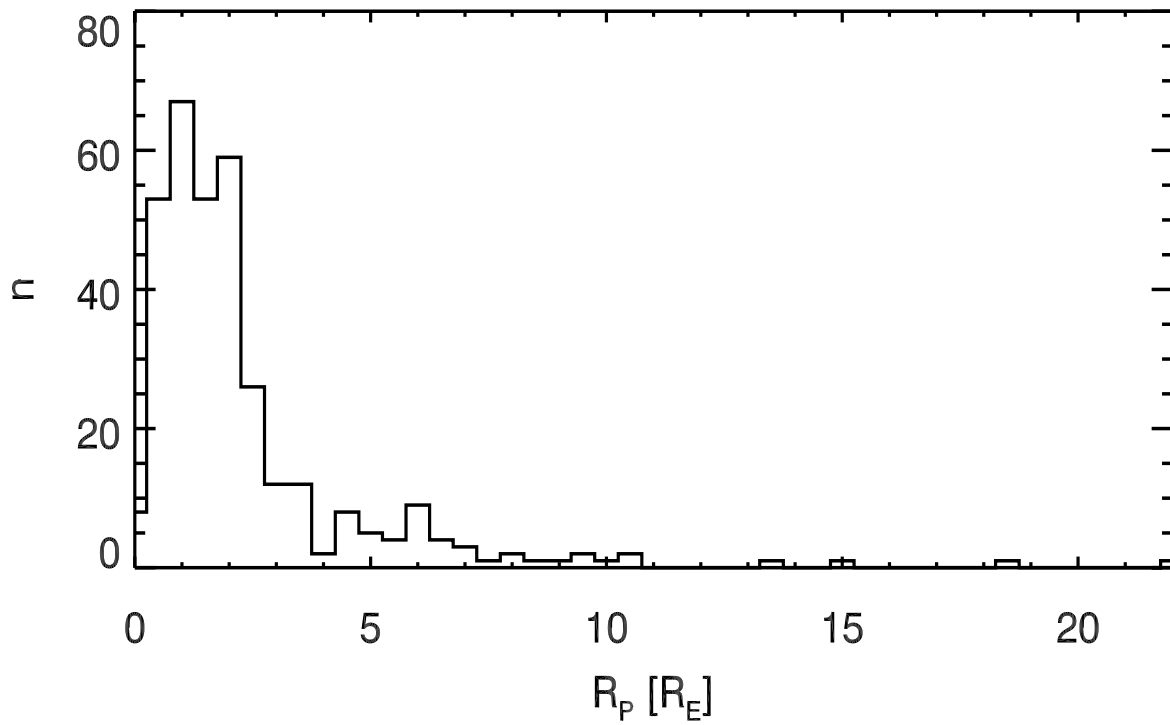


Fig. 3.— Distribution of planet radii from the iterative method for the bright multi-planet candidate systems from *Kepler*. Stellar and orbital properties can be found in Table 2 and Table 3.

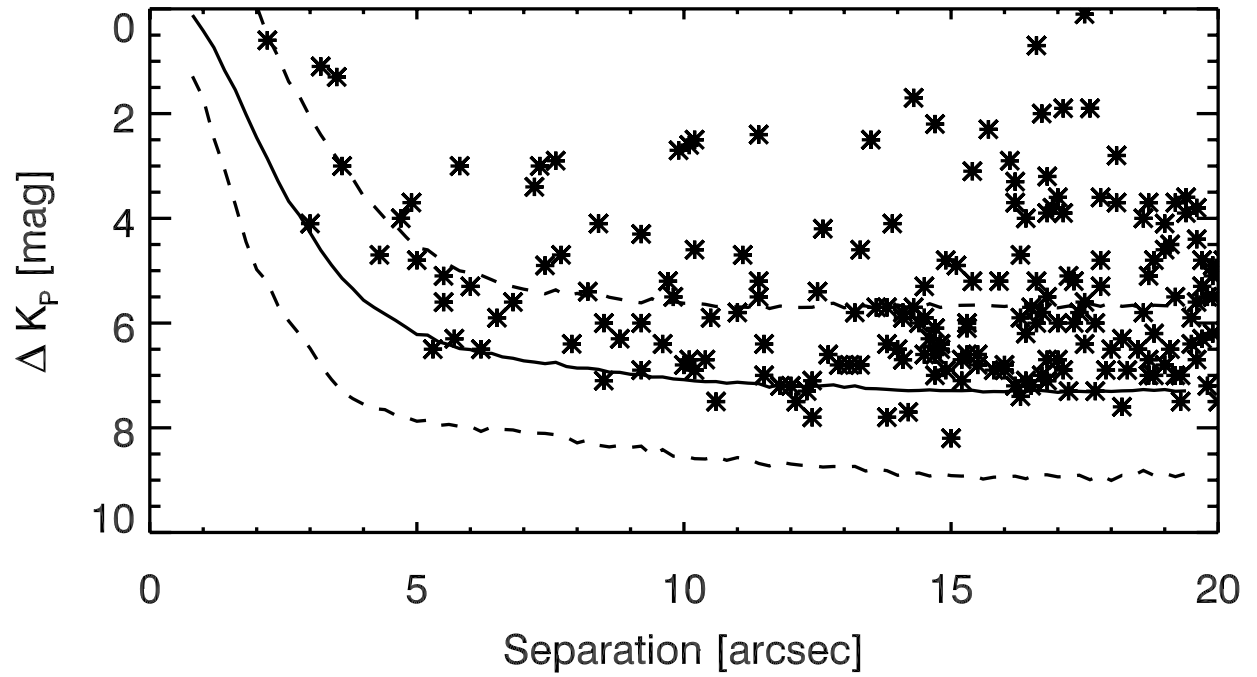


Fig. 4.— Averaged contrast curve for the UKIRT *J* band images. Dashed lines are $3\text{-}\sigma$ deviation of the contrast curve. Asterisks are detections of visual companions. A total of 177 visual companions within 20 arcsec of planet host stars are detected using UKIRT images and they are reported in Table 4.

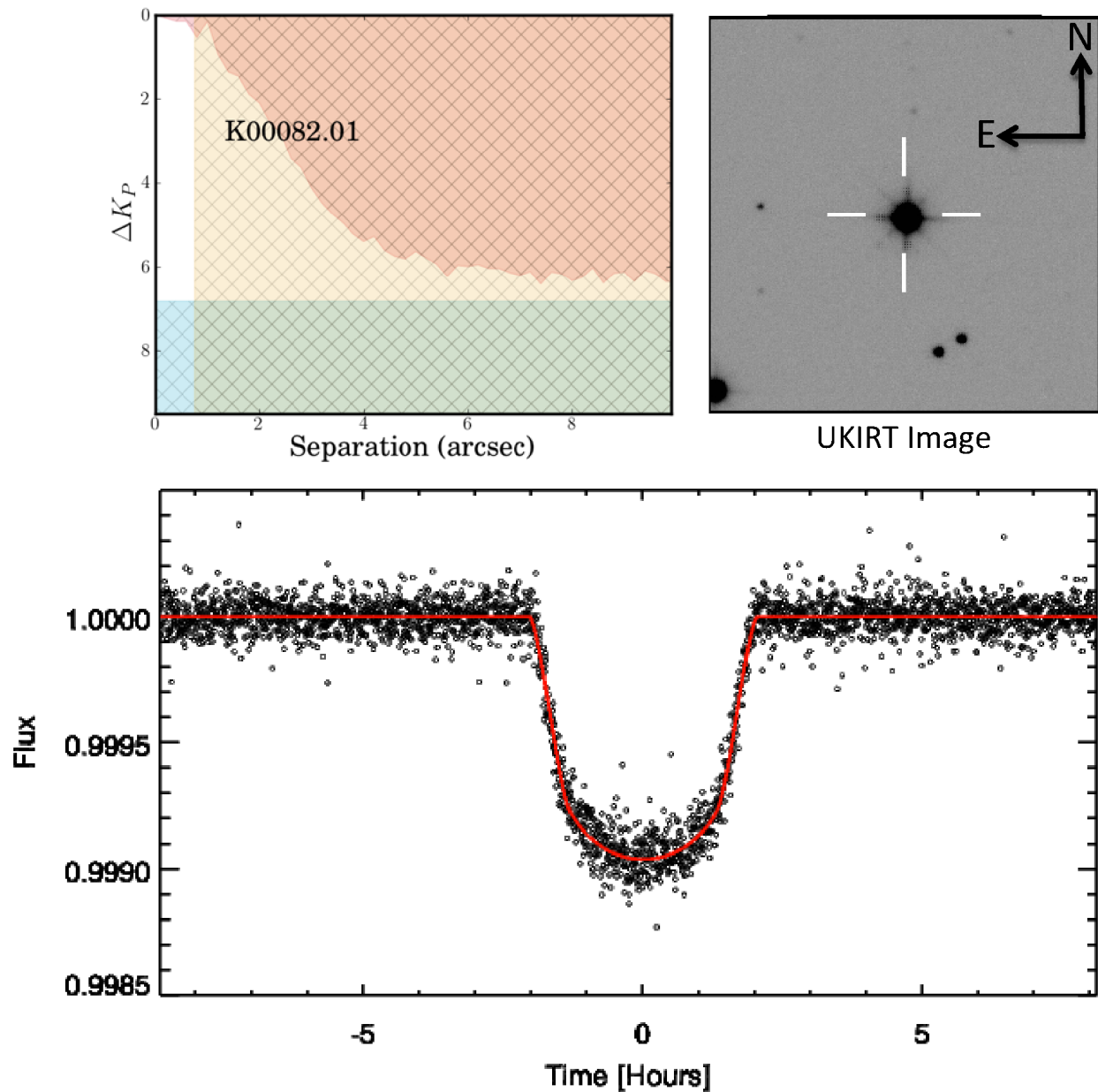


Fig. 5.— Top left: parameter space ($\Delta K_P - a$) for a possible contamination source around KOI 82. Yellow region is excluded by pixel centroid offset analysis, red region is excluded by contrast curve and cyan region is excluded by transit depth analysis. The remaining white region is the possible parameter space for a contamination source. Top right: the UKIRT image for KOI 82. Bottom: folded light curve for KOI 82.01 (black open circles) with the best-fit transit model (red solid line).

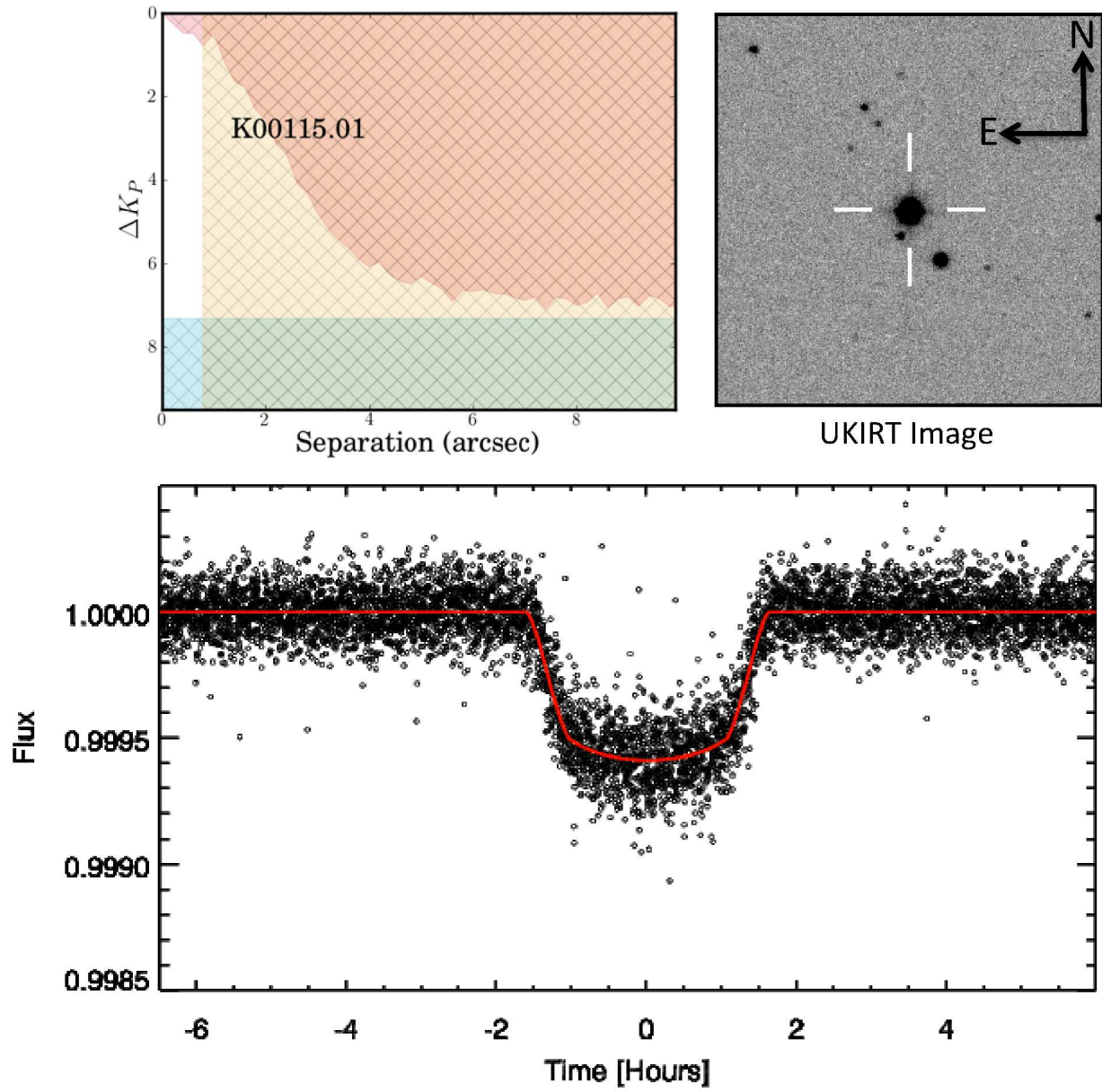


Fig. 6.— Same as Fig. 5 but for KOI 115.01.

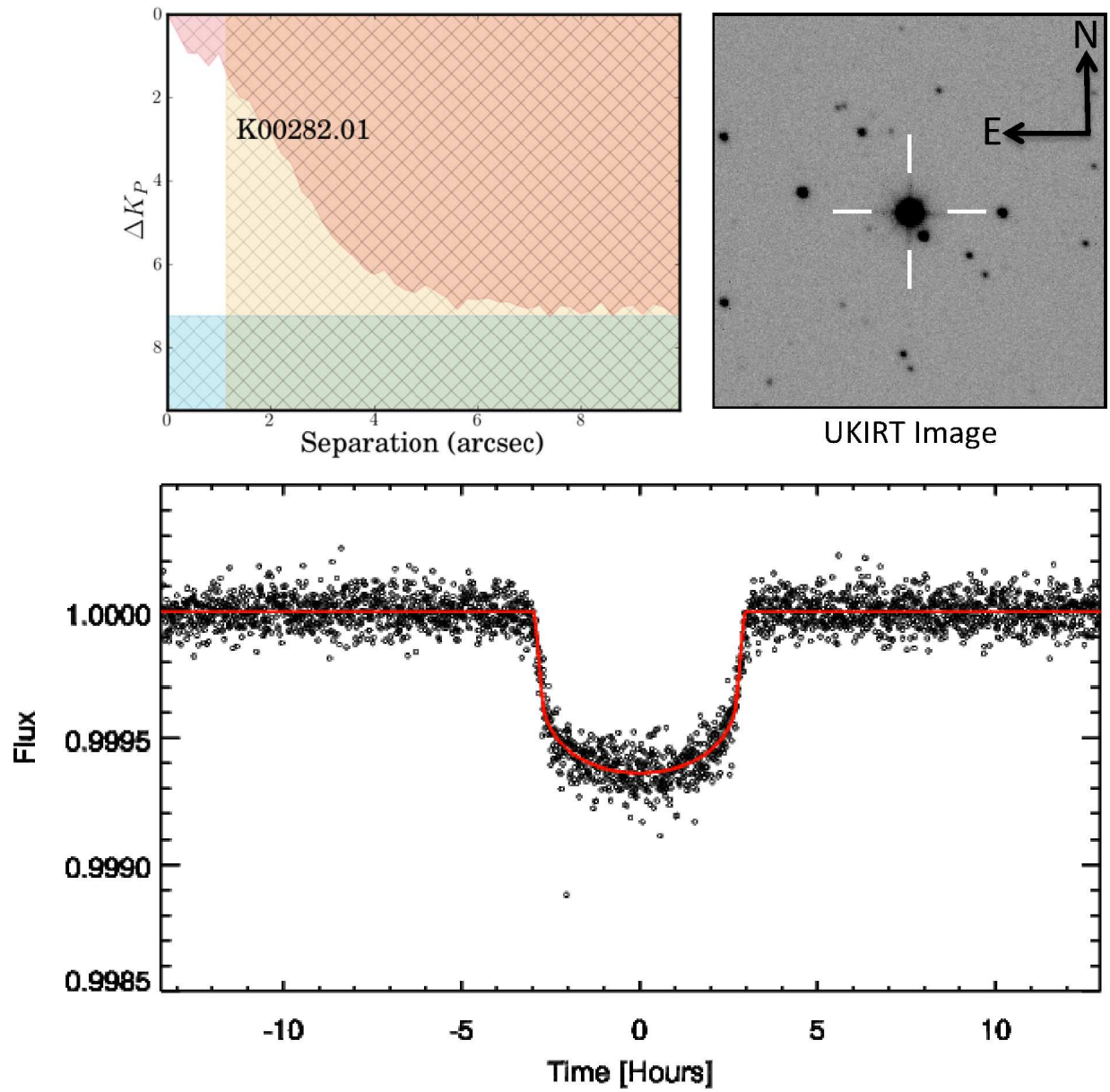


Fig. 7.— Same as Fig. 5 but for KOI 282.01.

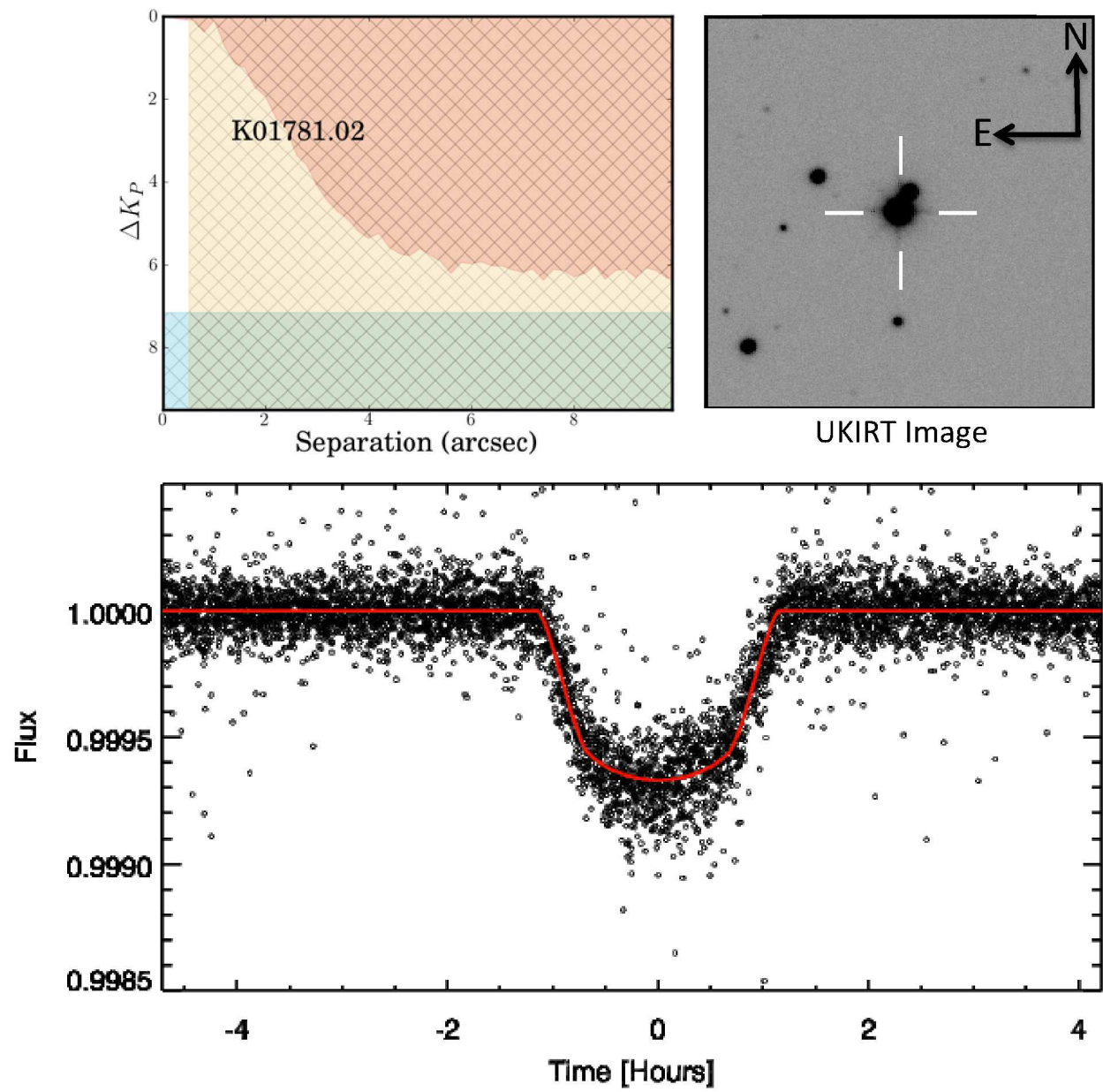


Fig. 8.— Same as Fig. 5 but for KOI 1781.02.

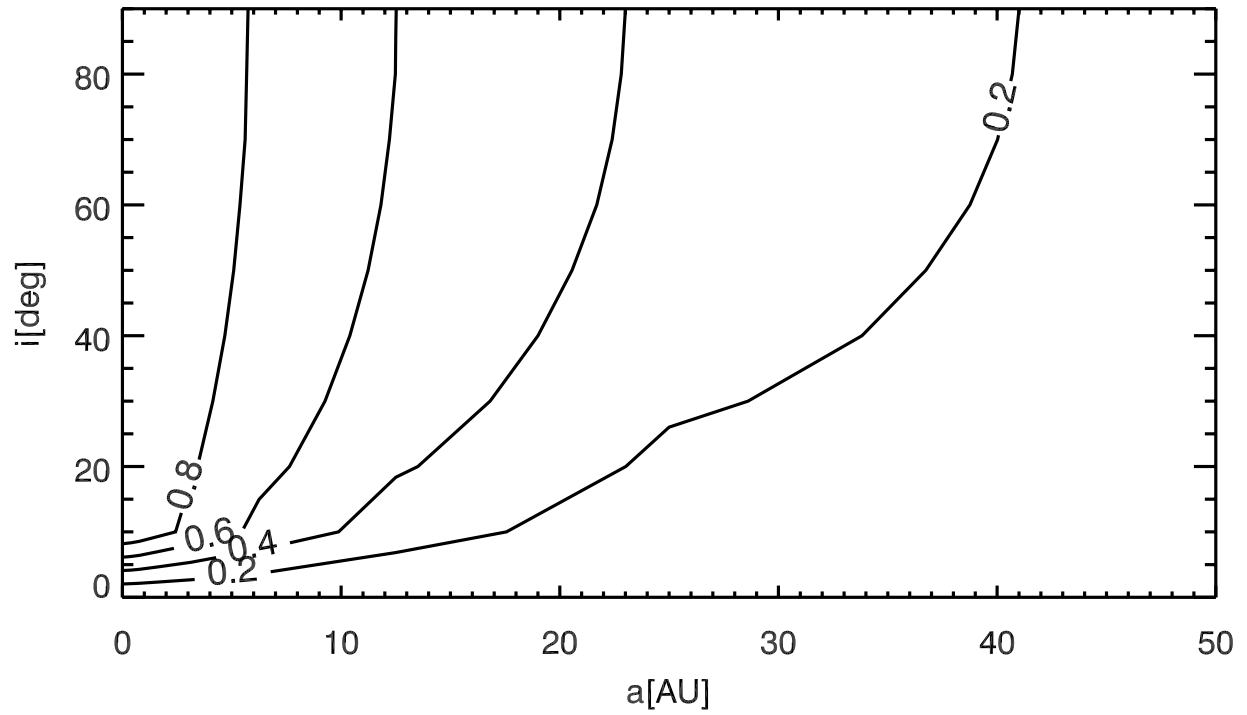


Fig. 9.— Averaged RV completeness contours for 23 systems in our sample with Doppler measurements. The Doppler measurements from CFOP are reported in Table 5. The Doppler technique is sensitive to companions at high inclinations and short separations.

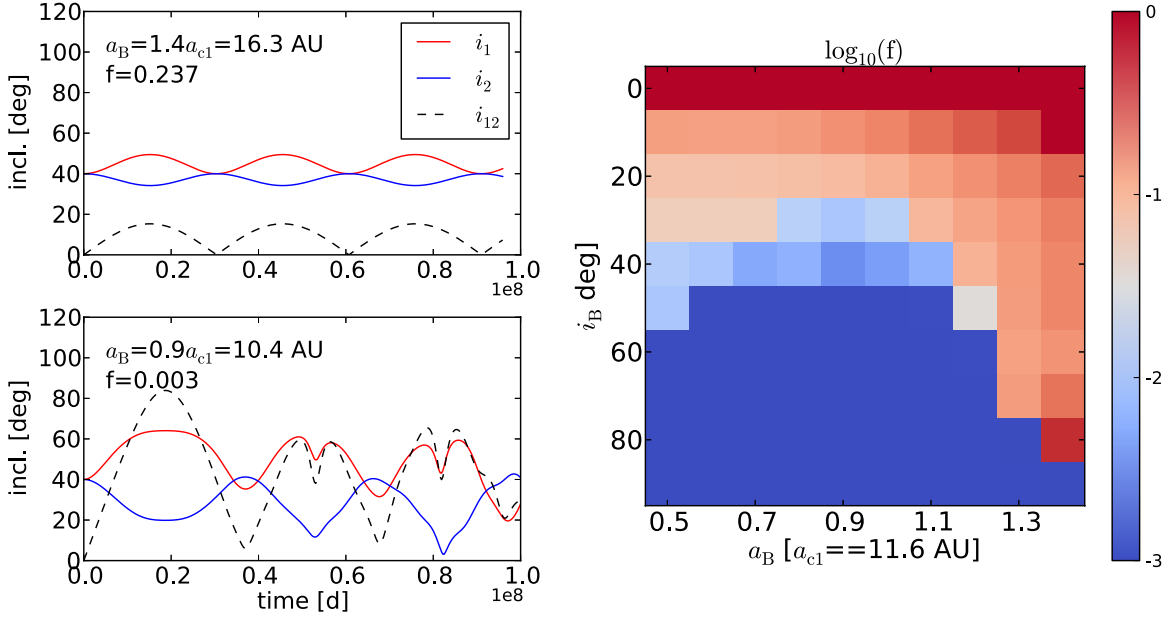


Fig. 10.— An example of dynamical analysis for KOI 275 system, which has two planet candidates KOI-275.01 and KOI 275.02. The left two panels show the evolutions of their orbital inclinations relative to the orbit plane of the proposed stellar companion (i_1 and i_2) and their mutual orbit inclination (i_{12}) in the cases of $a_B = 16.3$ AU (top) and $a_B = 10.4$ AU (bottom). In both cases, the initial orbital inclination of the binary relative to the planet candidates is set to $i_B = 40^\circ$. These two cases correspond to two grids in the right panel, which maps the time fraction (f) that both planet candidates stay in a coplanar configuration with $i_{12} < 5^\circ$ ($f = 0.237$ and $f = 0.003$ for the two cases shown in the left panels, respectively). Since orbital plane of a transiting planet is almost perpendicular to the sky plane, and thus here $i_B = 90^\circ - i$, where i is the orbital inclination with respect to the sky (used in Fig. 9 and 11)

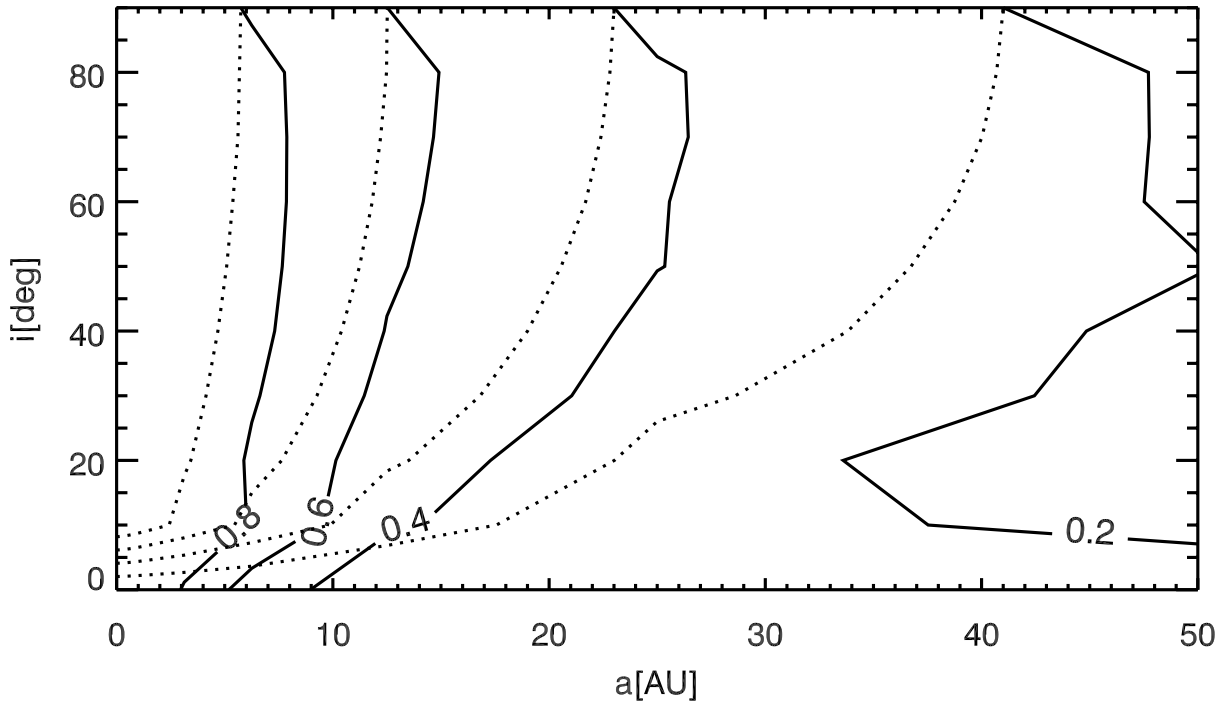


Fig. 11.— Averaged completeness contours for Doppler measurements and the dynamical stability analysis. Contours for RV-only completeness from Fig. 9 are over plotted as dotted lines. The completeness is improved by the sensitivity to stellar companions with low i values by the dynamical stability analysis.

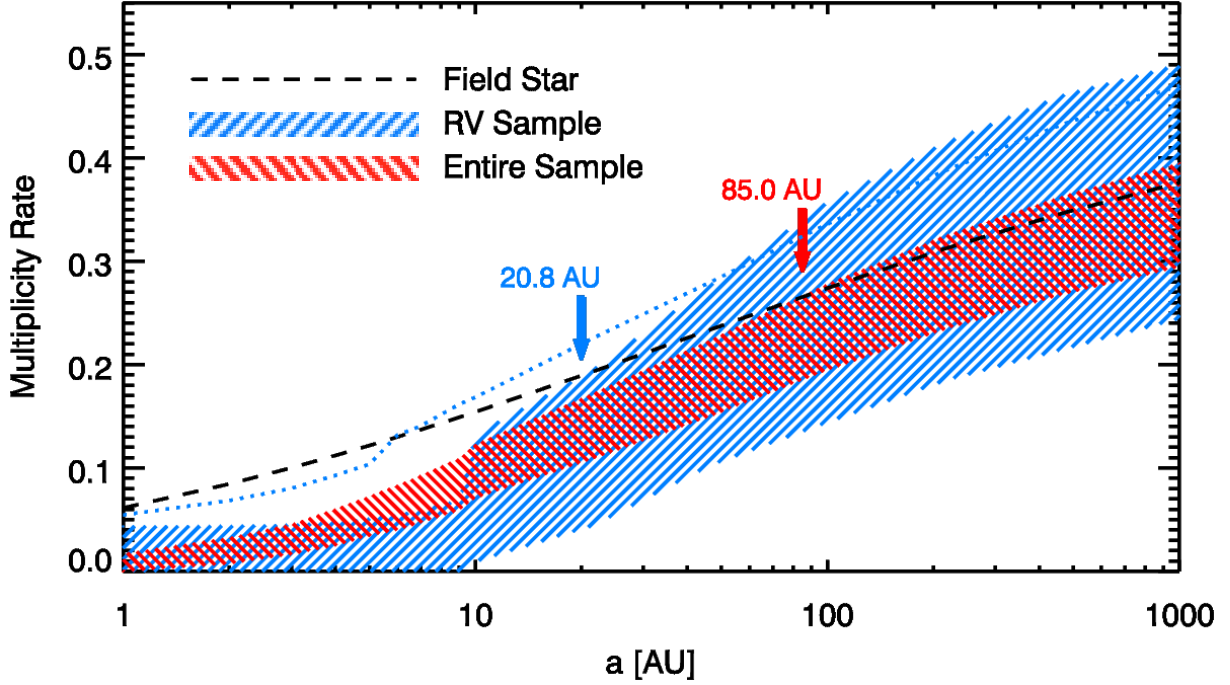


Fig. 12.— The comparison of field star multiplicity rate and the stellar multiplicity rate for planet host stars. Dashed line represents the stellar multiplicity rate for field stars. Blue hatched area represents $1\text{-}\sigma$ uncertainty region of stellar multiplicity rate for 23 KOIs with both RV measurements and dynamical analyses. There is a significant deficiency of stellar companions within 20.8 AU, indicating that planet formation and evolution may be suppressed by a close-in stellar companion. If only dynamical analysis is used for the RV sample, the $1\text{-}\sigma$ upper envelope is shown by the blue dotted line. In this case the difference between the field star multiplicity rate and that for the planet host stars is less distinct due to less constraint from observation and larger statistical errors, which emphasizes the important role of followup RV observations. Red hatched area represents $1\text{-}\sigma$ uncertainty region of the stellar multiplicity rate for 138 KOIs with dynamical analyses including 23 KOIs with RV measurements. The red hatched area suggests a wider effective separation below which planet formation and evolution may be significantly affected, but incompleteness beyond 20 AU prevents us from concluding whether the wider effective separation is due to stellar companion perturbation or an incomplete search and exclusion for stellar companion.

Table 1. List of references on stellar multiplicity study of planet host stars.

Reference	Multiplicity	Sample Size	Technique
Luhman & Jayawardhana (2002)	16%	25	AO
Patience et al. (2002)	27%	11	AO
Eggenberger et al. (2007, 2011)	13.2%±5.1% less than that of control group	130	AO
Daemgen et al. (2009)	21%	14	Lucky Imaging
Mugrauer & Neuhäuser (2009)	17%	250	wide field imaging
Raghavan et al. (2010)	30%	36	interferometry, CPP and RV
Roell et al. (2012)	>12%	477	literature review and catalog search
Adams et al. (2012, 2013)	60%, 20% and 7% within 6, 2 and 0.5 arcsec	90	AO
Ginski et al. (2012)	1.5%	71	Lucky Imaging
Lillo-Box et al. (2012)	12%-18%	98	Lucky Imaging
Bergfors et al. (2013)	>38%	31	Lucky Imaging

Table 2. Stellar Parameters

KOI [†]	KIC [†]	KOI						Derived Values						
		α^\dagger (deg)	δ^\dagger (deg)	K_P^\dagger (mag)	T_{eff}^\dagger (K)	$\log g^\dagger$ (cgs)	$[\text{Fe}/\text{H}]^\dagger$ (dex)	T_{eff} (K)	$\log g$ (cgs)	$[\text{Fe}/\text{H}]$ (dex)	M_* (M_\odot)	R_* (R_\odot)	L_* (L_\odot)	ρ_* (g cm^{-3})
K00005	8554498	289.739716	44.647419	11.66	5861	4.19	0.12	5865 ⁺⁶⁰ ₋₅₈	4.17 ^{+0.07} _{-0.08}	0.11 ^{+0.49} _{-0.47}	1.13 ^{+0.09} _{-0.11}	1.44 ^{+0.16} _{-0.15}	2.19 ^{+0.79} _{-0.60}	0.53 ± 0.18
K00041	6521045	291.385986	41.990269	11.20	5909	4.30	-0.12	5902 ⁺⁵³ ₋₇₄	3.62 ^{+0.20} _{-0.12}	-0.13 ^{+0.43} _{-0.38}	1.23 ^{+0.21} _{-0.13}	2.86 ^{+0.53} _{-0.65}	4.73 ^{+3.63} _{-2.22}	0.07 ± 0.05
K00070	6850504	287.697998	42.338718	12.50	5443	4.45	-0.15	5444 ⁺⁴⁴ ₋₄₃	4.43 ^{+0.07} _{-0.07}	-0.17 ^{+0.52} _{-0.47}	0.88 ^{+0.08} _{-0.12}	0.94 ^{+0.09} _{-0.08}	0.66 ^{+0.26} _{-0.19}	1.49 ± 0.45
K00072	11904151	285.679382	50.241299	10.96	5627	4.39	-0.81	5627 ⁺⁶¹ ₋₅₃	4.35 ^{+0.06} _{-0.07}	-0.80 ^{+0.48} _{-0.51}	0.79 ^{+0.11} _{-0.07}	0.98 ^{+0.09} _{-0.08}	0.67 ^{+0.28} _{-0.16}	1.16 ± 0.32
K00082	10187017	281.482727	47.208031	11.49	4908	4.61	0.20	4909 ⁺⁴¹ ₋₄₁	4.58 ^{+0.08} _{-0.07}	0.18 ^{+0.42} _{-0.47}	0.81 ^{+0.04} _{-0.09}	0.76 ^{+0.07} _{-0.07}	0.28 ^{+0.05} _{-0.06}	2.61 ± 0.75
K00085	5866724	288.688690	41.151180	11.02	6172	4.36	-0.05	6170 ⁺⁴⁷ ₋₄₈	4.33 ^{+0.08} _{-0.07}	-0.03 ^{+0.48} _{-0.48}	1.18 ^{+0.12} _{-0.15}	1.22 ^{+0.13} _{-0.11}	1.76 ^{+0.72} _{-0.46}	0.92 ± 0.30
K00089	8056665	299.821167	43.814270	11.64	7713	3.90	0.06	7715 ⁺¹⁹⁴ ₋₃₆	3.88 ^{+0.18} _{-0.12}	0.06 ^{+0.51} _{-0.48}	1.96 ^{+0.14} _{-0.20}	2.68 ^{+1.06} _{-0.62}	24.99 ^{+11.94} _{-9.49}	0.14 ± 0.13
K00094	6462863	297.333069	41.891121	12.21	6184	4.18	-0.76	6182 ⁺⁶⁰ ₋₅₂	4.17 ^{+0.04} _{-0.05}	-0.74 ^{+0.48} _{-0.49}	1.05 ^{+0.18} _{-0.09}	1.40 ^{+0.14} _{-0.10}	2.19 ^{+1.06} _{-0.56}	0.53 ± 0.15
K00102	8456679	299.704742	44.435749	12.57	5838	4.42	-0.36	5836 ⁺⁵² ₋₅₁	4.41 ^{+0.06} _{-0.08}	-0.33 ^{+0.49} _{-0.52}	0.99 ^{+0.13} _{-0.13}	1.03 ^{+0.11} _{-0.09}	0.92 ^{+0.31} _{-0.27}	1.28 ± 0.41
K00108	4914423	288.984558	40.064529	12.29	5975	4.33	-0.10	5973 ⁺⁴¹ ₋₄₁	4.30 ^{+0.07} _{-0.07}	-0.06 ^{+0.51} _{-0.51}	1.11 ^{+0.16} _{-0.16}	1.22 ^{+0.12} _{-0.11}	1.52 ^{+0.88} _{-0.45}	0.86 ± 0.27
K00111	6678383	287.604614	42.166779	12.60	5711	4.41	-0.78	5706 ⁺⁴⁵ ₋₃₈	4.32 ^{+0.06} _{-0.05}	-0.71 ^{+0.49} _{-0.49}	0.80 ^{+0.10} _{-0.08}	1.02 ^{+0.08} _{-0.08}	0.87 ^{+0.30} _{-0.23}	1.07 ± 0.27
K00112	10984090	295.648712	48.495560	12.77	5853	4.46	-0.59	5853 ⁺⁵⁶ ₋₅₀	4.43 ^{+0.06} _{-0.06}	-0.52 ^{+0.48} _{-0.48}	0.92 ^{+0.10} _{-0.10}	0.98 ^{+0.08} _{-0.08}	0.79 ^{+0.19} _{-0.19}	1.38 ± 0.40
K00115	9579641	287.887329	46.276241	12.79	6398	4.25	-0.22	6397 ⁺⁹⁵ ₋₉₅	4.15 ^{+0.20} _{-0.23}	-0.22 ^{+0.47} _{-0.48}	1.28 ^{+0.12} _{-0.19}	1.58 ^{+0.53} _{-0.37}	4.05 ^{+2.24} _{-1.80}	0.46 ± 0.40
K00116	8395660	300.863983	44.337551	12.88	5865	4.41	-0.36	5868 ⁺⁸⁶ ₋₄₆	4.36 ^{+0.10} _{-0.09}	-0.35 ^{+0.47} _{-0.47}	0.97 ^{+0.13} _{-0.12}	1.07 ^{+0.18} _{-0.13}	1.13 ^{+0.57} _{-0.37}	1.11 ± 0.51
K00117	10875245	297.028259	48.208611	12.49	5949	4.37	-0.09	5944 ⁺⁵⁵ ₋₄₆	4.12 ^{+0.39} _{-0.60}	-0.10 ^{+0.49} _{-0.50}	1.28 ^{+0.37} _{-0.21}	1.62 ^{+1.76} _{-0.64}	3.39 ^{+9.02} _{-2.09}	0.42 ± 0.94
K00119	9471974	294.559174	46.062328	12.65	5632	4.44	-0.03	5623 ⁺¹²⁴ ₋₁₃₄	4.13 ^{+0.19} _{-0.18}	-0.05 ^{+0.48} _{-0.50}	0.98 ^{+0.13} _{-0.10}	1.41 ^{+0.38} _{-0.30}	1.54 ^{+1.17} _{-0.55}	0.49 ± 0.36
K00123	5094751	290.392731	40.284870	12.37	5871	4.15	-0.05	5869 ⁺³⁹ ₋₃₉	4.14 ^{+0.06} _{-0.08}	-0.04 ^{+0.51} _{-0.51}	1.05 ^{+0.09} _{-0.09}	1.43 ^{+0.12} _{-0.12}	1.88 ^{+0.65} _{-0.41}	0.50 ± 0.15
K00124	11086270	292.929138	48.602810	12.94	5899	4.07	-0.15	5899 ⁺⁴⁸ ₋₅₀	4.02 ^{+0.07} _{-0.07}	-0.11 ^{+0.44} _{-0.49}	1.06 ^{+0.07} _{-0.07}	1.67 ^{+0.16} _{-0.13}	2.40 ^{+1.20} _{-0.75}	0.32 ± 0.08
K00139	8559644	291.653168	44.688271	13.49	5952	4.38	0.01	5950 ⁺⁴² ₋₄₂	4.37 ^{+0.07} _{-0.07}	0.03 ^{+0.50} _{-0.50}	1.11 ^{+0.10} _{-0.14}	1.13 ^{+0.12} _{-0.10}	1.32 ^{+0.52} _{-0.34}	1.10 ± 0.35
K00148	5735762	299.139221	40.949020	13.04	5190	4.49	-0.22	5194 ⁺³⁷ ₋₄₃	4.44 ^{+0.05} _{-0.07}	-0.18 ^{+0.51} _{-0.48}	0.82 ^{+0.07} _{-0.12}	0.90 ^{+0.08} _{-0.07}	0.44 ^{+0.11} _{-0.13}	1.61 ± 0.45
K00153	12252424	287.997894	50.944328	13.46	4725	4.64	0.17	4722 ⁺⁴⁷ ₋₅₇	4.46 ^{+0.08} _{-0.09}	0.12 ^{+0.45} _{-0.49}	0.76 ^{+0.04} _{-0.09}	0.83 ^{+0.10} _{-0.09}	0.22 ^{+0.05} _{-0.04}	1.84 ± 0.63
K00159	8972058	297.711853	45.261921	13.43	6069	4.30	-0.08	6072 ⁺⁹⁷ ₋₈₆	4.15 ^{+0.15} _{-0.15}	-0.11 ^{+0.49} _{-0.46}	1.10 ^{+0.11} _{-0.11}	1.46 ^{+0.31} _{-0.24}	2.27 ^{+1.21} _{-0.63}	0.50 ± 0.29
K00168	11512246	294.218933	49.479221	13.44	6142	3.97	-0.33	6149 ⁺¹¹⁹ ₋₁₂₁	3.85 ^{+0.17} _{-0.24}	-0.30 ^{+0.46} _{-0.56}	1.16 ^{+0.13} _{-0.08}	2.14 ^{+0.74} _{-0.40}	4.31 ^{+2.68} _{-1.89}	0.17 ± 0.14
K00244	4349452	286.638397	39.487881	10.73	6103	4.07	...	6103 ⁺⁴² ₋₄₉	4.07 ^{+0.05} _{-0.05}	0.04 ^{+0.48} _{-0.48}	1.19 ^{+0.09} _{-0.09}	1.66 ^{+0.13} _{-0.13}	3.11 ^{+1.40} _{-0.82}	0.37 ± 0.09
K00245	8478994	284.059540	44.518215	9.71	5288	4.59	...	5283 ⁺⁴⁸ ₋₃₇	4.57 ^{+0.07} _{-0.07}	0.02 ^{+0.49} _{-0.51}	0.86 ^{+0.07} _{-0.11}	0.79 ^{+0.08} _{-0.07}	0.53 ^{+0.21} _{-0.17}	2.46 ± 0.72
K00246	11295426	291.032318	49.040272	10.00	5793	4.28	0.15	5794 ⁺⁴¹ ₋₄₄	4.28 ^{+0.01} _{-0.01}	0.18 ^{+0.42} _{-0.45}	1.06 ^{+0.03} _{-0.03}	1.24 ^{+0.02} _{-0.18}	1.46 ^{+0.21} _{-0.13}	0.79 ± 0.06
K00260	8292840	289.347321	44.208511	10.50	6164	4.28	...	6164 ⁺⁵⁷ ₋₅₇	4.23 ^{+0.07} _{-0.07}	0.04 ^{+0.40} _{-0.49}	1.18 ^{+0.11} _{-0.15}	1.37 ^{+0.13} _{-0.12}	2.42 ^{+0.79} _{-0.70}	0.65 ± 0.19
K00262	11807274	288.100861	50.033718	10.42	6058	3.98	-0.35	6060 ⁺⁵¹ ₋₅₂	3.91 ^{+0.07} _{-0.07}	-0.31 ^{+0.48} _{-0.48}	1.19 ^{+0.11} _{-0.11}	2.03 ^{+0.16} _{-0.18}	4.94 ^{+1.81} _{-1.98}	0.20 ± 0.05
K00270	6528464	293.732819	41.900829	11.41	5552	4.08	...	5551 ⁺⁵⁵ ₋₅₇	4.04 ^{+0.07} _{-0.06}	-0.01 ^{+0.52} _{-0.49}	0.94 ^{+0.05} _{-0.06}	1.52 ^{+0.12} _{-0.13}	1.46 ^{+0.76} _{-0.41}	0.38 ± 0.10
K00271	9451706	285.190002	46.027962	11.48	6169	4.33	-0.15	6167 ⁺⁵² ₋₄₅	4.30 ^{+0.06} _{-0.08}	-0.20 ^{+0.55} _{-0.42}	1.16 ^{+0.12} _{-0.14}	1.25 ^{+0.15} _{-0.10}	1.66 ^{+0.64} _{-0.44}	0.84 ± 0.27
K00274	8077137	282.492218	43.980209	11.39	6090	4.13	-0.05	6092 ⁺⁹¹ ₋₉₄	4.11 ^{+0.08} _{-0.07}	-0.02 ^{+0.50} _{-0.50}	1.19 ^{+0.10} _{-0.12}	1.58 ^{+0.17} _{-0.16}	2.94 ^{+1.00} _{-0.80}	0.42 ± 0.14
K00275	10586004	285.311249	47.848564	11.70	5795	4.24	...	5799 ⁺⁴⁴ ₋₄₄	4.20 ^{+0.07} _{-0.06}	0.03 ^{+0.49} _{-0.52}	1.12 ^{+0.10} _{-0.13}	1.38 ^{+0.15} _{-0.14}	1.76 ^{+0.77} _{-0.54}	0.60 ± 0.20
K00277	11401755	291.250183	49.231834	11.87	5973	4.06	...	5970 ⁺⁴⁹ ₋₄₇	4.01 ^{+0.06} _{-0.07}	-0.01 ^{+0.46} _{-0.47}	1.10 ^{+0.08} _{-0.14}	1.72 ^{+0.18} _{-0.18}	2.52 ^{+1.43} _{-0.75}	0.31 ± 0.09
K00279	12314973	295.486511	51.013500	11.68	6418	4.28	-0.34	6418 ⁺⁷² ₋₆₂	4.02 ^{+0.12} _{-0.15}	-0.32 ^{+0.52} _{-0.54}	1.31 ^{+0.15} _{-0.15}	1.84 ^{+0.40} _{-0.27}	5.22 ^{+3.59} _{-1.95}	0.29 ± 0.16
K00282	5088536	288.450653	40.245327	11.53	5873	4.33	...	5879 ⁺⁴⁸ ₋₅₁	4.29 ^{+0.07} _{-0.06}	0.02 ^{+0.46} _{-0.46}	1.00 ^{+0.09} _{-0.10}	1.17 ^{+0.10} _{-0.09}	1.43 ^{+0.32} _{-0.30}	0.87 ± 0.23
K00283	5695396	288.530823	40.942299	11.53	5687	4.42	0.06	5686 ⁺⁴⁴ ₋₄₄	4.40 ^{+0.07} _{-0.07}	0.06 ^{+0.47} _{-0.47}	1.00 ^{+0.12} _{-0.12}	1.03 ^{+0.09} _{-0.09}	0.99 ^{+0.40} _{-0.27}	1.28 ± 0.38
K00284	6021275	283.235809	41.343040	11.82	5925	4.40	-0.05	5924 ⁺⁵⁴ ₋₅₃	4.38 ^{+0.08} _{-0.07}	-0.03 ^{+0.48} _{-0.49}	1.02 ^{+0.13} _{-0.12}	1.07 ^{+0.12} _{-0.10}	1.37 ^{+0.52} _{-0.45}	1.17 ± 0.38
K00285	6196457	289.086060	41.562958	11.56	5883	4.14	...	5882 ⁺⁵⁸ ₋₄₈	4.09 ^{+0.08} _{-0.06}	0.05 ^{+0.47} _{-0.47}	1.16 ^{+0.10} _{-0.10}	1.61 ^{+0.16} _{-0.16}	2.76 ^{+0.99} _{-0.76}	0.39 ± 0.11
K00289	10386922	282.945648	47.574905	12.75	5812	4.46	...	5839 ⁺⁴⁸¹ ₋₄₈₆	4.25 ^{+0.43} _{-0.36}	-0.02 ^{+0.50} _{-0.51}	1.02 ^{+0.24} _{-0.15}	1.25 ^{+0.78} _{-0.50}	1.41 ^{+1.61} _{-0.72}	0.74 ± 1.15
K00291	10933561	297.277985	48.320332	12.85	5600	4.19	-0.16	5598 ⁺⁵³ ₋₅₂	4.15 ^{+0.07} _{-0.07}	-0.12 ^{+0.47} _{-0.47}	0.98 ^{+0.06} _{-0.14}	1.39 ^{+0.14} _{-0.14}	1.61 ^{+0.78} _{-0.41}	0.52 ± 0.16
K00295	11547513	284.739044	49.598400	12.32	5936	4.41	...	6044 ⁺³⁹⁶ ₋₅₀₆	3.66 ^{+0.15} _{-0.16}	-0.10 ^{+0.45} _{-0.49}	1.22 ^{+0.77} _{-0.26}	2.82 ^{+0.59} _{-0.62}	4.04 ^{+10.61} _{-2.02}	0.08 ± 0.06
K00298	12785320	290.494263	52.055519	12.71	5445	4.48	...	5472 ⁺⁴³⁰ ₋₄₉₈	4.29 ^{+0.39} _{-0.37}	0.02 ^{+0.48} _{-0.53}	0.98 ^{+0.25} _{-0.16}	1.17 ^{+0.89} _{-0.47}	1.04 ^{+1.97} _{-0.65}	0.86 ± 1.50
K00301	3642289	290.495117	38.795479	12.73	6337	4.33	0.04	6337 ⁺⁹⁴ ₋₉₄	4.22 ^{+0.13} _{-0.13}	0.09 ^{+0.48} _{-0.48}	1.34 ^{+0.19} _{-0.19}	1.46 ^{+0.18} _{-0.18}	3.91 ^{+1.65} _{-1.65}	0.60 ± 0.29
K00304	6029239	287.089966	41.373878	12.55	6150	3.98	-0.09	6147 ⁺⁷⁹ ₋₈₈	3.91 ^{+0.19} _{-0.22}	-0.10 ^{+0.52} _{-0.45}	1.17 ^{+0.13} _{-0.12}	2.01 ^{+0.60} _{-0.42}	3.09 ^{+2.55} _{-1.02}	0.20 ± 0.16
K00307	6289257	293.180328	41.617760	12.80	6141	4.42	-0.31	6141 ⁺⁵⁸ ₋₅₃	4.38 ^{+0.08} _{-0.08}	-0.28 ^{+0.44} _{-0.49}	1.10 ^{+0.12} _{-0.12}	1.12 ^{+0.11} _{-0.11}	1.36 ^{+0.43} _{-0.34}	

Table 2—Continued

KOI [†]	KIC [†]	KOI						Derived Values						
		α^\dagger (deg)	δ^\dagger (deg)	K_P^\dagger (mag)	T_{eff}^\dagger (K)	$\log g^\dagger$ (cgs)	$[\text{Fe}/\text{H}]^\dagger$ (dex)	T_{eff} (K)	$\log g$ (cgs)	$[\text{Fe}/\text{H}]$ (dex)	M_* (M_\odot)	R_* (R_\odot)	L_* (L_\odot)	ρ_* (g cm^{-3})
K00321	8753657	291.848053	44.968220	12.52	5538	4.34	-0.19	5541 ⁺⁴² ₋₄₄	4.30 ^{+0.05} _{-0.06}	-0.17 ^{+0.50} _{-0.45}	0.91 ^{+0.09} _{-0.10}	1.12 ^{+0.10} _{-0.09}	0.94 ^{+0.28} _{-0.25}	0.92 ± 0.25
K00326	9880467	286.656036	46.783543	12.96	4746	2.54	...	4747 ⁺⁴⁸ ₋₄₉	3.50 ^{+0.00} _{-0.00}	-0.02 ^{+0.47} _{-0.41}	1.96 ^{+0.11} _{-0.12}	4.12 ^{+0.11} _{-0.13}	34.33 ^{+13.95} _{-9.06}	0.04 ± 0.00
K00327	9881662	287.369476	46.768219	13.00	6206	4.39	-0.09	6209 ⁺⁵⁹ ₋₆₂	4.35 ^{+0.08} _{-0.08}	-0.04 ^{+0.49} _{-0.53}	1.19 ^{+0.12} _{-0.15}	1.20 ^{+0.12} _{-0.11}	1.73 ^{+0.60} _{-0.47}	0.96 ± 0.29
K00332	10290666	297.650940	47.396290	13.05	5719	4.33	-0.28	5720 ⁺⁷¹ ₋₆₁	4.27 ^{+0.06} _{-0.05}	-0.24 ^{+0.47} _{-0.51}	1.02 ^{+0.09} _{-0.12}	1.21 ^{+0.13} _{-0.11}	1.09 ^{+0.46} _{-0.25}	0.80 ± 0.24
K00338	10552611	297.970886	47.731682	13.45	4104	1.87	0.54	4112 ⁺⁴⁸ ₋₅₂	3.50 ^{+0.00} _{-0.00}	0.54 ^{+0.06} _{-0.41}	0.92 ^{+0.02} _{-0.04}	2.83 ^{+0.03} _{-0.06}	4.95 ^{+0.45} _{-0.55}	0.06 ± 0.00
K00341	10878263	297.961548	48.244362	13.34	5536	4.48	0.01	5535 ⁺⁴⁸ ₋₅₀	4.46 ^{+0.06} _{-0.07}	0.04 ^{+0.44} _{-0.52}	0.95 ^{+0.07} _{-0.14}	0.94 ^{+0.09} _{-0.08}	0.74 ^{+0.25} _{-0.23}	1.63 ± 0.47
K00343	10982872	295.118896	48.481281	13.20	5744	4.32	-0.27	5747 ⁺⁴⁵ ₋₅₃	4.27 ^{+0.06} _{-0.08}	-0.28 ^{+0.46} _{-0.50}	0.95 ^{+0.09} _{-0.11}	1.17 ^{+0.13} _{-0.11}	1.24 ^{+0.42} _{-0.36}	0.82 ± 0.26
K00353	11566064	295.212677	49.562180	13.37	6858	4.33	-0.09	6863 ⁺⁹⁹ ₋₁₁₄	4.24 ^{+0.21} _{-0.20}	-0.06 ^{+0.48} _{-0.53}	1.49 ^{+0.17} _{-0.21}	1.51 ^{+0.47} _{-0.33}	4.52 ^{+2.01} _{-1.53}	0.61 ± 0.49
K00354	11568987	296.418549	49.540100	13.23	5935	4.44	-0.84	5934 ⁺⁶⁵ ₋₅₇	4.40 ^{+0.08} _{-0.07}	-0.84 ^{+0.54} _{-0.47}	0.90 ^{+0.14} _{-0.08}	0.99 ^{+0.10} _{-0.10}	0.77 ^{+0.31} _{-0.16}	1.28 ± 0.41
K00369	7175184	281.915680	42.775509	11.99	6377	4.41	-0.33	6380 ⁺⁵⁸ ₋₅₈	4.41 ^{+0.15} _{-0.15}	-0.34 ^{+0.50} _{-0.48}	1.20 ^{+0.16} _{-0.17}	1.13 ^{+0.20} _{-0.20}	2.12 ^{+0.85} _{-0.72}	1.18 ± 0.74
K00370	8494142	291.387756	44.529110	11.93	6022	3.95	-0.67	6019 ⁺⁵⁶ ₋₅₂	3.92 ^{+0.06} _{-0.08}	-0.71 ^{+0.53} _{-0.44}	1.18 ^{+0.12} _{-0.09}	1.99 ^{+0.19} _{-0.16}	6.18 ^{+1.73} _{-1.89}	0.21 ± 0.06
K00623	12068975	295.226440	50.558979	11.81	5877	4.23	-0.53	5880 ⁺⁴⁶ ₋₅₅	4.18 ^{+0.08} _{-0.07}	-0.52 ^{+0.49} _{-0.43}	0.89 ^{+0.07} _{-0.07}	1.26 ^{+0.12} _{-0.12}	1.39 ^{+0.56} _{-0.21}	0.62 ± 0.18
K00626	4478168	295.193390	39.539669	13.49	6157	4.41	-0.28	6158 ⁺⁵³ ₋₅₅	4.40 ^{+0.07} _{-0.06}	-0.25 ^{+0.48} _{-0.45}	1.11 ^{+0.14} _{-0.15}	1.09 ^{+0.10} _{-0.10}	1.48 ^{+0.75} _{-0.44}	1.20 ± 0.36
K00627	4563268	292.150452	39.637581	13.31	6125	4.37	0.09	6127 ⁺⁶¹ ₋₅₇	4.35 ^{+0.06} _{-0.07}	0.09 ^{+0.48} _{-0.49}	1.20 ^{+0.09} _{-0.21}	1.20 ^{+0.10} _{-0.09}	1.68 ^{+0.58} _{-0.49}	0.99 ± 0.27
K00655	5966154	293.626038	41.272820	13.00	6133	4.32	-0.28	6136 ⁺⁵⁵ ₋₅₆	4.28 ^{+0.07} _{-0.07}	-0.26 ^{+0.44} _{-0.45}	1.11 ^{+0.13} _{-0.14}	1.26 ^{+0.13} _{-0.11}	1.71 ^{+0.89} _{-0.48}	0.78 ± 0.25
K00664	6442340	291.634674	41.833858	13.48	5986	4.24	-0.15	5986 ⁺⁹¹ ₋₈₈	4.12 ^{+0.15} _{-0.18}	-0.17 ^{+0.45} _{-0.49}	1.04 ^{+0.09} _{-0.10}	1.46 ^{+0.38} _{-0.27}	1.91 ^{+1.44} _{-0.42}	0.47 ± 0.31
K00665	6685609	290.030518	42.166050	13.18	6080	4.37	-0.02	6085 ⁺⁸⁰ ₋₉₂	4.16 ^{+0.16} _{-0.16}	0.02 ^{+0.48} _{-0.51}	1.18 ^{+0.15} _{-0.15}	1.48 ^{+0.27} _{-0.21}	2.62 ^{+1.64} _{-0.95}	0.51 ± 0.31
K00678	7509886	285.439148	43.168480	13.28	5174	3.91	0.11	5169 ⁺⁹⁰ ₋₇₅	3.50 ^{+0.00} _{-0.00}	0.00 ^{+0.54} _{-0.43}	0.93 ^{+0.04} _{-0.03}	2.83 ^{+0.05} _{-0.07}	1.50 ^{+0.86} _{-0.41}	0.06 ± 0.00
K00679	7515212	287.620819	43.141647	13.18	5913	4.37	...	5912 ⁺⁴⁸ ₋₃₅	4.18 ^{+0.08} _{-0.38}	0.02 ^{+0.48} _{-0.53}	1.24 ^{+0.18} _{-0.18}	1.46 ^{+0.55} _{-0.55}	2.59 ^{+1.31} _{-1.31}	0.56 ± 1.01
K00710	9590976	293.037750	46.277519	13.29	6653	4.31	...	6654 ⁺⁵²⁵ ₋₅₂₃	3.63 ^{+0.36} _{-0.13}	-0.01 ^{+0.46} _{-0.53}	1.23 ^{+0.97} _{-0.26}	2.84 ^{+1.08} _{-1.05}	3.90 ^{+26.82} _{-1.73}	0.08 ± 0.09
K00717	9873254	282.212921	46.717819	13.39	5686	4.41	-0.35	5687 ⁺⁴⁹ ₋₄₈	4.28 ^{+0.24} _{-0.31}	-0.32 ^{+0.45} _{-0.53}	1.08 ^{+0.31} _{-0.35}	1.24 ^{+0.74} _{-0.74}	1.31 ^{+4.04} _{-0.48}	0.79 ± 1.06
K00719	9950612	291.506165	46.895741	13.18	4689	4.66	...	4689 ⁺⁵⁶ ₋₅₆	4.64 ^{+0.07} _{-0.07}	-0.02 ^{+0.53} _{-0.49}	0.72 ^{+0.05} _{-0.09}	0.67 ^{+0.06} _{-0.06}	0.18 ^{+0.04} _{-0.04}	3.46 ± 1.03
K00972	11013201	282.000305	48.542221	9.28	8002	3.82	-0.06	7993 ⁺²⁰⁴ ₋₁₈₄	3.59 ^{+0.28} _{-0.09}	-0.08 ^{+0.51} _{-0.50}	2.14 ^{+0.15} _{-0.17}	3.90 ^{+0.45} _{-1.15}	42.54 ^{+16.71} _{-15.17}	0.05 ± 0.03
K01001	1871056	292.044617	37.376240	13.04	6235	3.80	-0.19	6225 ⁺¹²¹ ₋₁₀₉	3.53 ^{+0.23} _{-0.03}	-0.18 ^{+0.43} _{-0.45}	1.36 ^{+0.11} _{-0.11}	3.28 ^{+0.73} _{-0.73}	7.24 ^{+4.59} _{-3.01}	0.05 ± 0.03
K01151	8280511	283.002960	44.284229	13.04	5759	4.43	-0.95	5728 ⁺¹²⁵ ₋₆₈	3.80 ^{+0.09} _{-0.06}	-1.09 ^{+0.58} _{-0.29}	1.02 ^{+0.11} _{-0.10}	2.15 ^{+0.11} _{-0.25}	5.45 ^{+3.27} _{-1.84}	0.15 ± 0.04
K01175	10350571	295.920654	47.448608	13.29	5610	4.03	-0.50	5609 ⁺⁵³ ₋₅₃	4.00 ^{+0.08} _{-0.08}	-0.50 ^{+0.52} _{-0.47}	0.99 ^{+0.08} _{-0.08}	1.65 ^{+0.16} _{-0.17}	2.77 ^{+0.89} _{-0.87}	0.31 ± 0.10
K01215	3939150	286.583160	39.077202	13.42	5946	4.08	-0.32	5943 ⁺⁵⁶ ₋₅₃	3.50 ^{+0.15} _{-0.00}	-0.36 ^{+0.49} _{-0.49}	1.14 ^{+0.10} _{-0.06}	3.12 ^{+0.12} _{-0.47}	4.27 ^{+2.17} _{-1.72}	0.05 ± 0.02
K01221	3640905	290.107178	38.702229	11.58	5128	3.94	0.42	5125 ⁺⁵¹ ₋₄₆	3.91 ^{+0.06} _{-0.07}	0.42 ^{+0.18} _{-0.54}	1.03 ^{+0.08} _{-0.10}	1.87 ^{+0.18} _{-0.15}	2.07 ^{+0.66} _{-0.48}	0.22 ± 0.06
K01241	6448890	293.758362	41.871868	12.44	4931	3.58	0.16	4927 ⁺⁴⁹ ₋₄₈	3.50 ^{+0.00} _{-0.00}	0.15 ^{+0.40} _{-0.47}	1.31 ^{+0.13} _{-0.13}	3.35 ^{+0.20} _{-0.20}	6.05 ^{+6.66} _{-2.22}	0.05 ± 0.01
K01316	10794087	290.552368	48.126263	11.93	5721	4.00	...	5723 ⁺⁴⁴ ₋₅₆	3.66 ^{+0.26} _{-0.16}	0.03 ^{+0.50} _{-0.53}	1.17 ^{+0.12} _{-0.08}	2.65 ^{+0.54} _{-0.69}	3.41 ^{+1.77} _{-1.19}	0.09 ± 0.06
K01445	11336883	283.936798	49.110329	12.32	6182	4.35	0.06	6183 ⁺⁴⁸ ₋₄₉	4.30 ^{+0.07} _{-0.07}	0.07 ^{+0.47} _{-0.45}	1.21 ^{+0.11} _{-0.14}	1.28 ^{+0.11} _{-0.11}	1.96 ^{+0.98} _{-0.49}	0.81 ± 0.23
K01525	7869917	281.971252	43.672771	12.08	6905	4.24	0.01	6907 ⁺⁸¹ ₋₈₈	4.11 ^{+0.18} _{-0.25}	-0.01 ^{+0.50} _{-0.48}	1.68 ^{+0.21} _{-0.31}	1.85 ^{+0.75} _{-0.41}	11.64 ^{+9.02} _{-7.06}	0.37 ± 0.35
K01534	4741126	290.090820	39.816990	13.47	6401	4.40	-0.06	6401 ⁺⁹⁴ ₋₈₆	4.25 ^{+0.18} _{-0.18}	-0.06 ^{+0.51} _{-0.46}	1.31 ^{+0.17} _{-0.17}	1.41 ^{+0.33} _{-0.33}	2.60 ^{+1.52} _{-0.79}	0.66 ± 0.44
K01613	6268648	285.476593	41.632717	11.05	5945	4.41	...	5997 ⁺⁴⁷⁹ ₋₅₅₅	4.09 ^{+0.30} _{-0.28}	-0.04 ^{+0.50} _{-0.44}	1.09 ^{+0.30} _{-0.17}	1.57 ^{+0.72} _{-0.51}	2.07 ^{+2.40} _{-0.98}	0.39 ± 0.47
K01628	6975129	288.395752	42.459751	12.95	6197	4.38	0.08	6198 ⁺⁴⁸ ₋₅₂	4.36 ^{+0.07} _{-0.08}	0.11 ^{+0.47} _{-0.51}	1.22 ^{+0.09} _{-0.15}	1.19 ^{+0.13} _{-0.11}	1.81 ^{+0.47} _{-0.54}	1.02 ± 0.31
K01692	6616218	294.674103	42.075581	12.56	5501	4.49	0.16	5501 ⁺⁵⁴ ₋₅₃	4.47 ^{+0.06} _{-0.06}	0.19 ^{+0.47} _{-0.47}	0.98 ^{+0.11} _{-0.11}	0.94 ^{+0.07} _{-0.07}	0.65 ^{+0.14} _{-0.13}	1.64 ± 0.40
K01779	9909735	298.482819	46.793621	13.30	5812	4.14	0.14	5813 ⁺¹⁰⁷ ₋₁₁₃	3.95 ^{+0.18} _{-0.12}	0.18 ^{+0.42} _{-0.54}	0.97 ^{+0.08} _{-0.09}	1.73 ^{+0.27} _{-0.35}	1.46 ^{+0.95} _{-0.27}	0.26 ± 0.14
K01781	11551692	287.605591	49.523258	12.23	4977	4.59	0.22	4974 ⁺⁴⁴ ₋₅₁	4.54 ^{+0.07} _{-0.07}	0.23 ^{+0.47} _{-0.48}	0.83 ^{+0.10} _{-0.10}	0.79 ^{+0.06} _{-0.06}	0.31 ^{+0.07} _{-0.07}	2.33 ± 0.60
K01806	9529744	293.213562	46.175129	13.47	6440	4.41	-0.24	6442 ⁺⁸⁶ ₋₈₁	4.31 ^{+0.19} _{-0.20}	-0.24 ^{+0.47} _{-0.48}	1.07 ^{+0.24} _{-0.17}	1.19 ^{+0.34} _{-0.26}	2.14 ^{+1.27} _{-0.44}	0.89 ± 0.69
K01809	8240797	294.453857	44.145973	12.71	5692	4.47	...	5733 ⁺⁵¹⁹ ₋₇₃₃	4.13 ^{+0.22} _{-0.14}	-0.04 ^{+0.52} _{-0.44}	1.06 ^{+0.23} _{-0.23}	1.49 ^{+0.56} _{-0.38}	1.69 ^{+1.61} _{-0.82}	0.45 ± 0.43
K01824	2989404	291.382233	38.127468	12.72	6255	4.21	-0.08	6256 ⁺⁷³ ₋₈₇	4.12 ^{+0.14} _{-0.14}	-0.03 ^{+0.49} _{-0.52}	1.21 ^{+0.13} _{-0.15}	1.58 ^{+0.33} _{-0.27}	3.25 ^{+1.65} _{-1.07}	0.44 ± 0.25
K01909	10130039	287.140656	47.115189	12.78	6095	4.46	-0.07	6100 ⁺⁷⁰ ₋₆₇	4.35 ^{+0.14} _{-0.14}	-0.02 ^{+0.46} _{-0.48}	1.19 ^{+0.12} _{-0.16}	1.20 ^{+0.24} _{-0.21}	1.71 ^{+0.99} _{-0.45}	0.97 ± 0.56
K01929	10136549	290.060486	47.163960	12.73	5900	4.12	-0.13	5899 ⁺⁷² ₋₇₃	3.86 ^{+0.20} _{-0.24}	-0.10 ^{+0.51} _{-0.52}	1.02 ^{+0.07} _{-0.07}	1.98 ^{+0.42} _{-0.42}	1.88 ^{+1.60} _{-0.43}	0.18 ± 0.14
K01930	5511081	282.978973	40.784351	12.12	5897	4.12	-0.11	5899 ⁺⁵³ ₋₅₉	4.06 ^{+0.07} _{-0.07}	-0.05 ^{+0.48} _{-0.52}	1.09 ^{+0.08} _{-0.08}	1.61 ^{+0.14} _{-0.14}	2.42 ^{+1.09} _{-0.66}	0.37 ± 0.10
K01932	5202905	295.933472	40.300571	12.35	8229	3.86	-0.09	8232 ⁺²⁰⁵ ₋₂₀₉	3.74 ^{+0.20} _{-0.20}	-0.09 ^{+0.52} _{-0.48}	2.15 ^{+0.22} _{-0.19}	3.27 ^{+1.02} _{-0.72}	42	

Table 2—Continued

KOI [†]	KIC [†]	KOI						Derived Values						
		α^\dagger (deg)	δ^\dagger (deg)	K_P^\dagger (mag)	T_{eff}^\dagger (K)	$\log g^\dagger$ (cgs)	$[\text{Fe}/\text{H}]^\dagger$ (dex)	T_{eff} (K)	$\log g$ (cgs)	$[\text{Fe}/\text{H}]$ (dex)	M_* (M_\odot)	R_* (R_\odot)	L_* (L_\odot)	ρ_* (g cm^{-3})
K02053	2307415	292.421082	37.682819	12.99	6310	4.34	-0.33	6313 ⁺⁸¹ ₋₈₂	4.25 ^{+0.18} _{-0.17}	-0.30 ^{+0.51} _{-0.48}	1.21 ^{+0.19} _{-0.18}	1.35 ^{+0.37} _{-0.28}	2.70 ^{+2.35} _{-1.19}	0.69 ± 0.51
K02059	12301181	287.590088	51.060570	12.91	4790	4.63	-1.13	4787 ⁺⁶² ₋₆₂	4.45 ^{+0.18} _{-0.16}	-1.15 ^{+0.53} _{-0.45}	0.58 ^{+0.07} _{-0.05}	0.76 ^{+0.16} _{-0.15}	0.15 ^{+0.05} _{-0.03}	1.87 ± 1.16
K02148	6021193	283.192078	41.305389	13.35	5604	3.90	0.30	5613 ⁺¹²⁵ ₋₁₃₀	3.78 ^{+0.21} _{-0.27}	0.33 ^{+0.27} _{-0.49}	1.05 ^{+0.15} _{-0.10}	2.23 ^{+0.97} _{-0.51}	2.00 ^{+1.30} _{-0.68}	0.13 ± 0.11
K02158	5211199	297.651428	40.352551	13.05	5404	4.02	-0.09	5406 ⁺⁶⁸ ₋₆₈	3.92 ^{+0.17} _{-0.17}	-0.07 ^{+0.48} _{-0.43}	0.91 ^{+0.05} _{-0.06}	1.74 ^{+0.36} _{-0.32}	1.39 ^{+0.74} _{-0.40}	0.24 ± 0.14
K02169	9006186	285.207489	45.384350	12.40	5447	4.42	0.03	5451 ⁺⁶⁶ ₋₇₆	4.31 ^{+0.14} _{-0.14}	-0.02 ^{+0.15} _{-0.47}	0.90 ^{+0.15} _{-0.11}	1.10 ^{+0.20} _{-0.20}	0.96 ^{+0.28} _{-0.28}	0.96 ± 0.53
K02173	11774991	297.292419	49.981628	12.88	4739	4.64	0.25	4740 ⁺⁶⁵ ₋₇₂	4.48 ^{+0.16} _{-0.17}	0.27 ^{+0.33} _{-0.49}	0.75 ^{+0.05} _{-0.09}	0.82 ^{+0.20} _{-0.14}	0.25 ^{+0.10} _{-0.06}	1.93 ± 1.22
K02175	9022166	291.880035	45.387932	12.85	5293	4.58	-0.49	5293 ⁺²⁰⁰ ₋₂₄	4.35 ^{+0.24} _{-0.23}	-0.49 ^{+0.48} _{-0.49}	0.85 ^{+0.16} _{-0.12}	1.00 ^{+0.42} _{-0.26}	0.52 ^{+0.97} _{-0.21}	1.19 ± 1.22
K02289	3867615	295.701111	38.945831	13.36	6255	4.38	-0.04	6251 ⁺⁸⁷ ₋₈₇	4.28 ^{+0.20} _{-0.21}	-0.03 ^{+0.49} _{-0.47}	1.27 ^{+0.17} _{-0.19}	1.34 ^{+0.45} _{-0.29}	2.73 ^{+2.56} _{-1.12}	0.75 ± 0.63
K02311	4247991	287.241180	39.332760	12.57	5765	4.48	-0.29	5763 ⁺⁴⁷ ₋₄₅	4.33 ^{+0.45} _{-0.45}	-0.29 ^{+0.52} _{-0.51}	1.19 ^{+0.61} _{-0.35}	1.21 ^{+1.21} _{-0.85}	1.71 ^{+8.32} _{-5.21}	0.94 ± 2.04
K02352	8013439	285.182800	43.831078	10.42	6638	4.32	...	6670 ⁺⁴⁵ ₋₅₂	4.08 ^{+0.25} _{-0.25}	0.02 ^{+0.50} _{-0.48}	1.13 ^{+0.34} _{-0.19}	1.61 ^{+0.57} _{-0.37}	2.55 ^{+2.89} _{-0.99}	0.38 ± 0.35
K02541	12306058	290.621826	51.057301	13.01	5214	3.74	0.02	5213 ⁺⁸⁹ ₋₈₇	3.50 ^{+0.25} _{-0.00}	-0.04 ^{+0.45} _{-0.45}	1.19 ^{+0.10} _{-0.09}	3.10 ^{+0.18} _{-0.70}	3.64 ^{+2.13} _{-0.90}	0.06 ± 0.02
K02585	7673841	288.660767	43.368080	13.46	6482	4.20	-0.30	6490 ⁺⁷⁸ ₋₇₅	3.89 ^{+0.32} _{-0.17}	-0.31 ^{+0.48} _{-0.48}	1.32 ^{+0.14} _{-0.14}	2.19 ^{+0.52} _{-0.79}	5.30 ^{+5.21} _{-2.08}	0.18 ± 0.16
K02595	8883329	290.995270	45.192211	13.22	6742	4.11	-0.22	6740 ⁺¹¹⁹ ₋₁₁₆	3.81 ^{+0.16} _{-0.14}	-0.20 ^{+0.49} _{-0.52}	1.51 ^{+0.18} _{-0.12}	2.54 ^{+0.53} _{-0.47}	10.30 ^{+6.92} _{-4.26}	0.13 ± 0.08
K02672	11253827	296.132812	48.977402	11.92	5565	4.33	-0.13	5568 ⁺⁵⁶ ₋₆₁	4.28 ^{+0.20} _{-0.21}	-0.12 ^{+0.50} _{-0.49}	0.89 ^{+0.05} _{-0.03}	1.11 ^{+0.34} _{-0.23}	1.07 ^{+0.42} _{-0.30}	0.92 ± 0.71
K02674	8022489	289.651245	43.824421	13.35	5973	4.26	-0.12	5966 ⁺⁸⁸ ₋₈₈	4.05 ^{+0.38} _{-0.35}	-0.15 ^{+0.47} _{-0.51}	1.03 ^{+0.09} _{-0.10}	1.60 ^{+0.76} _{-0.61}	1.87 ^{+1.23} _{-0.49}	0.35 ± 0.46
K02675	5794570	292.971252	41.035770	12.43	5706	4.56	-0.35	5704 ⁺⁵⁹ ₋₆₀	4.46 ^{+0.13} _{-0.20}	-0.32 ^{+0.51} _{-0.48}	1.03 ^{+0.19} _{-0.16}	0.96 ^{+0.32} _{-0.14}	0.85 ^{+0.53} _{-0.29}	1.61 ± 1.20
K02687	7202957	292.615112	42.764252	10.16	5803	3.91	0.15	5800 ⁺⁷⁵ ₋₆₀	3.55 ^{+0.05} _{-0.05}	0.12 ^{+0.48} _{-0.47}	1.15 ^{+0.12} _{-0.12}	2.93 ^{+0.97} _{-0.91}	2.85 ^{+1.12} _{-1.12}	0.06 ± 0.04
K02693	5185897	291.468658	40.343849	13.26	4476	4.73	-0.05	4477 ⁺⁵⁶ ₋₅₉	4.63 ^{+0.15} _{-0.13}	-0.04 ^{+0.48} _{-0.47}	0.70 ^{+0.07} _{-0.08}	0.67 ^{+0.11} _{-0.12}	0.14 ^{+0.03} _{-0.03}	3.23 ± 1.71
K02696	11071200	284.415924	48.658020	13.00	7036	4.15	-0.14	7033 ⁺⁹⁴ ₋₁₀₄	4.02 ^{+0.19} _{-0.19}	-0.15 ^{+0.49} _{-0.49}	1.64 ^{+0.22} _{-0.22}	2.06 ^{+0.59} _{-0.42}	11.82 ^{+8.06} _{-5.35}	0.27 ± 0.20
K02714	12206313	290.082764	50.863480	13.31	6362	4.19	-0.30	6356 ⁺⁹⁴ ₋₈₅	3.94 ^{+0.23} _{-0.16}	-0.24 ^{+0.50} _{-0.53}	1.26 ^{+0.12} _{-0.12}	1.97 ^{+0.48} _{-0.48}	4.54 ^{+2.71} _{-1.60}	0.23 ± 0.17
K02722	7673192	288.370239	43.354610	13.27	6534	4.34	-0.22	6535 ⁺¹⁰³ ₋₁₀₅	4.24 ^{+0.12} _{-0.12}	-0.23 ^{+0.53} _{-0.49}	1.32 ^{+0.19} _{-0.21}	1.42 ^{+0.33} _{-0.24}	3.19 ^{+2.81} _{-1.24}	0.65 ± 0.39
K02732	9886361	289.921448	46.744560	12.80	6303	4.44	-0.14	6303 ⁺⁷³ ₋₇₀	4.19 ^{+0.29} _{-0.25}	-0.17 ^{+0.50} _{-0.47}	1.44 ^{+0.52} _{-0.24}	1.55 ^{+0.80} _{-0.46}	3.37 ^{+7.50} _{-1.50}	0.54 ± 0.68
K02949	6026737	285.875793	41.332432	13.31	6176	4.00	-0.07	6175 ⁺⁹⁴ ₋₉₂	3.87 ^{+0.21} _{-0.28}	-0.07 ^{+0.48} _{-0.49}	1.16 ^{+0.10} _{-0.09}	2.10 ^{+0.79} _{-0.48}	3.03 ^{+2.18} _{-0.82}	0.18 ± 0.16
K03083	7106173	287.978851	42.679359	12.86	5923	4.53	-0.07	5915 ⁺⁹⁶ ₋₇₉	4.43 ^{+0.22} _{-0.27}	-0.07 ^{+0.48} _{-0.48}	1.15 ^{+0.18} _{-0.18}	1.05 ^{+0.25} _{-0.25}	1.32 ^{+0.46} _{-0.46}	1.39 ± 1.44
K03097	7582689	281.112335	43.227791	11.97	6306	4.01	-0.29	6307 ⁺⁷³ ₋₆₉	3.92 ^{+0.20} _{-0.27}	-0.28 ^{+0.48} _{-0.47}	1.19 ^{+0.11} _{-0.10}	2.00 ^{+0.76} _{-0.44}	3.75 ^{+2.59} _{-1.22}	0.21 ± 0.19
K03111	8581240	298.576874	44.621609	12.86	6034	3.92	-0.06	6038 ⁺⁹² ₋₁₁₈	3.79 ^{+0.14} _{-0.19}	-0.03 ^{+0.47} _{-0.47}	1.18 ^{+0.17} _{-0.11}	2.33 ^{+0.58} _{-0.49}	3.34 ^{+2.93} _{-1.31}	0.13 ± 0.08
K03158 ^{††}	6278762	289.752289	41.634605	8.72	5105	5106 ⁺⁷² ₋₆₄	4.56 ^{+0.05} _{-0.05}	0.14 ^{+0.41} _{-0.36}	0.86 ^{+0.05} _{-0.07}	0.81 ^{+0.05} _{-0.07}	0.39 ^{+0.07} _{-0.07}	2.30 ± 0.56
K03196 ^{††}	9002538	283.350464	45.339111	11.53	6408	...	-0.07	6490 ⁺⁴³⁶ ₋₄₀₄	4.33 ^{+0.05} _{-0.07}	-0.03 ^{+0.46} _{-0.40}	1.04 ^{+0.22} _{-0.12}	1.17 ^{+0.16} _{-0.12}	1.45 ^{+1.08} _{-0.51}	0.90 ± 0.36
K03384 ^{††}	8644365	298.095428	44.737061	13.20	5962	...	-0.18	6092 ⁺⁴⁵⁶ ₋₄₅₁	4.35 ^{+0.09} _{-0.09}	-0.10 ^{+0.48} _{-0.41}	1.00 ^{+0.17} _{-0.12}	1.10 ^{+0.20} _{-0.17}	1.23 ^{+0.83} _{-0.45}	1.05 ± 0.54
K03398 ^{††}	3561464	295.498108	38.644501	13.49	6483	...	-0.43	6578 ⁺⁴³⁹ ₋₄₄₃	4.32 ^{+0.05} _{-0.14}	-0.35 ^{+0.47} _{-0.47}	1.00 ^{+0.23} _{-0.12}	1.16 ^{+0.25} _{-0.13}	1.61 ^{+1.34} _{-0.55}	0.89 ± 0.46
K03403 ^{††}	11754430	286.646423	49.937778	13.10	6011	...	-0.15	6167 ⁺⁴¹⁶ ₋₄₄₂	4.33 ^{+0.11} _{-0.15}	-0.05 ^{+0.46} _{-0.44}	1.02 ^{+0.20} _{-0.17}	1.15 ^{+0.26} _{-0.17}	1.35 ^{+1.08} _{-0.53}	0.95 ± 0.55
K03425 ^{††}	9117416	300.316193	45.495380	13.27	5133	5243 ⁺⁴²¹ ₋₄₀₆	4.52 ^{+0.11} _{-0.36}	0.05 ^{+0.47} _{-0.45}	0.89 ^{+0.16} _{-0.13}	0.86 ^{+0.49} _{-0.27}	0.53 ^{+1.02} _{-0.27}	1.97 ± 2.25
K03500 ^{††}	6058816	296.354614	41.335560	13.21	6086	...	-0.26	6187 ⁺⁴⁹² ₋₄₁₉	4.34 ^{+0.13} _{-0.11}	-0.19 ^{+0.49} _{-0.47}	1.00 ^{+0.17} _{-0.12}	1.12 ^{+0.18} _{-0.13}	1.29 ^{+0.98} _{-0.49}	1.01 ± 0.49
K03681 ^{††}	2581316	292.627472	37.860142	11.69	6294	6302 ⁺¹⁹¹ ₋₁₈₅	4.25 ^{+0.09} _{-0.09}	0.11 ^{+0.42} _{-0.46}	1.05 ^{+0.21} _{-0.13}	1.29 ^{+0.18} _{-0.13}	1.71 ^{+0.88} _{-0.53}	0.70 ± 0.27
K03864 ^{††}	4164922	293.344971	39.257809	12.91	5013	...	-0.26	5030 ⁺⁴⁸³ ₋₄₀₈	4.62 ^{+0.07} _{-0.11}	-0.18 ^{+0.45} _{-0.47}	0.78 ^{+0.12} _{-0.10}	0.72 ^{+0.15} _{-0.14}	0.30 ^{+0.28} _{-0.14}	2.96 ± 1.58
K04021 ^{††}	11967788	294.034363	50.371651	13.17	6456	...	-0.17	6473 ⁺¹⁷⁶ ₋₁₅₃	4.25 ^{+0.06} _{-0.08}	-0.09 ^{+0.47} _{-0.46}	1.05 ^{+0.22} _{-0.12}	1.27 ^{+0.18} _{-0.11}	1.85 ^{+1.11} _{-0.58}	0.72 ± 0.28
K04032 ^{††}	7100673	285.728485	42.654530	12.64	5730	...	-0.26	5907 ⁺⁴⁷¹ ₋₄₄₃	4.36 ^{+0.16} _{-0.11}	-0.13 ^{+0.47} _{-0.43}	0.98 ^{+0.15} _{-0.12}	1.08 ^{+0.22} _{-0.21}	1.10 ^{+0.87} _{-0.46}	1.10 ± 0.68
K04097 ^{††}	5688683	285.690002	40.994530	13.44	4350	...	-0.18	4259 ⁺⁴¹⁹ ₋₄₂₄	4.73 ^{+0.03} _{-0.04}	-0.17 ^{+0.49} _{-0.40}	0.61 ^{+0.09} _{-0.07}	0.56 ^{+0.06} _{-0.04}	0.09 ^{+0.07} _{-0.04}	4.97 ± 1.60
K04269 ^{††}	8890924	293.796844	45.160728	13.26	5106	...	-0.04	5165 ⁺⁴³¹ ₋₄₂₆	4.58 ^{+0.08} _{-0.22}	0.02 ^{+0.45} _{-0.41}	0.85 ^{+0.14} _{-0.12}	0.78 ^{+0.28} _{-0.11}	0.40 ^{+0.49} _{-0.18}	2.47 ± 1.90
K04288 ^{††}	4548011	287.371246	39.603569	12.40	6207	...	-0.08	6299 ⁺⁴⁵⁶ ₋₄₁₅	4.33 ^{+0.66} _{-0.09}	0.02 ^{+0.42} _{-0.46}	1.03 ^{+0.21} _{-0.13}	1.16 ^{+0.21} _{-0.13}	1.41 ^{+1.08} _{-0.52}	0.92 ± 0.43

Note. — Columns marked with a [†] are values from NASA Exoplanet Archive. Stars marked with a ^{††} have missing T_{eff} . Their T_{eff} values are estimated based on $g - r$ and $g - i$ values (Pinsonneault et al. 2012), the adopted T_{eff} is the average of the results. There are three exceptions, values of T_{eff} for K03158 and K0368 are adopted from Ammons et al. (2006) and T_{eff} for K04021 is based on the infrared flux method in Pinsonneault et al. (2012)

Table 3. Orbital Parameters

KOI	KIC	T_0 (BKJD)	Period (d)	Impact Parameter	R_{PL}/R_*	e	ω (radian)	R_{PL} (R_{\oplus})	Inclination (deg)	a/R_*	a (AU)	T_{PL} (K)	Depth (ppm)	Dur (hr)	Sig (σ)	p1	p2
K00005.01	8554498	132.9733	4.78033 ^{+0.00001} _{-0.0001}	0.93 ^{+0.01} _{-0.01}	0.045 ^{+0.001} _{-0.002}	0.00 ^{+0.02} _{-0.00}	0.00 ^{+0.13} _{-0.00}	8.07 ± 0.64	82.72 ^{+0.61} _{-0.46}	7.6 ^{+0.5} _{-0.4}	0.059 ± 0.002	1434 ± 45	983 ± 3	2.3	5.1	0.932	0.997
K00005.02	8554498	133.3670	7.05186 ^{+0.00000} _{-0.00000}	0.92 ^{+0.16} _{-0.17}	0.003 ^{+0.001} _{-0.001}	0.00 ^{+0.00} _{-0.00}	0.04 ^{+0.05} _{-0.04}	0.51 ± 0.26	85.30 ^{+0.72} _{-0.60}	11.2 ^{+1.0} _{-1.0}	0.075 ± 0.002	1159 ± 69	12 ± 4	1.9	0.4	0.015	0.278
K00041.01	6521045	122.9506	12.81574 ^{+0.00004} _{-0.00005}	0.57 ^{+0.20} _{-0.55}	0.014 ^{+0.001} _{-0.001}	0.00 ^{+0.30} _{-0.00}	0.00 ^{+0.88} _{-0.00}	3.08 ± 0.74	87.33 ^{+2.57} _{-2.06}	12.0 ^{+2.5} _{-2.4}	0.114 ± 0.005	1120 ± 130	219 ± 5	6.7	1.5	0.615	0.988
K00041.02	6521045	133.1758	6.88710 ^{+0.00016} _{-0.00015}	0.90 ^{+0.02} _{-0.09}	0.009 ^{+0.001} _{-0.001}	0.11 ^{+0.19} _{-0.11}	0.01 ^{+0.11} _{-0.01}	3.13 ± 0.58	81.11 ^{+1.65} _{-1.50}	5.4 ^{+1.3} _{-0.5}	0.076 ± 0.003	1628 ± 119	72 ± 4	4.4	0.3	0.067	0.783
K00041.03	6521045	153.9839	35.33314 ^{+0.00109} _{-0.00204}	0.93 ^{+0.10} _{-0.14}	0.012 ^{+0.000} _{-0.003}	0.00 ^{+0.22} _{-0.00}	0.00 ^{+3.09} _{-0.55}	3.78 ± 0.88	86.88 ^{+0.83} _{-0.78}	17.0 ^{+4.8} _{-2.4}	0.226 ± 0.010	947 ± 106	96 ± 10	6.3	1.0	0.077	0.807
K00070.01	6850504	138.6075	10.85409 ^{+0.00002} _{-0.00003}	0.31 ^{+0.26} _{-0.31}	0.028 ^{+0.002} _{-0.001}	0.00 ^{+0.41} _{-0.00}	0.16 ^{+3.20} _{-0.16}	2.94 ± 0.26	89.13 ^{+0.87} _{-0.87}	20.4 ^{+1.1} _{-1.2}	0.092 ± 0.003	803 ± 32	1060 ± 9	4.0	0.5	0.959	0.999
K00070.02	6850504	134.5009	3.69612 ^{+0.00002} _{-0.00002}	0.36 ^{+0.17} _{-0.36}	0.017 ^{+0.001} _{-0.001}	0.00 ^{+0.27} _{-0.00}	0.00 ^{+0.24} _{-0.00}	1.77 ± 0.18	87.96 ^{+2.04} _{-1.23}	10.1 ^{+0.7} _{-0.7}	0.045 ± 0.002	1140 ± 53	400 ± 5	2.7	1.7	0.821	0.996
K00070.03	6850504	164.7276	77.61153 ^{+0.00017} _{-0.00022}	0.32 ^{+0.21} _{-0.32}	0.026 ^{+0.001} _{-0.000}	0.00 ^{+0.07} _{-0.00}	0.00 ^{+0.23} _{-0.00}	2.68 ± 0.27	89.76 ^{+0.24} _{-0.18}	77.4 ^{+6.0} _{-6.4}	0.341 ± 0.012	409 ± 20	834 ± 28	7.4	0.5	0.549	0.984
K00070.04	6850504	135.9338	6.09850 ^{+0.00018} _{-0.00022}	0.07 ^{+0.59} _{-0.07}	0.008 ^{+0.000} _{-0.002}	0.52 ^{+0.19} _{-0.50}	3.16 ^{+1.61} _{-2.67}	0.82 ± 0.13	89.70 ^{+0.30} _{-2.46}	14.3 ^{+1.2} _{-1.1}	0.063 ± 0.002	951 ± 54	74 ± 7	2.8	0.3	0.037	0.657
K00070.05	6850504	135.2142	19.57709 ^{+0.00077} _{-0.00066}	0.34 ^{+0.44} _{-0.31}	0.009 ^{+0.002} _{-0.001}	0.01 ^{+0.37} _{-0.01}	0.00 ^{+1.02} _{-0.00}	0.89 ± 0.16	89.37 ^{+0.58} _{-0.83}	31.0 ^{+2.4} _{-2.5}	0.136 ± 0.005	646 ± 35	104 ± 13	4.5	1.5	0.023	0.538
K00072.01	11904151	131.5744	0.83749 ^{+0.00000} _{-0.00000}	0.00 ^{+0.00} _{-0.00}	0.011 ^{+0.001} _{-0.001}	0.00 ^{+0.00} _{-0.00}	0.00 ^{+0.50} _{-0.00}	1.25 ± 0.13	90.00 ^{+0.00} _{-3.73}	3.4 ^{+1.2} _{-0.2}	0.016 ± 0.001	2068 ± 92	190 ± 1	2.0	5.5	0.936	0.997
K00072.02	11904151	138.6781	45.29404 ^{+0.00011} _{-0.00011}	0.00 ^{+0.39} _{-0.00}	0.020 ^{+0.001} _{-0.000}	0.00 ^{+0.11} _{-0.00}	0.00 ^{+0.24} _{-0.00}	2.10 ± 0.18	90.00 ^{+0.00} _{-0.48}	50.5 ^{+3.4} _{-3.9}	0.230 ± 0.009	527 ± 21	480 ± 13	7.0	0.6	0.775	0.989
K00082.01	10187017	134.7534	16.14569 ^{+0.00003} _{-0.00003}	0.25 ^{+0.31} _{-0.28}	0.026 ^{+0.003} _{-0.003}	0.00 ^{+0.40} _{-0.00}	0.00 ^{+4.10} _{-0.23}	2.19 ± 0.18	89.56 ^{+0.44} _{-0.34}	32.0 ^{+1.6} _{-1.6}	0.117 ± 0.003	579 ± 26	974 ± 7	3.9	1.1	0.974	0.999
K00082.02	10187017	134.0798	10.31173 ^{+0.00006} _{-0.00010}	0.28 ^{+0.26} _{-0.28}	0.014 ^{+0.002} _{-0.000}	0.00 ^{+0.23} _{-0.00}	0.00 ^{+0.17} _{-0.00}	1.19 ± 0.12	89.31 ^{+0.69} _{-0.72}	24.1 ^{+1.8} _{-1.5}	0.086 ± 0.002	669 ± 32	276 ± 5	3.2	0.5	0.637	0.989
K00082.03	10187017	145.0258	27.45362 ^{+0.00070} _{-0.00064}	0.02 ^{+0.59} _{-0.02}	0.010 ^{+0.001} _{-0.000}	0.34 ^{+0.30} _{-0.33}	0.26 ^{+3.23} _{-0.26}	0.82 ± 0.12	89.97 ^{+0.03} _{-0.75}	46.8 ^{+4.1} _{-3.7}	0.166 ± 0.004	476 ± 27	145 ± 9	3.9	0.7	0.066	0.779
K00082.04	10187017	139.9875	7.07134 ^{+0.00019} _{-0.00019}	0.22 ^{+0.22} _{-0.22}	0.008 ^{+0.001} _{-0.001}	0.00 ^{+0.00} _{-0.00}	0.00 ^{+0.00} _{-0.00}	0.64 ± 0.08	89.34 ^{+1.12} _{-0.99}	19.0 ^{+1.5} _{-1.5}	0.067 ± 0.002	749 ± 41	79 ± 5	2.8	0.6	0.068	0.784
K00082.05	10187017	135.8466	5.28698 ^{+0.00020} _{-0.00020}	0.68 ^{+1.07} _{-0.04}	0.006 ^{+0.034} _{-0.000}	0.00 ^{+0.14} _{-0.00}	0.02 ^{+1.57} _{-0.00}	0.51 ± 1.43	87.09 ^{+0.09} _{-3.30}	15.5 ^{+1.4} _{-1.3}	0.055 ± 0.001	890 ± 67	41 ± 4	2.2	0.6	0.038	0.665
K00085.01	5866724	132.0395	5.85993 ^{+0.00002} _{-0.00002}	0.53 ^{+0.53} _{-0.53}	0.020 ^{+0.004} _{-0.004}	0.77 ^{+0.58} _{-0.58}	4.60 ^{+1.44} _{-1.44}	2.60 ± 0.47	87.36 ^{+0.61} _{-0.61}	11.8 ^{+1.0} _{-1.0}	0.067 ± 0.003	1203 ± 74	321 ± 3	4.4	5.2	0.939	0.999
K00085.02	5866724	133.4963	2.15492 ^{+0.00013} _{-0.00011}	0.00 ^{+0.37} _{-0.00}	0.009 ^{+0.000} _{-0.000}	0.00 ^{+0.14} _{-0.00}	0.01 ^{+1.78} _{-0.01}	1.29 ± 0.13	90.00 ^{+0.00} _{-3.96}	5.5 ^{+0.4} _{-0.3}	0.035 ± 0.001	1786 ± 82	99 ± 2	3.2	3.7	0.657	0.990
K00085.03	5866724	137.9953	8.13115 ^{+0.00009} _{-0.00006}	0.62 ^{+0.13} _{-0.13}	0.010 ^{+0.000} _{-0.000}	0.00 ^{+0.61} _{-0.00}	0.00 ^{+1.45} _{-0.23}	1.62 ± 0.13	86.86 ^{+2.45} _{-1.00}	12.7 ^{+0.5} _{-0.5}	0.085 ± 0.003	1215 ± 52	116 ± 4	4.3	1.6	0.382	0.969
K00089.01	8056665	150.5651	84.68895 ^{+0.00010} _{-0.00010}	0.54 ^{+0.54} _{-0.54}	0.017 ^{+0.002} _{-0.001}	0.00 ^{+0.57} _{-0.00}	0.00 ^{+0.79} _{-0.00}	4.97 ± 1.65	89.29 ^{+0.62} _{-0.62}	38.1 ^{+10.0} _{-11.0}	0.473 ± 0.014	775 ± 120	402 ± 17	12.6	0.7	0.019	0.323
K00089.02	8056665	289.8688	207.60349 ^{+0.00047} _{-0.00036}	0.94 ^{+1.41} _{-1.10}	0.032 ^{+0.000} _{-0.013}	0.01 ^{+0.66} _{-0.01}	0.00 ^{+1.57} _{-0.00}	10.66 ± 3.82	89.24 ^{+0.27} _{-0.61}	61.6 ^{+20.4} _{-16.2}	0.861 ± 0.023	608 ± 98	490 ± 33	9.6	0.6	0.038	0.495
K00094.01	6462863	132.7405	22.34300 ^{+0.00001} _{-0.00001}	0.45 ^{+0.20} _{-0.20}	0.069 ^{+0.001} _{-0.001}	0.00 ^{+0.00} _{-0.00}	0.00 ^{+0.00} _{-0.00}	10.51 ± 0.97	88.93 ^{+0.46} _{-0.46}	24.3 ^{+1.5} _{-1.5}	0.158 ± 0.007	833 ± 35	5426 ± 27	6.8	13.6	0.978	1.000
K00094.02	6462863	138.0072	10.42371 ^{+0.00003} _{-0.00003}	0.40 ^{+0.40} _{-0.40}	0.026 ^{+0.000} _{-0.001}	0.00 ^{+0.10} _{-0.00}	0.00 ^{+0.44} _{-0.00}	3.98 ± 0.32	88.36 ^{+1.64} _{-0.00}	14.5 ^{+0.8} _{-0.8}	0.095 ± 0.004	1078 ± 39	769 ± 11	5.1	3.0	0.246	0.942
K00094.03	6462863	161.2400	54.31993 ^{+0.00006} _{-0.00019}	0.39 ^{+0.20} _{-0.21}	0.043 ^{+0.003} _{-0.000}	0.00 ^{+0.09} _{-0.04}	0.00 ^{+0.16} _{-0.19}	6.60 ± 0.60	89.49 ^{+0.37} _{-0.32}	44.0 ^{+2.6} _{-2.6}	0.285 ± 0.012	614 ± 27	2494 ± 37	8.9	3.7	0.464	0.977
K00094.04	6462863	131.6139	3.74324 ^{+0.00006} _{-0.00009}	0.00 ^{+0.21} _{-0.00}	0.010 ^{+0.000} _{-0.001}	0.00 ^{+0.04} _{-0.00}	0.00 ^{+0.00} _{-0.00}	1.49 ± 0.15	90.00 ^{+0.00} _{-1.65}	7.3 ^{+0.5} _{-0.4}	0.048 ± 0.002	1513 ± 61	125 ± 7	3.9	1.7	0.085	0.823
K00102.01	8456679	135.0591	1.73514 ^{+0.00000} _{-0.00000}	0.56 ^{+0.03} _{-0.03}	0.034 ^{+0.000} _{-0.000}	0.78 ^{+0.04} _{-0.09}	4.70 ^{+0.06} _{-0.06}	3.85 ± 0.38	84.57 ^{+0.77} _{-0.76}	5.9 ^{+0.4} _{-0.4}	0.028 ± 0.001	1592 ± 104	946 ± 3	2.7	27.2	0.906	0.996
K00102.02	8456679	132.2635	4.06853 ^{+0.00008} _{-0.00015}	0.51 ^{+0.49} _{-0.49}	0.008 ^{+0.009} _{-0.002}	0.71 ^{+0.71} _{-0.71}	3.62 ^{+3.60} _{-3.60}	0.94 ± 0.62	87.13 ^{+2.70} _{-1.79}	10.3 ^{+0.9} _{-0.8}	0.050 ± 0.002	1210 ± 73	98 ± 6	3.0	2.6	0.008	0.168
K00108.01	4914423	142.1763	15.96535 ^{+0.00006} _{-0.00006}	0.51 ^{+0.11} _{-0.32}	0.020 ^{+0.001} _{-0.001}	0.00 ^{+0.35} _{-0.00}	0.03 ^{+0.53} _{-0.03}	2.66 ± 0.28	88.69 ^{+0.87} _{-0.40}	22.3 ^{+1.7} _{-1.7}	0.128 ± 0.005	840 ± 42	492 ± 8	4.8	0.3	0.719	0.985
K00108.02	4914423	295.3304	179.60101 ^{+0.00008} _{-0.00003}	0.00 ^{+0.44} _{-0.00}	0.032 ^{+0.002} _{-0.002}	0.00 ^{+0.00} _{-0.00}	0.00 ^{+0.00} _{-0.00}	4.38 ± 0.45	90.00 ^{+0.00} _{-0.25}	109.4 ^{+6.8} _{-5.3}	0.647 ± 0.025	382 ± 16	1296 ± 35	13.0	0.8	0.171	0.838
K00111.01	6678383	137.6139	11.42751 ^{+0.00004} _{-0.00005}	0.00 ^{+0.41} _{-0.40}	0.020 ^{+0.001} _{-0.001}	0.00 ^{+0.24} _{-0.00}	0.01 ^{+3.85} _{-0.01}	2.21 ± 0.19	90.00 ^{+0.00} _{-1.32}	19.5 ^{+1.4} _{-1.1}	0.092 ± 0.004	871 ± 35	509 ± 8	4.7	1.8	0.752	0.993
K00111.02	6678383	132.7129	23.66834 ^{+0.00011} _{-0.00011}	0.00 ^{+0.42} _{-0.00}	0.019 ^{+0.001} _{-0.000}	0.00 ^{+0.08} _{-0.00}	0.00 ^{+1.38} _{-0.00}	2.07 ± 0.17	90.00 ^{+0.00} _{-0.81}	32.5 ^{+1.9} _{-2.0}	0.149 ± 0.005	673 ± 27	480 ± 12	5.8	1.1	0.550	0.984
K00111.03	6678383	271.0832	51.75627 ^{+0.00023} _{-0.00024}	0.00 ^{+0.45} _{-0.00}	0.022 ^{+0.002} _{-0.000}	0.00 ^{+0.02} _{-0.00}	0.04 ^{+3.87} _{-0.49}	2.31 ± 0.22	90.00 ^{+0.00} _{-0.49}	56.2 ^{+4.0} _{-4.1}	0.251 ± 0.010	510 ± 25	621 ± 19	7.3	0.3	0.464	0.977
K00112.01	10984090	185.1795	51.07931 ^{+0.00014} _{-0.00022}	0.24 ^{+0.14} _{-0.21}	0.024 ^{+0.001} _{-0.002}	0.05 ^{+0.22} _{-0.05}	0.00 ^{+0.29} _{-0.00}	2.55 ± 0.24	89.76 ^{+0.24} _{-0.15}	58.0 ^{+4.0} _{-4.4}	0.262 ± 0.011	512 ± 24	749 ± 19	6.7	0.4		

Table 3—Continued

KOI	KIC	T_0 (BKJD)	Period (d)	Impact Parameter	R_{PL}/R_*	e	ω (radian)	R_{PL} (R_{\oplus})	Inclination (deg)	a/ R_*	a (AU)	T_{PL} (K)	Depth (ppm)	Dur (hr)	Sig (σ)	p1	p2
K00124.01	11086270	137.1212	12.69115 ^{+0.00020} _{-0.00014}	0.85 ^{+0.04} _{-0.16}	0.016 ^{+0.000} _{-0.002}	0.06 ^{+0.56} _{-0.06}	0.00 ^{+1.01} _{-0.16}	2.98 ± 0.33	86.46 ^{+0.92} _{-0.58}	14.0 ^{+1.1} _{-1.1}	0.108 ± 0.002	1056 ± 53	256 ± 9	4.0	1.0	0.421	0.948
K00124.02	11086270	142.8190	31.71987 ^{+0.00025} _{-0.00034}	0.86 ^{+0.05} _{-0.08}	0.020 ^{+0.001} _{-0.001}	0.00 ^{+0.18} _{-0.00}	0.00 ^{+0.50} _{-0.00}	3.57 ± 0.43	88.10 ^{+0.39} _{-0.37}	26.1 ^{+2.6} _{-1.9}	0.200 ± 0.004	771 ± 50	369 ± 15	5.2	0.4	0.363	0.934
K00139.01	8559644	142.0874	224.79712 ^{+0.00003} _{-0.00001}	0.18 ^{+0.42} _{-0.18}	0.047 ^{+0.009} _{-0.001}	0.00 ^{+0.03} _{-0.00}	0.10 ^{+4.60} _{-0.10}	5.83 ± 0.80	89.93 ^{+0.07} _{-0.19}	141.8 ^{+12.4} _{-10.4}	0.749 ± 0.028	330 ± 19	3395 ± 68	12.4	0.8	0.422	0.948
K00139.02	8559644	141.3521	3.34184 ^{+0.00005} _{-0.00007}	0.00 ^{+0.41} _{-0.00}	0.011 ^{+0.000} _{-0.000}	0.00 ^{+0.08} _{-0.00}	0.00 ^{+0.19} _{-0.00}	1.39 ± 0.15	90.00 ^{+0.00} _{-3.08}	8.2 ^{+0.6} _{-0.4}	0.045 ± 0.002	1387 ± 64	167 ± 7	3.2	0.5	0.197	0.860
K00148.01	5735762	124.0630	4.77798 ^{+0.00003} _{-0.00004}	0.20 ^{+0.31} _{-0.20}	0.018 ^{+0.001} _{-0.000}	0.00 ^{+0.10} _{-0.00}	0.00 ^{+0.36} _{-0.00}	1.75 ± 0.17	89.07 ^{+0.93} _{-1.67}	12.4 ^{+0.8} _{-0.9}	0.052 ± 0.002	992 ± 48	489 ± 8	3.0	2.1	0.352	0.964
K00148.02	5735762	125.3398	9.67393 ^{+0.00003} _{-0.00003}	0.39 ^{+0.19} _{-0.37}	0.027 ^{+0.002} _{-0.001}	0.00 ^{+0.11} _{-0.00}	0.00 ^{+0.34} _{-0.00}	2.60 ± 0.26	88.89 ^{+1.07} _{-0.71}	20.1 ^{+1.4} _{-1.3}	0.083 ± 0.003	772 ± 37	987 ± 12	3.5	2.3	0.632	0.988
K00148.03	5735762	146.0657	42.89592 ^{+0.00051} _{-0.00048}	0.19 ^{+0.35} _{-0.19}	0.021 ^{+0.002} _{-0.000}	0.00 ^{+0.31} _{-0.00}	0.00 ^{+0.31} _{-0.00}	1.97 ± 0.21	89.80 ^{+0.20} _{-0.40}	54.5 ^{+4.8} _{-4.1}	0.224 ± 0.009	467 ± 25	599 ± 28	6.0	1.1	0.089	0.830
K00153.01	12252424	139.7122	8.92511 ^{+0.00005} _{-0.00005}	0.63 ^{+0.13} _{-0.09}	0.034 ^{+0.004} _{-0.002}	0.50 ^{+0.26} _{-0.27}	4.24 ^{+0.46} _{-1.97}	2.86 ± 0.67	88.21 ^{+0.56} _{-0.75}	20.9 ^{+4.3} _{-3.1}	0.077 ± 0.002	698 ± 78	997 ± 15	3.1	1.0	0.871	0.994
K00153.02	12252424	128.5467	4.75399 ^{+0.00002} _{-0.00002}	0.38 ^{+0.24} _{-0.38}	0.023 ^{+0.001} _{-0.001}	0.00 ^{+0.35} _{-0.00}	0.00 ^{+1.44} _{-0.00}	2.12 ± 0.28	88.28 ^{+1.72} _{-1.47}	12.9 ^{+1.3} _{-1.2}	0.050 ± 0.001	883 ± 57	780 ± 10	2.7	0.5	0.889	0.995
K00159.01	8972058	136.7363	8.99092 ^{+0.00001} _{-0.00001}	0.59 ^{+0.20} _{-0.57}	0.020 ^{+0.002} _{-0.001}	0.00 ^{+0.39} _{-0.00}	0.00 ^{+0.73} _{-0.00}	3.14 ± 0.65	87.39 ^{+2.52} _{-1.86}	12.8 ^{+2.5} _{-2.1}	0.087 ± 0.003	1120 ± 123	466 ± 12	4.4	0.5	0.306	0.917
K00159.02	8972058	134.7278	2.40365 ^{+0.00002} _{-0.00002}	0.93 ^{+0.03} _{-0.04}	0.013 ^{+0.003} _{-0.003}	0.05 ^{+0.05} _{-0.05}	0.17 ^{+0.17} _{-0.17}	2.41 ± 0.34	78.01 ^{+1.48} _{-2.03}	4.5 ^{+0.4} _{-0.4}	0.036 ± 0.001	1905 ± 100	82 ± 6	1.7	0.6	0.090	0.711
K00168.01	11512246	133.2871	10.74245 ^{+0.00006} _{-0.00006}	0.37 ^{+0.41} _{-0.37}	0.016 ^{+0.004} _{-0.000}	0.00 ^{+0.19} _{-0.00}	0.00 ^{+0.50} _{-0.00}	3.79 ± 1.14	87.97 ^{+2.03} _{-3.91}	10.1 ^{+2.2} _{-2.5}	0.100 ± 0.003	1258 ± 158	426 ± 13	7.4	0.2	0.332	0.961
K00168.02	11512246	147.5788	15.27448 ^{+0.00046} _{-0.00040}	0.00 ^{+0.69} _{-0.23}	0.011 ^{+0.003} _{-0.002}	0.08 ^{+0.39} _{-0.06}	1.93 ^{+2.10} _{-0.93}	2.26 ± 0.66	89.98 ^{+0.02} _{-3.15}	14.0 ^{+2.7} _{-3.2}	0.126 ± 0.004	1062 ± 138	210 ± 17	7.5	0.4	0.157	0.903
K00168.03	11512246	138.3254	7.10690 ^{+0.00029} _{-0.00022}	0.18 ^{+0.40} _{-0.18}	0.008 ^{+0.002} _{-0.001}	0.04 ^{+0.18} _{-0.04}	0.02 ^{+0.35} _{-0.02}	1.91 ± 0.54	88.79 ^{+1.21} _{-3.31}	7.8 ^{+1.9} _{-1.7}	0.076 ± 0.002	1404 ± 188	107 ± 11	6.4	0.1	0.093	0.837
K00244.01	4349452	178.5274	12.72036 ^{+0.00002} _{-0.00002}	0.92 ^{+0.07} _{-0.02}	0.039 ^{+0.002} _{-0.001}	0.01 ^{+0.18} _{-0.01}	0.00 ^{+0.81} _{-0.00}	7.06 ± 0.63	86.47 ^{+0.32} _{-0.58}	14.6 ^{+1.0} _{-0.9}	0.113 ± 0.003	1046 ± 40	1183 ± 4	3.1	37.2	0.973	0.999
K00244.02	4349452	171.7046	6.23856 ^{+0.00001} _{-0.00001}	0.68 ^{+0.68} _{-0.68}	0.019 ^{+0.001} _{-0.003}	0.00 ^{+0.45} _{-0.00}	0.00 ^{+0.15} _{-0.00}	3.50 ± 0.48	85.83 ^{+1.17} _{-1.20}	9.0 ^{+0.9} _{-0.8}	0.070 ± 0.002	1327 ± 85	421 ± 3	3.9	15.9	0.953	0.998
K00245.01	8478994	175.2497	39.79219 ^{+0.00006} _{-0.00006}	0.50 ^{+0.09} _{-0.50}	0.028 ^{+0.000} _{-0.001}	0.00 ^{+0.45} _{-0.00}	0.00 ^{+0.15} _{-0.00}	1.92 ± 0.19	89.51 ^{+0.49} _{-0.12}	58.6 ^{+4.8} _{-4.7}	0.217 ± 0.008	460 ± 24	607 ± 5	4.7	7.1	0.947	0.999
K00245.02	8478994	191.8385	21.30185 ^{+0.00019} _{-0.00019}	0.35 ^{+0.35} _{-0.35}	0.002 ^{+0.000} _{-0.000}	0.20 ^{+0.20} _{-0.20}	3.50 ^{+3.46} _{-3.46}	0.70 ± 0.11	89.47 ^{+0.45} _{-0.45}	38.5 ^{+3.2} _{-3.2}	0.143 ± 0.005	568 ± 30	91 ± 4	4.2	3.3	0.196	0.924
K00245.03	8478994	184.0333	13.36727 ^{+0.00042} _{-0.00061}	0.80 ^{+0.43} _{-0.43}	0.004 ^{+0.003} _{-0.001}	0.00 ^{+0.05} _{-0.00}	0.16 ^{+0.86} _{-0.16}	0.37 ± 0.21	88.40 ^{+0.95} _{-0.80}	28.4 ^{+2.5} _{-2.2}	0.105 ± 0.003	657 ± 38	17 ± 3	2.2	1.1	0.044	0.699
K00245.04	8478994	195.7268	51.19880 ^{+0.00016} _{-0.02033}	0.68 ^{+0.81} _{-0.68}	0.004 ^{+0.007} _{-0.002}	0.24 ^{+0.20} _{-0.24}	0.06 ^{+0.26} _{-0.06}	0.34 ± 0.36	89.45 ^{+0.55} _{-0.64}	69.9 ^{+5.8} _{-5.8}	0.256 ± 0.009	415 ± 23	15 ± 7	4.1	0.3	0.044	0.699
K00246.01	11295426	173.8571	5.39877 ^{+0.00001} _{-0.00001}	0.38 ^{+0.20} _{-0.93}	0.016 ^{+0.002} _{-0.000}	0.00 ^{+0.40} _{-0.00}	0.00 ^{+4.72} _{-0.00}	2.20 ± 0.13	87.98 ^{+0.18} _{-1.10}	10.7 ^{+0.2} _{-0.1}	0.061 ± 0.001	1177 ± 12	349 ± 2	3.6	8.4	0.972	0.999
K00246.02	11295426	136.3854	9.60487 ^{+0.00021} _{-0.00029}	0.44 ^{+0.03} _{-0.16}	0.007 ^{+0.001} _{-0.001}	0.45 ^{+0.26} _{-0.25}	2.02 ^{+2.29} _{-1.79}	0.92 ± 0.13	88.41 ^{+0.59} _{-0.95}	15.7 ^{+0.2} _{-0.3}	0.090 ± 0.001	967 ± 10	58 ± 3	2.9	0.7	0.094	0.721
K00260.01	8292840	172.7904	10.49570 ^{+0.00010} _{-0.00005}	0.65 ^{+0.04} _{-0.04}	0.010 ^{+0.000} _{-0.000}	0.00 ^{+0.40} _{-0.00}	0.00 ^{+0.21} _{-0.00}	1.79 ± 0.17	86.86 ^{+0.94} _{-0.94}	13.5 ^{+1.0} _{-1.0}	0.101 ± 0.003	1185 ± 56	119 ± 3	5.2	1.6	0.300	0.955
K00260.02	8292840	245.0413	100.28340 ^{+0.00028} _{-0.00085}	0.15 ^{+0.41} _{-0.15}	0.016 ^{+0.002} _{-0.001}	0.00 ^{+0.03} _{-0.00}	0.00 ^{+0.12} _{-0.00}	2.43 ± 0.29	89.87 ^{+0.13} _{-0.39}	69.6 ^{+6.0} _{-5.0}	0.447 ± 0.016	492 ± 25	326 ± 14	11.1	0.6	0.379	0.968
K00260.03	8292840	140.2944	21.86964 ^{+0.00018} _{-0.00023}	0.56 ^{+0.16} _{-0.23}	0.010 ^{+0.001} _{-0.001}	0.10 ^{+0.37} _{-0.10}	0.00 ^{+0.24} _{-0.00}	1.56 ± 0.19	88.66 ^{+0.62} _{-0.54}	24.6 ^{+2.2} _{-2.2}	0.162 ± 0.006	837 ± 42	127 ± 5	5.9	1.4	0.200	0.926
K00262.01	11807274	172.6319	7.81251 ^{+0.00011} _{-0.00011}	0.76 ^{+0.04} _{-0.04}	0.009 ^{+0.000} _{-0.000}	0.09 ^{+0.26} _{-0.09}	0.25 ^{+0.59} _{-0.25}	2.08 ± 0.23	84.82 ^{+0.67} _{-1.14}	9.7 ^{+0.8} _{-0.6}	0.082 ± 0.002	1388 ± 69	90 ± 3	4.8	0.6	0.316	0.920
K00262.02	11807274	136.9686	9.37614 ^{+0.00023} _{-0.00016}	0.94 ^{+0.04} _{-0.00}	0.015 ^{+0.000} _{-0.000}	0.00 ^{+0.08} _{-0.00}	0.00 ^{+0.70} _{-0.00}	3.52 ± 0.41	83.55 ^{+0.36} _{-0.81}	8.2 ^{+1.0} _{-1.0}	0.092 ± 0.003	1388 ± 68	94 ± 4	3.2	1.1	0.397	0.943
K00270.01	6528464	175.0152	12.58250 ^{+0.00011} _{-0.00013}	0.00 ^{+0.22} _{-0.00}	0.009 ^{+0.001} _{-0.000}	0.00 ^{+0.42} _{-0.00}	0.00 ^{+0.15} _{-0.00}	1.50 ± 0.14	90.00 ^{+0.00} _{-0.92}	14.6 ^{+1.3} _{-1.0}	0.104 ± 0.002	965 ± 51	108 ± 5	6.6	2.1	0.208	0.868
K00270.02	6528464	162.0396	33.67312 ^{+0.00039} _{-0.00022}	0.45 ^{+0.16} _{-0.45}	0.012 ^{+0.001} _{-0.000}	0.00 ^{+0.55} _{-0.00}	0.00 ^{+0.09} _{-0.00}	1.96 ± 0.20	89.07 ^{+0.93} _{-0.41}	28.2 ^{+2.2} _{-2.4}	0.200 ± 0.004	700 ± 36	165 ± 10	8.4	1.1	0.185	0.851
K00271.01	9451706	172.5460	48.63057 ^{+0.00009} _{-0.00014}	0.51 ^{+0.44} _{-0.44}	0.018 ^{+0.001} _{-0.001}	0.00 ^{+0.00} _{-0.00}	0.00 ^{+0.00} _{-0.00}	2.44 ± 0.26	89.37 ^{+0.24} _{-0.24}	47.0 ^{+1.3} _{-4.4}	0.274 ± 0.011	599 ± 32	358 ± 13	6.9	3.7	0.581	0.986
K00271.02	9451706	209.0731	29.39241 ^{+0.00009} _{-0.00013}	0.00 ^{+0.41} _{-0.00}	0.016 ^{+0.001} _{-0.000}	0.00 ^{+0.04} _{-0.00}	0.48 ^{+0.33} _{-0.48}	2.20 ± 0.22	90.00 ^{+0.00} _{-0.76}	32.9 ^{+2.3} _{-2.8}	0.196 ± 0.007	719 ± 34	316 ± 10	7.0	3.4	0.656	0.990
K00271.03	9451706	141.5109	14.43593 ^{+0.00034} _{-0.00039}	0.13 ^{+0.66} _{-0.13}	0.010 ^{+0.000} _{-0.002}	0.49 ^{+0.22} _{-0.10}	1.10 ^{+2.42} _{-1.10}	1.31 ± 0.21	89.65 ^{+0.35} _{-1.94}	21.1 ^{+1.8} _{-1.9}	0.122 ± 0.005	892 ± 56	105 ± 6	3.2	3.0	0.235	0.939
K00274.01	8077137	175.9276	15.09205 ^{+0.00088} _{-0.00060}	0.13 ^{+0.48} _{-0.13}	0.004 ^{+0.001} _{-0.001}	0.00 ^{+0.16} _{-0.00}	0.02 ^{+0.28} _{-0.02}	0.77 ± 0.13	89.57 ^{+0.43} _{-1.58}	17.1 ^{+1.7} _{-1.4}	0.127 ± 0.004	970 ± 64	24 ± 6	6.6	0.7	0.029	0.426
K00274.02	8077137	153.4920	22.79519 ^{+0.00089} _{-0.00132}	0.48 ^{+0.27} _{-0.48}	0.003 ^{+0.002} _{-0.000}	0.07 ^{+0.29} _{-0.07}	0.29 ^{+1.31} _{-0.29}	0.58 ± 0.23	88.80 ^{+1.01} _{-0.65}	22.4 ^{+2.2} _{-1.6}	0.167 ± 0.005	843 ± 54	18 ± 8	6.6	0.6	0.025	0.390
K00275.01	10586004	176.8205	15.79186 ^{+0.00009} _{-0.00009}	0.00 ^{+0.30} _{-0.00}	0.013 ^{+0.000} _{-0.000}	0.00 ^{+0.00} _{-0.00}	0.00 ^{+0.00} _{-0.00}	2.10 ± 0.24	90.00 ^{+0.00} _{-0.67}	18.9 ^{+1.9} _{-1.5}	0.129 ± 0.004	909 ± 47	206 ± 9	6.8	0.6	0.352	0.931
K00275.02	10586004	208.7874	82.19970 ^{+0.00024} _{-0.00026}	0.18 ^{+0.34} _{-0.18}	0.014 ^{+0.002} _{-0.000}	0.00 ^{+0.23} _{-0.00}	0.00 ^{+0.15} _{-0.00}	2.05 ± 0.24	89.82 ^{+0.18} _{-0.36}	59.6 ^{+5.1} _{-4.4}							

Table 3—Continued

KOI	KIC	T_0 (BKJD)	Period (d)	Impact Parameter	R_{PL}/R_*	e	ω (radian)	R_{PL} (R_{\oplus})	Inclination (deg)	a/ R_*	a (AU)	T_{PL} (K)	Depth (ppm)	Dur (hr)	Sig (σ)	p1	p2
K00285.01	6196457	179.2804	13.74878 ^{+0.00005} _{-0.00005}	0.59 ^{+0.08} _{-0.10}	0.022 ^{+0.000} _{-0.002}	0.48 ^{+0.17} _{-0.01}	4.47 ^{+0.69} _{-0.33}	3.95 ± 0.38	87.82 ^{+0.31} _{-0.53}	15.8 ^{+1.5} _{-1.1}	0.118 ± 0.003	990 ± 58	419 ± 7	6.3	1.0	0.830	0.996
K00285.02	6196457	147.9103	26.72428 ^{+0.00022} _{-0.00024}	0.52 ^{+0.10} _{-0.26}	0.016 ^{+0.002} _{-0.004}	0.87 ^{+0.03} _{-0.66}	4.67 ^{+0.38} _{-0.77}	2.79 ± 0.55	88.80 ^{+0.59} _{-0.30}	24.9 ^{+2.7} _{-1.9}	0.183 ± 0.006	784 ± 48	193 ± 11	9.9	0.5	0.391	0.970
K00285.03	6196457	134.2716	49.35899 ^{+0.00071} _{-0.00089}	0.52 ^{+0.39} _{-0.50}	0.011 ^{+0.001} _{-0.001}	0.00 ^{+0.28} _{-0.00}	0.00 ^{+3.79} _{-0.00}	1.96 ± 0.26	89.20 ^{+0.77} _{-0.65}	37.4 ^{+3.8} _{-2.9}	0.275 ± 0.008	640 ± 39	129 ± 16	8.8	0.5	0.070	0.789
K00289.01	10386922	138.7360	26.62940 ^{+0.00258} _{-0.00057}	0.65 ^{+0.20} _{-0.56}	0.021 ^{+0.002} _{-0.001}	0.00 ^{+0.24} _{-0.00}	0.00 ^{+0.72} _{-0.00}	4.51 ± 1.64	88.19 ^{+1.61} _{-1.62}	19.9 ^{+6.2} _{-6.2}	0.185 ± 0.017	854 ± 139	482 ± 16	7.8	0.1	0.508	0.963
K00289.02	10386922	403.6729	296.63709 ^{+0.00042} _{-0.00044}	0.65 ^{+0.22} _{-0.61}	0.051 ^{+0.003} _{-0.005}	0.09 ^{+0.35} _{-0.09}	1.65 ^{+0.76} _{-1.65}	9.86 ± 3.07	89.66 ^{+0.32} _{-0.33}	113.5 ^{+20.3} _{-34.9}	0.908 ± 0.062	366 ± 59	2838 ± 67	16.2	0.1	0.397	0.943
K00291.01	10933561	185.1521	31.51789 ^{+0.00028} _{-0.00028}	0.40 ^{+0.17} _{-0.40}	0.017 ^{+0.001} _{-0.001}	0.00 ^{+0.21} _{-0.00}	0.00 ^{+0.26} _{-0.00}	2.60 ± 0.30	89.21 ^{+0.79} _{-0.37}	30.1 ^{+2.6} _{-2.7}	0.194 ± 0.005	688 ± 41	361 ± 20	7.7	0.5	0.121	0.775
K00291.02	10933561	134.1052	8.12986 ^{+0.00017} _{-0.00014}	0.90 ^{+0.06} _{-0.02}	0.015 ^{+0.002} _{-0.001}	0.09 ^{+0.09} _{-0.09}	0.04 ^{+0.97} _{-0.04}	2.32 ± 0.31	85.40 ^{+0.46} _{-0.70}	11.7 ^{+1.1} _{-0.8}	0.079 ± 0.002	1107 ± 58	138 ± 9	2.7	1.1	0.119	0.772
K00295.01	11547513	171.8763	5.31743 ^{+0.00006} _{-0.00006}	0.94 ^{+0.01} _{-0.05}	0.020 ^{+0.003} _{-0.001}	0.00 ^{+0.06} _{-0.00}	0.00 ^{+0.52} _{-0.00}	6.23 ± 1.47	78.93 ^{+2.69} _{-1.83}	5.0 ^{+1.1} _{-0.8}	0.064 ± 0.009	1811 ± 216	288 ± 6	3.3	1.3	0.678	0.981
K00295.02	11547513	135.5088	10.10575 ^{+0.00030} _{-0.00030}	0.98 ^{+0.03} _{-0.03}	0.012 ^{+0.001} _{-0.001}	0.00 ^{+0.07} _{-0.00}	0.00 ^{+0.66} _{-0.00}	3.00 ± 1.15	83.90 ^{+0.95} _{-1.03}	9.1 ^{+1.6} _{-1.8}	0.096 ± 0.010	1298 ± 156	113 ± 8	2.3	0.7	0.124	0.779
K00298.01	12785320	178.3053	19.96000 ^{+0.00079} _{-0.00087}	0.93 ^{+0.50} _{-0.82}	0.008 ^{+0.006} _{-0.006}	0.00 ^{+0.03} _{-0.00}	0.20 ^{+0.34} _{-0.20}	1.00 ± 0.96	85.10 ^{+4.67} _{-2.90}	26.3 ^{+15.2} _{-10.1}	0.143 ± 0.010	1101 ± 1394	81 ± 17	5.4	0.2	0.039	0.505
K00298.02	12785320	170.7233	57.38425 ^{+0.00016} _{-0.00016}	0.67 ^{+0.18} _{-0.67}	0.014 ^{+0.004} _{-0.003}	0.00 ^{+0.59} _{-0.00}	0.00 ^{+0.47} _{-0.00}	1.71 ± 0.99	89.40 ^{+1.61} _{-0.61}	54.0 ^{+18.0} _{-20.5}	0.289 ± 0.019	455 ± 122	237 ± 27	5.2	0.7	0.025	0.386
K00301.01	3642289	171.7134	6.00255 ^{+0.00009} _{-0.00009}	0.30 ^{+0.11} _{-0.30}	0.012 ^{+0.001} _{-0.001}	0.00 ^{+0.28} _{-0.00}	0.00 ^{+1.15} _{-0.00}	1.96 ± 0.33	88.34 ^{+1.66} _{-0.82}	10.4 ^{+1.2} _{-1.5}	0.071 ± 0.003	1296 ± 96	199 ± 6	4.2	0.9	0.135	0.797
K00301.02	3642289	141.3742	11.44883 ^{+0.00048} _{-0.00048}	0.20 ^{+0.36} _{-0.36}	0.008 ^{+0.001} _{-0.001}	0.00 ^{+0.20} _{-0.00}	0.00 ^{+0.24} _{-0.00}	1.23 ± 0.35	89.29 ^{+0.71} _{-0.36}	15.7 ^{+4.2} _{-3.3}	0.109 ± 0.005	1040 ± 141	79 ± 9	5.3	0.3	0.016	0.291
K00304.01	6029239	174.9087	8.51205 ^{+0.00005} _{-0.00005}	0.95 ^{+0.35} _{-0.07}	0.027 ^{+0.003} _{-0.004}	0.08 ^{+0.31} _{-0.08}	0.00 ^{+1.49} _{-0.00}	6.02 ± 1.73	84.54 ^{+1.39} _{-6.28}	9.2 ^{+2.3} _{-2.1}	0.086 ± 0.003	1291 ± 177	588 ± 7	2.6	1.1	0.465	0.956
K00304.02	6029239	136.5633	5.51835 ^{+0.00019} _{-0.00022}	0.85 ^{+0.22} _{-0.22}	0.006 ^{+0.000} _{-0.003}	0.24 ^{+0.08} _{-0.24}	0.00 ^{+0.43} _{-0.00}	1.41 ± 0.47	83.05 ^{+2.84} _{-1.4}	6.7 ^{+1.8} _{-1.4}	0.064 ± 0.002	1535 ± 241	34 ± 6	3.5	0.3	0.020	0.341
K00307.01	6289257	176.2694	19.67423 ^{+0.00043} _{-0.00036}	0.60 ^{+0.15} _{-0.59}	0.013 ^{+0.002} _{-0.001}	0.27 ^{+0.27} _{-0.27}	0.38 ^{+1.14} _{-0.38}	1.56 ± 0.22	88.78 ^{+1.19} _{-0.40}	28.1 ^{+1.7} _{-2.1}	0.147 ± 0.006	765 ± 42	221 ± 11	4.1	1.9	0.079	0.681
K00307.02	6289257	131.5367	5.21106 ^{+0.00015} _{-0.00012}	0.44 ^{+0.13} _{-0.44}	0.009 ^{+0.007} _{-0.000}	0.43 ^{+0.46} _{-0.43}	3.66 ^{+1.14} _{-3.66}	1.09 ± 0.44	87.79 ^{+2.21} _{-0.89}	11.7 ^{+1.0} _{-1.0}	0.061 ± 0.003	1201 ± 71	103 ± 5	3.6	2.0	0.023	0.371
K00312.01	7050989	175.5857	11.57894 ^{+0.00010} _{-0.00010}	0.63 ^{+0.19} _{-0.19}	0.014 ^{+0.002} _{-0.002}	0.05 ^{+0.05} _{-0.05}	0.00 ^{+0.00} _{-0.00}	1.78 ± 0.26	88.15 ^{+0.55} _{-0.55}	18.9 ^{+1.8} _{-1.4}	0.106 ± 0.004	924 ± 53	236 ± 8	3.6	0.4	0.065	0.636
K00312.02	7050989	131.9683	16.39922 ^{+0.00015} _{-0.00010}	0.01 ^{+0.64} _{-0.01}	0.013 ^{+0.003} _{-0.002}	0.72 ^{+0.08} _{-0.61}	6.28 ^{+0.00} _{-6.22}	1.76 ± 0.34	89.97 ^{+0.03} _{-1.66}	23.8 ^{+2.1} _{-1.9}	0.134 ± 0.005	832 ± 51	224 ± 10	3.6	0.5	0.053	0.584
K00313.01	7419318	177.6356	18.73572 ^{+0.00015} _{-0.00015}	0.63 ^{+0.09} _{-0.26}	0.022 ^{+0.001} _{-0.001}	0.00 ^{+0.43} _{-0.00}	0.00 ^{+0.87} _{-0.25}	2.11 ± 0.26	88.91 ^{+0.51} _{-1.52}	32.8 ^{+2.8} _{-1.7}	0.134 ± 0.004	616 ± 32	604 ± 15	3.4	1.0	0.542	0.967
K00313.02	7419318	179.8861	8.43640 ^{+0.00010} _{-0.00011}	0.00 ^{+0.23} _{-0.00}	0.016 ^{+0.001} _{-0.001}	0.00 ^{+0.11} _{-0.00}	0.00 ^{+0.23} _{-0.00}	1.54 ± 0.15	90.00 ^{+0.00} _{-0.72}	18.9 ^{+1.4} _{-1.4}	0.079 ± 0.003	814 ± 35	350 ± 10	3.4	0.3	0.369	0.936
K00314.01	7603200	177.8521	13.78105 ^{+0.00010} _{-0.00008}	1.14 ^{+0.29} _{-0.30}	0.032 ^{+0.001} _{-0.010}	0.19 ^{+0.25} _{-0.17}	1.04 ^{+2.41} _{-1.01}	6.06 ± 3.45	85.13 ^{+2.88} _{-2.80}	13.2 ^{+12.7} _{-3.4}	0.105 ± 0.013	713 ± 210	729 ± 10	2.7	0.4	0.797	0.995
K00314.02	7603200	171.0047	23.08945 ^{+0.00018} _{-0.00018}	0.87 ^{+0.14} _{-0.24}	0.027 ^{+0.001} _{-0.005}	0.01 ^{+0.01} _{-0.01}	4.67 ^{+4.67} _{-4.67}	2.50 ± 1.35	88.67 ^{+0.71} _{-0.92}	33.8 ^{+10.4} _{-10.4}	0.134 ± 0.011	428 ± 107	498 ± 16	2.5	4.3	0.699	0.991
K00314.03	7603200	133.5522	10.31202 ^{+0.00022} _{-0.00028}	0.76 ^{+0.41} _{-0.36}	0.008 ^{+0.000} _{-0.004}	0.00 ^{+0.12} _{-0.00}	0.00 ^{+0.28} _{-0.00}	0.70 ± 0.46	88.02 ^{+0.91} _{-0.91}	19.7 ^{+10.3} _{-7.7}	0.079 ± 0.007	552 ± 173	57 ± 9	2.3	0.5	0.040	0.678
K00316.01	8008067	137.5880	15.77120 ^{+0.00015} _{-0.00015}	0.86 ^{+0.09} _{-0.09}	0.024 ^{+0.002} _{-0.003}	0.00 ^{+0.41} _{-0.00}	0.00 ^{+1.59} _{-0.00}	6.43 ± 2.24	85.99 ^{+2.69} _{-0.93}	11.5 ^{+5.1} _{-2.7}	0.129 ± 0.005	1061 ± 205	534 ± 13	5.4	11.7	0.408	0.972
K00316.02	8008067	481.2644	157.07021 ^{+0.00048} _{-0.00129}	0.92 ^{+0.04} _{-0.33}	0.026 ^{+0.018} _{-0.006}	0.00 ^{+0.45} _{-0.00}	0.00 ^{+4.59} _{-0.00}	6.35 ± 4.04	89.16 ^{+0.51} _{-1.84}	59.0 ^{+41.3} _{-18.4}	0.597 ± 0.025	472 ± 119	537 ± 41	8.7	2.6	0.173	0.913
K00316.03	8008067	131.7801	7.30569 ^{+0.00008} _{-0.00009}	0.96 ^{+0.01} _{-0.00}	0.026 ^{+0.004} _{-0.000}	0.00 ^{+0.03} _{-0.00}	0.00 ^{+0.22} _{-0.00}	5.00 ± 1.70	84.48 ^{+1.68} _{-1.52}	9.3 ^{+3.4} _{-1.7}	0.077 ± 0.003	1186 ± 166	254 ± 8	2.1	8.3	0.241	0.941
K00321.01	8753657	170.4543	2.42631 ^{+0.00002} _{-0.00002}	0.00 ^{+0.36} _{-0.00}	0.011 ^{+0.001} _{-0.000}	0.00 ^{+0.10} _{-0.00}	0.00 ^{+4.00} _{-0.00}	1.37 ± 0.13	90.00 ^{+0.00} _{-3.31}	6.6 ^{+0.4} _{-0.4}	0.034 ± 0.001	1434 ± 57	193 ± 3	2.9	0.7	0.451	0.954
K00321.02	8753657	132.3660	4.62339 ^{+0.00009} _{-0.00009}	0.00 ^{+0.51} _{-0.00}	0.007 ^{+0.001} _{-0.001}	0.37 ^{+0.08} _{-0.37}	0.00 ^{+0.18} _{-0.00}	0.82 ± 0.11	90.00 ^{+0.00} _{-2.87}	10.5 ^{+0.8} _{-0.9}	0.053 ± 0.002	1134 ± 61	63 ± 5	3.1	0.5	0.024	0.377
K00326.01	9880467	171.0311	8.97350 ^{+0.00010} _{-0.00016}	2.77 ^{+0.22} _{-0.22}	0.031 ^{+0.000} _{-0.000}	0.72 ^{+0.09} _{-0.09}	1.80 ^{+1.57} _{-1.57}	13.90 ± 1.49	60.00 ^{+13.81} _{-0.00}	5.5 ^{+0.0} _{-0.0}	0.106 ± 0.002	1340 ± 17	959 ± 34	3.7	9.5	0.855	0.993
K00326.02	9880467	151.2420	108.52770 ^{+0.00080} _{-0.00176}	0.95 ^{+0.21} _{-0.35}	0.041 ^{+0.002} _{-0.023}	0.00 ^{+0.62} _{-0.00}	0.00 ^{+1.52} _{-0.43}	18.62 ± 4.93	88.14 ^{+0.64} _{-0.30}	29.1 ^{+0.3} _{-0.3}	0.557 ± 0.011	583 ± 7	743 ± 128	12.4	1.4	0.855	0.993
K00327.01	9881662	172.6615	3.25428 ^{+0.00005} _{-0.00005}	0.11 ^{+0.35} _{-0.11}	0.011 ^{+0.001} _{-0.002}	0.00 ^{+0.24} _{-0.00}	0.00 ^{+2.00} _{-0.00}	1.43 ± 0.17	89.21 ^{+0.79} _{-2.62}	8.1 ^{+0.7} _{-0.7}	0.045 ± 0.002	1459 ± 77	166 ± 5	3.1	2.5	0.434	0.950
K00327.02	9881662	189.6005	91.35250 ^{+0.00655} _{-0.00037}	0.00 ^{+0.67} _{-0.00}	0.014 ^{+0.001} _{-0.001}	0.51 ^{+0.19} _{-0.48}	0.01 ^{+0.11} _{-0.01}	1.76 ± 0.24	90.00 ^{+0.00} _{-0.50}	75.8 ^{+8.0} _{-5.8}	0.420 ± 0.015	470 ± 31	190 ± 30	7.8	0.9	0.110	0.756
K00332.01	10290666	172.0875	5.45851 ^{+0.00006} _{-0.00006}	0.01 ^{+0.31} _{-0.01}	0.014 ^{+0.000} _{-0.001}	0.00 ^{+0.10} _{-0.00}	0.00 ^{+0.24} _{-0.00}	1.93 ± 0.20	89.92 ^{+0.08} _{-1.76}	10.6 ^{+0.8} _{-1.1}	0.061 ± 0.002	1175 ± 50	269 ± 8	4.0	0.8	0.172	0.838
K00332.02	10290666	135.3520	6.86687 ^{+0.00023} _{-0.00026}	0.61 ^{+0.19} _{-0.61}	0.006 ^{+0.002} _{-0.002}	0.60 ^{+0.23} _{-0.60}	3.48 ^{+3.48} _{-3.48}	0.80 ± 0.23	87.40 ^{+2.60} _{-0.78}	13.2 ^{+1.1} _{-1.1}	0.070 ± 0.003	1039 ± 60	42 ± 9	3.5	0.0	0.022	0.363
K00338.01	10552611	174.5747	7.01062 ^{+0.00012} _{-0.00010}	0.96 ^{+0.07} _{-0.05}	0.020 ^{+0.007} _{-0.000}	0.00 ^{+0.21} _{-0.00}	0.01 ^{+6.27} _{-0.01}	6.15 ± 1.16	79.62 ^{+0.75} _{-0.70}	5.3 ^{+0.0} _{-0.0}	0.070 ± 0.001	1182					

Table 3—Continued

KOI	KIC	T_0 (BKJD)	Period (d)	Impact Parameter	R_{PL}/R_*	e	ω (radian)	R_{PL} (R_{\oplus})	Inclination (deg)	a/ R_*	a (AU)	T_{PL} (K)	Depth (ppm)	Dur (hr)	Sig (σ)	p1	p2
K00623.01	12068975	174.0660	10.34968 ^{+0.00023} _{-0.00020}	0.43 ^{+0.26} _{-0.22}	0.010 ^{+0.001} _{-0.001}	0.15 ^{+0.39} _{-0.15}	0.34 ^{+3.17} _{-0.34}	1.35 ± 0.17	88.38 ^{+1.62} _{-1.20}	15.1 ^{+1.5} _{-2.2}	0.089 ± 0.002	1007 ± 59	123 ± 6	4.6	1.3	0.080	0.813
K00623.02	12068975	179.4702	15.67757 ^{+0.00034} _{-0.00033}	0.47 ^{+0.22} _{-0.47}	0.010 ^{+0.001} _{-0.000}	0.08 ^{+0.48} _{-0.08}	0.04 ^{+0.57} _{-0.04}	1.37 ± 0.16	88.58 ^{+1.42} _{-0.80}	19.7 ^{+2.2} _{-1.7}	0.118 ± 0.003	891 ± 52	111 ± 8	5.5	1.3	0.064	0.773
K00623.03	12068975	171.4706	5.59935 ^{+0.00011} _{-0.00010}	0.01 ^{+0.76} _{-0.01}	0.008 ^{+0.001} _{-0.000}	0.43 ^{+0.14} _{-0.43}	0.02 ^{+0.30} _{-0.02}	1.13 ± 0.13	89.97 ^{+0.03} _{-5.38}	10.1 ^{+0.9} _{-0.8}	0.059 ± 0.002	1256 ± 96	89 ± 4	4.0	1.9	0.027	0.578
K00623.04	12068975	154.4160	25.20971 ^{+0.00091} _{-0.00091}	0.82 ^{+0.09} _{-0.09}	0.008 ^{+0.006} _{-0.006}	0.68 ^{+0.31} _{-0.62}	0.00 ^{+0.00} _{-0.00}	1.06 ± 1.48	87.95 ^{+0.49} _{-1.36}	28.5 ^{+2.3} _{-2.6}	0.161 ± 0.004	813 ± 102	75 ± 10	5.5	0.4	0.014	0.410
K00626.01	4478168	172.2186	14.58667 ^{+0.00021} _{-0.00020}	0.32 ^{+0.13} _{-0.32}	0.016 ^{+0.001} _{-0.001}	0.00 ^{+0.12} _{-0.00}	0.00 ^{+0.20} _{-0.00}	1.96 ± 0.22	89.24 ^{+0.76} _{-0.35}	23.7 ^{+2.0} _{-1.7}	0.121 ± 0.005	832 ± 43	390 ± 19	4.4	0.5	0.085	0.700
K00626.02	4478168	132.8298	8.02901 ^{+0.00023} _{-0.00022}	0.36 ^{+0.34} _{-0.36}	0.007 ^{+0.001} _{-0.001}	0.13 ^{+0.38} _{-0.13}	2.85 ^{+1.81} _{-2.67}	0.82 ± 0.17	88.73 ^{+1.27} _{-1.22}	16.0 ^{+1.3} _{-1.3}	0.081 ± 0.004	1016 ± 57	68 ± 13	3.4	0.4	0.013	0.243
K00627.01	4563268	176.1730	7.75191 ^{+0.00007} _{-0.00008}	0.34 ^{+0.14} _{-0.34}	0.017 ^{+0.001} _{-0.001}	0.02 ^{+0.30} _{-0.02}	0.00 ^{+0.22} _{-0.00}	2.23 ± 0.22	88.69 ^{+0.31} _{-0.68}	14.5 ^{+1.1} _{-1.0}	0.081 ± 0.003	1061 ± 53	413 ± 11	3.9	3.3	0.190	0.854
K00627.02	4563268	132.0230	4.16547 ^{+0.00006} _{-0.00009}	0.00 ^{+0.24} _{-0.19}	0.009 ^{+0.001} _{-0.001}	0.00 ^{+0.04} _{-0.00}	0.00 ^{+0.23} _{-0.00}	1.22 ± 0.14	90.00 ^{+0.00} _{-1.54}	9.5 ^{+0.8} _{-0.7}	0.054 ± 0.002	1318 ± 72	123 ± 8	3.4	2.5	0.018	0.319
K00655.01	5966154	192.0969	25.67210 ^{+0.00018} _{-0.00020}	0.47 ^{+0.17} _{-0.25}	0.018 ^{+0.001} _{-0.000}	0.00 ^{+0.23} _{-0.00}	3.39 ^{+2.12} _{-3.39}	2.46 ± 0.26	89.09 ^{+0.50} _{-0.42}	30.1 ^{+2.6} _{-2.4}	0.176 ± 0.007	748 ± 39	394 ± 14	5.9	0.9	0.189	0.853
K00655.02	5966154	176.4103	151.88600 ^{+0.00240} _{-0.00052}	0.19 ^{+0.26} _{-0.19}	0.017 ^{+0.001} _{-0.000}	0.00 ^{+0.00} _{-0.00}	0.00 ^{+0.11} _{-0.00}	2.35 ± 0.27	89.89 ^{+0.11} _{-0.16}	99.2 ^{+8.6} _{-7.1}	0.578 ± 0.026	410 ± 22	362 ± 36	11.7	0.7	0.080	0.686
K00664.01	6442340	170.2279	13.13742 ^{+0.00024} _{-0.00026}	0.42 ^{+0.42} _{-0.42}	0.014 ^{+0.002} _{-0.002}	0.41 ^{+0.41} _{-0.41}	0.27 ^{+0.27} _{-0.27}	2.18 ± 0.53	88.53 ^{+1.47} _{-1.35}	16.1 ^{+3.0} _{-3.0}	0.110 ± 0.003	980 ± 113	233 ± 14	4.8	0.1	0.132	0.884
K00664.02	6442340	133.5821	7.78220 ^{+0.00032} _{-0.00030}	0.00 ^{+0.65} _{-0.00}	0.009 ^{+0.005} _{-0.001}	0.40 ^{+0.40} _{-0.40}	2.60 ^{+2.08} _{-2.60}	1.43 ± 0.59	90.00 ^{+0.00} _{-4.31}	11.2 ^{+3.0} _{-2.2}	0.078 ± 0.003	1187 ± 188	102 ± 10	4.1	0.5	0.115	0.867
K00664.03	6442340	152.0300	23.44194 ^{+0.00054} _{-0.00054}	0.47 ^{+0.31} _{-0.31}	0.008 ^{+0.001} _{-0.001}	0.00 ^{+0.18} _{-0.00}	0.00 ^{+0.25} _{-0.00}	1.26 ± 0.41	88.96 ^{+0.95} _{-0.78}	24.0 ^{+7.2} _{-7.2}	0.162 ± 0.005	780 ± 131	82 ± 18	6.1	0.7	0.115	0.867
K00665.01	6685609	170.3240	5.86805 ^{+0.00003} _{-0.00004}	0.52 ^{+0.17} _{-0.52}	0.019 ^{+0.001} _{-0.001}	0.00 ^{+0.50} _{-0.00}	0.00 ^{+1.55} _{-0.00}	3.04 ± 0.63	86.79 ^{+3.21} _{-1.81}	9.7 ^{+1.4} _{-1.8}	0.067 ± 0.003	1321 ± 125	434 ± 8	4.2	0.2	0.598	0.987
K00665.02	6685609	133.5707	1.61188 ^{+0.00007} _{-0.00007}	0.37 ^{+0.26} _{-0.37}	0.009 ^{+0.001} _{-0.001}	0.00 ^{+0.22} _{-0.00}	0.12 ^{+1.03} _{-0.12}	1.61 ± 0.31	83.88 ^{+6.02} _{-6.02}	3.6 ^{+0.5} _{-0.6}	0.029 ± 0.001	2153 ± 191	99 ± 4	3.3	0.8	0.066	0.779
K00665.03	6685609	133.3015	3.07156 ^{+0.00006} _{-0.00008}	0.14 ^{+0.36} _{-0.14}	0.008 ^{+0.001} _{-0.001}	0.00 ^{+0.30} _{-0.00}	0.00 ^{+0.30} _{-0.00}	1.46 ± 0.37	88.57 ^{+1.43} _{-4.27}	5.8 ^{+1.5} _{-1.0}	0.044 ± 0.002	1712 ± 192	93 ± 6	4.2	0.3	0.040	0.677
K00678.01	7509886	172.5935	6.04047 ^{+0.00009} _{-0.00012}	1.01 ^{+0.06} _{-0.05}	0.017 ^{+0.007} _{-0.001}	0.05 ^{+0.07} _{-0.05}	0.57 ^{+0.99} _{-0.57}	1.16 ± 1.31	77.92 ^{+0.94} _{-0.71}	4.8 ^{+0.1} _{-0.0}	0.063 ± 0.001	1561 ± 46	264 ± 9	2.5	0.9	0.420	0.948
K00678.02	7509886	132.0163	4.13855 ^{+0.00005} _{-0.00006}	0.99 ^{+0.03} _{-0.03}	0.020 ^{+0.000} _{-0.000}	0.05 ^{+0.05} _{-0.05}	0.36 ^{+0.36} _{-0.36}	6.12 ± 0.60	74.66 ^{+1.16} _{-0.43}	3.7 ^{+3.0} _{-0.0}	0.049 ± 0.001	1770 ± 35	254 ± 7	2.7	1.5	0.473	0.957
K00679.01	7515212	190.2473	31.80526 ^{+0.00020} _{-0.00019}	0.89 ^{+0.02} _{-0.07}	0.019 ^{+0.001} _{-0.001}	0.01 ^{+0.11} _{-0.01}	0.00 ^{+0.01} _{-0.00}	7.44 ± 0.94	86.30 ^{+0.83} _{-0.27}	13.6 ^{+2.3} _{-0.4}	0.227 ± 0.012	1054 ± 62	338 ± 18	8.7	0.7	0.251	0.894
K00679.02	7515212	139.6350	16.25831 ^{+0.00113} _{-0.00107}	0.89 ^{+3.29} _{-1.19}	0.007 ^{+0.027} _{-0.001}	0.00 ^{+0.04} _{-0.00}	0.00 ^{+0.29} _{-0.00}	1.17 ± 2.45	83.98 ^{+0.83} _{-0.57}	19.6 ^{+11.2} _{-9.0}	0.135 ± 0.008	1345 ± 1355	51 ± 13	6.8	0.2	0.018	0.312
K00710.01	9590976	170.9513	5.37485 ^{+0.00015} _{-0.00011}	0.92 ^{+0.00} _{-0.07}	0.014 ^{+0.001} _{-0.001}	0.14 ^{+0.11} _{-0.14}	0.00 ^{+0.56} _{-0.00}	4.59 ± 0.72	77.99 ^{+2.75} _{-0.72}	4.4 ^{+0.7} _{-0.2}	0.064 ± 0.008	2118 ± 211	155 ± 7	4.2	2.7	0.310	0.957
K00710.02	9590976	137.9585	8.58604 ^{+0.00035} _{-0.00033}	0.96 ^{+0.05} _{-0.06}	0.010 ^{+0.004} _{-0.000}	0.00 ^{+0.12} _{-0.00}	0.00 ^{+1.33} _{-0.00}	3.23 ± 0.72	80.86 ^{+1.88} _{-1.12}	6.0 ^{+0.5} _{-0.4}	0.085 ± 0.006	1817 ± 170	99 ± 9	3.5	1.9	0.116	0.867
K00710.03	9590976	132.4974	3.88683 ^{+0.00012} _{-0.00012}	0.81 ^{+0.07} _{-0.07}	0.008 ^{+0.005} _{-0.002}	0.36 ^{+0.36} _{-0.36}	3.41 ^{+3.41} _{-3.41}	2.38 ± 1.38	79.03 ^{+1.07} _{-3.49}	3.8 ^{+3.9} _{-0.4}	0.052 ± 0.009	2138 ± 803	58 ± 6	4.7	1.1	0.036	0.649
K00717.01	9873254	175.7916	14.70751 ^{+0.00033} _{-0.00036}	0.65 ^{+0.22} _{-0.62}	0.015 ^{+0.003} _{-0.002}	0.00 ^{+0.45} _{-0.00}	0.00 ^{+1.15} _{-0.00}	2.00 ± 0.85	88.41 ^{+1.52} _{-1.29}	20.9 ^{+7.0} _{-6.0}	0.121 ± 0.008	781 ± 120	273 ± 16	3.8	0.4	0.264	0.900
K00717.02	9873254	132.2130	0.90039 ^{+0.00005} _{-0.00006}	1.32 ^{+0.18} _{-0.18}	0.005 ^{+0.000} _{-0.001}	0.79 ^{+0.05} _{-0.01}	1.60 ^{+0.71} _{-0.01}	1.04 ± 0.41	60.64 ^{+27.64} _{-2.53}	2.4 ^{+1.2} _{-0.6}	0.019 ± 0.001	2297 ± 445	31 ± 3	1.2	0.1	0.082	0.692
K00719.01	9506112	134.8770	9.03420 ^{+0.00015} _{-0.00013}	0.78 ^{+0.05} _{-0.12}	0.024 ^{+0.001} _{-0.003}	0.00 ^{+0.00} _{-0.00}	0.00 ^{+0.00} _{-0.00}	1.74 ± 0.21	88.24 ^{+0.42} _{-0.30}	24.9 ^{+1.9} _{-1.8}	0.077 ± 0.002	618 ± 34	554 ± 8	1.8	0.9	0.634	0.989
K00719.02	9506112	146.9200	28.12230 ^{+0.00138} _{-0.00494}	0.05 ^{+0.38} _{-0.05}	0.012 ^{+0.001} _{-0.001}	0.00 ^{+0.13} _{-0.00}	0.00 ^{+0.38} _{-0.00}	0.86 ± 0.10	89.95 ^{+0.05} _{-0.45}	51.7 ^{+4.4} _{-4.2}	0.163 ± 0.005	432 ± 24	169 ± 14	4.2	0.6	0.027	0.579
K00719.03	9506112	166.5382	45.90000 ^{+0.00978} _{-0.00370}	0.00 ^{+0.44} _{-0.00}	0.013 ^{+0.002} _{-0.000}	0.32 ^{+0.20} _{-0.32}	0.00 ^{+0.23} _{-0.00}	0.97 ± 0.13	90.00 ^{+0.00} _{-0.35}	72.1 ^{+6.5} _{-5.9}	0.226 ± 0.008	364 ± 20	185 ± 24	4.6	0.2	0.038	0.664
K00719.04	9506112	133.7840	4.15982 ^{+0.00003} _{-0.00003}	0.40 ^{+0.17} _{-0.40}	0.010 ^{+0.001} _{-0.001}	0.00 ^{+0.21} _{-0.00}	0.00 ^{+0.38} _{-0.00}	0.69 ± 0.09	88.49 ^{+1.50} _{-0.78}	14.9 ^{+1.2} _{-1.0}	0.046 ± 0.001	797 ± 42	144 ± 5	1.9	0.2	0.067	0.781
K00972.01	11013201	261.5394	13.11891 ^{+0.00002} _{-0.00002}	0.82 ^{+0.13} _{-0.13}	0.022 ^{+0.004} _{-0.004}	0.16 ^{+0.16} _{-0.16}	4.73 ^{+4.73} _{-4.73}	9.32 ± 2.47	84.95 ^{+2.55} _{-1.97}	7.7 ^{+0.8} _{-0.8}	0.140 ± 0.004	1742 ± 289	375 ± 26	5.0	4.6	0.646	0.979
K00972.02	11013201	139.1430	7.82257 ^{+0.00044} _{-0.00018}	0.74 ^{+0.27} _{-0.25}	0.004 ^{+0.001} _{-0.002}	0.00 ^{+0.13} _{-0.00}	0.04 ^{+0.37} _{-0.04}	1.51 ± 0.64	84.12 ^{+1.97} _{-1.69}	6.4 ^{+1.8} _{-1.5}	0.099 ± 0.003	1972 ± 329	16 ± 20	5.6	0.2	0.089	0.710
K01001.01	1871056	155.7178	40.80686 ^{+0.00012} _{-0.00043}	0.00 ^{+0.76} _{-0.24}	0.016 ^{+0.002} _{-0.001}	0.69 ^{+0.12} _{-0.69}	0.00 ^{+0.11} _{-0.00}	6.00 ± 0.82	90.00 ^{+0.00} _{-2.68}	16.2 ^{+2.7} _{-2.7}	0.260 ± 0.010	1013 ± 73	328 ± 27	13.7	1.2	0.010	0.202
K01001.02	1871056	216.2450	140.09140 ^{+0.00229} _{-0.00164}	0.65 ^{+0.22} _{-0.57}	0.016 ^{+0.003} _{-0.000}	0.00 ^{+0.69} _{-0.00}	0.00 ^{+4.24} _{-0.00}	5.82 ± 1.03	89.14 ^{+0.76} _{-0.47}	37.6 ^{+11.4} _{-1.4}	0.585 ± 0.022	627 ± 71	300 ± 52	19.3	0.3	0.074	0.666
K01151.01	8280511	134.8157	5.21781 ^{+0.00021} _{-0.00019}	0.89 ^{+0.06} _{-0.04}	0.011 ^{+0.000} _{-0.001}	0.05 ^{+0.15} _{-0.05}	0.00 ^{+0.61} _{-0.00}	2.73 ± 0.34	80.79 ^{+0.69} _{-1.23}	5.7 ^{+0.7} _{-0.7}	0.060 ± 0.004	1615 ± 84	99 ± 9	3.6	1.0	0.039	0.672
K01151.02	8280511	135.7436	7.41105 ^{+0.00027} _{-0.00026}	0.89 ^{+0.04} _{-0.04}	0.013 ^{+0.001} _{-0.001}	0.10 ^{+0.05} _{-0.10}	0.00 ^{+0.24} _{-0.00}	3.13 ± 0.47	83.01 ^{+0.96} _{-1.55}	7.5 ^{+0.6} _{-0.7}	0.076 ± 0.006	1417 ± 118	124 ± 10	3.9	0.6	0.133	0.884
K01151.03	8280511	135.4660	5.24972 ^{+0.00010} _{-0.00012}	0.60 ^{+0.33} _{-0.45}	0.007 ^{+0.003} _{-0.001}	0.06 ^{+0.52} _{-0.06}	3.16 ^{+1.34} _{-3.16}	0.86 ± 0.38	86.95 ^{+2.39} _{-3.14}	11.3 ^{+2.7} _{-2.8}	0.057 ± 0.003	1138 ± 185	65 ± 9	2.9	1.0		

Table 3—Continued

KOI	KIC	T_0 (BKJD)	Period (d)	Impact Parameter	R_{PL}/R_*	e	ω (radian)	R_{PL} (R_{\oplus})	Inclination (deg)	a/ R_*	a (AU)	T_{PL} (K)	Depth (ppm)	Dur (hr)	Sig (σ)	p1	p2	
K01445.03	11336883	150.8360	20.01960	+0.00098 -0.00163	0.31+0.55 -0.22	0.004+0.003 -0.001	0.40+0.30 -0.35	3.93+1.29 -1.30	0.60 ± 0.28	89.33+0.67 -1.16	26.6+2.5 -2.1	0.154 ± 0.006	789 ± 49	20 ± 14	6.8	0.3	0.032	0.622
K01525.01	7869917	133.5535	7.71468	+0.00011 -0.00011	0.59+0.59 -0.50	0.016+0.003 -0.003	0.63+0.43 -0.43	4.53+0.06 -1.24	3.26 ± 1.07	86.62+3.38 -4.28	10.3+3.1 -2.5	0.091 ± 0.005	1447 ± 322	217 ± 10	4.7	0.2	0.486	0.959
K01525.02	7869917	138.2671	11.80609	+0.00036 -0.00046	0.37+0.30 -0.37	0.009+0.001 -0.002	0.00+0.18 -0.00	0.00+0.31 -0.00	1.46 ± 0.43	88.67+1.33 -1.36	15.1+4.1 -2.9	0.106 ± 0.009	1156 ± 163	120 ± 13	5.4	0.8	0.148	0.812
K01534.01	4741126	146.9846	20.42226	+0.00049 -0.00030	0.05+0.05 -0.41	0.012+0.001 -0.001	0.00+0.00 -0.00	0.00+0.00 -0.00	1.83 ± 0.45	89.88+1.26 -1.26	24.2+2.9 -4.1	0.160 ± 0.007	862 ± 110	187 ± 16	6.5	1.0	0.089	0.710
K01534.02	4741126	138.2340	7.63861	+0.00030 -0.00030	0.41+0.35 -0.41	0.008+0.001 -0.002	0.00+0.17 -0.00	0.00+0.33 -0.00	1.12 ± 0.34	88.24+1.76 -1.64	13.2+3.1 -2.9	0.083 ± 0.004	1160 ± 171	80 ± 10	4.0	0.8	0.023	0.371
K01613.01	6268648	141.0860	15.86621	+0.00058 -0.00057	0.34+0.65 -0.34	0.008+0.003 -0.001	0.52+0.32 -0.14	2.66+1.57 -1.57	1.32 ± 0.82	88.98+1.02 -3.05	17.8+8.8 -6.9	0.127 ± 0.010	900 ± 237	77 ± 6	4.3	0.8	0.028	0.422
K01613.02	6268648	196.7260	94.09329	+0.00438 -0.00051	0.48+0.51 -0.48	0.008+0.002 -0.002	0.00+0.20 -0.00	0.00+0.20 -0.00	1.31 ± 0.71	89.57+0.43 -0.68	59.2+32.3 -19.3	0.416 ± 0.031	496 ± 159	65 ± 17	10.0	1.2	0.013	0.254
K01628.01	6975129	147.1029	19.74747	+0.00031 -0.00040	0.71+0.12 -0.30	0.020+0.003 -0.002	0.08+0.41 -0.00	0.00+4.60 -0.00	2.62 ± 0.39	88.53+0.71 -0.41	27.1+2.5 -1.8	0.153 ± 0.005	784 ± 46	466 ± 17	4.0	1.2	0.165	0.832
K01628.02	6975129	132.0945	1.77243	+0.00003 -0.00003	0.00+0.00 -0.00	0.007+0.001 -0.001	0.00+0.06 -0.00	0.00+0.29 -0.00	0.94 ± 0.12	90.00+0.00 -2.07	5.5+0.5 -0.7	0.029 ± 0.001	1744 ± 91	74 ± 4	2.5	1.8	0.043	0.530
K01692.01	6616218	137.2639	5.96040	+0.00003 -0.00002	0.35+0.09 -0.35	0.024+0.000 -0.001	0.00+0.15 -0.00	0.00+0.38 -0.00	2.46 ± 0.21	88.64+1.36 -0.46	14.4+1.1 -1.0	0.064 ± 0.002	957 ± 40	829 ± 9	3.0	0.9	0.865	0.994
K01692.02	6616218	133.3133	2.46110	+0.00003 -0.00003	0.00+0.00 -0.00	0.008+0.001 -0.001	0.00+0.00 -0.00	0.00+0.00 -0.00	0.80 ± 0.10	90.00+0.00 -2.57	8.0+0.7 -0.6	0.035 ± 0.001	1288 ± 73	82 ± 6	2.4	0.7	0.026	0.404
K01779.01	9909735	134.0812	4.66272	+0.00001 -0.00001	0.84+0.06 -0.19	0.041+0.004 -0.001	0.00+0.43 -0.00	0.00+4.76 -0.00	7.84 ± 1.47	83.09+2.83 -1.84	6.7+1.6 -0.8	0.054 ± 0.002	1458 ± 171	1627 ± 10	3.1	0.8	0.636	0.978
K01779.02	9909735	133.0899	11.81502	+0.00009 -0.00009	0.93+0.24 -0.09	0.037+0.000 -0.001	0.00+0.34 -0.10	4.48+0.90 -0.30	6.54 ± 1.68	86.18+1.16 -0.83	13.5+3.1 -0.6	0.101 ± 0.003	1034 ± 155	1028 ± 18	3.0	1.4	0.170	0.836
K01781.01	11551692	135.2206	7.83445	+0.00001 -0.00001	0.33+0.31 -0.15	0.037+0.011 -0.000	0.00+0.66 -0.00	0.00+4.72 -0.00	3.24 ± 0.56	89.03+0.49 -1.08	19.4+1.4 -1.3	0.073 ± 0.002	753 ± 34	1954 ± 11	3.1	3.5	0.995	1.000
K01781.02	11551692	137.1027	3.00516	+0.00001 -0.00001	0.31+0.27 -0.30	0.022+0.003 -0.001	0.00+0.35 -0.00	0.00+4.31 -0.00	1.88 ± 0.20	88.27+1.73 -0.83	10.2+0.6 -0.8	0.038 ± 0.001	1040 ± 46	690 ± 5	2.2	0.9	0.979	1.000
K01781.03	11551692	151.8476	58.02125	+0.00020 -0.00013	0.50+0.47 -0.19	0.031+0.002 -0.000	0.00+0.28 -0.00	0.00+0.00 -0.00	2.61 ± 0.31	89.63+0.55 -0.16	76.0+6.4 -5.4	0.276 ± 0.007	377 ± 20	1338 ± 46	5.1	1.2	0.598	0.987
K01806.02	9529744	138.2171	17.93497	+0.00050 -0.00080	0.31+0.19 -0.31	0.012+0.000 -0.003	0.00+0.15 -0.00	0.00+0.23 -0.00	1.60 ± 0.40	89.30+0.70 -0.57	24.4+5.5 -4.8	0.137 ± 0.008	849 ± 109	176 ± 18	5.2	3.1	0.112	0.863
K01806.03	9529744	137.6755	8.37167	+0.00000 -0.00000	0.27+0.27 -0.27	0.008+0.002 -0.000	0.00+0.00 -0.00	0.00+0.00 -0.00	1.09 ± 0.32	88.99+1.33 -0.33	14.7+2.9 -2.9	0.083 ± 0.005	1087 ± 152	89 ± 13	4.0	4.1	0.034	0.640
K01809.01	8240797	144.5235	13.09392	+0.00016 -0.00017	0.96+0.45 -0.02	0.023+0.014 -0.003	0.00+0.38 -0.00	0.00+1.58 -0.00	6.15 ± 3.24	86.14+0.00 -6.28	10.0+3.9 -2.2	0.115 ± 0.014	1009 ± 145	390 ± 9	2.5	1.4	0.462	0.956
K01809.02	8240797	132.6958	4.91538	+0.00000 -0.00000	0.72+0.15 -0.15	0.015+0.003 -0.001	0.00+0.37 -0.00	0.00+0.94 -0.44	2.42 ± 0.85	85.24+2.85 -0.99	8.5+2.4 -0.6	0.058 ± 0.003	1293 ± 218	235 ± 6	3.1	1.1	0.263	0.899
K01824.01	2989404	134.6430	3.55380	+0.00004 -0.00002	0.50+0.41 -0.41	0.012+0.001 -0.001	0.00+0.33 -0.00	0.15+4.37 -0.15	2.07 ± 0.44	85.76+3.56 -2.65	6.6+1.0 -1.0	0.049 ± 0.002	1591 ± 150	197 ± 5	3.5	0.5	0.202	0.863
K01824.02	2989404	136.0502	1.67834	+0.00022 -0.00022	0.63+0.21 -0.44	0.011+0.001 -0.001	0.03+0.53 -0.03	0.08+2.53 -0.08	2.12 ± 0.49	79.91+7.73 -7.45	3.6+0.7 -0.6	0.030 ± 0.001	2196 ± 244	152 ± 3	2.9	0.3	0.184	0.849
K01909.01	10130039	133.9557	12.75808	+0.00023 -0.00011	0.28+0.28 -0.22	0.013+0.002 -0.002	0.44+0.44 -0.27	0.00+0.00 -0.00	1.65 ± 0.35	89.22+0.59 -1.11	20.3+3.6 -1.8	0.113 ± 0.004	888 ± 84	191 ± 9	4.2	0.4	0.210	0.930
K01909.02	10130039	131.4909	5.47037	+0.00011 -0.00008	0.22+0.41 -0.22	0.008+0.002 -0.000	0.00+0.27 -0.00	0.00+0.30 -0.00	1.11 ± 0.25	88.89+1.11 -2.56	11.1+2.1 -1.8	0.064 ± 0.003	1201 ± 120	110 ± 6	3.6	0.2	0.060	0.762
K01909.03	10130039	145.5671	25.09858	+0.00084 -0.00016	0.89+0.26 -0.26	0.015+0.002 -0.002	0.00+0.53 -0.00	0.00+1.40 -0.00	1.97 ± 0.58	88.36+0.73 -0.73	30.7+7.3 -3.2	0.178 ± 0.008	725 ± 94	187 ± 13	3.0	0.2	0.133	0.885
K01929.01	10136549	132.8155	9.69303	+0.00016 -0.00019	0.70+0.16 -0.59	0.011+0.001 -0.001	0.00+0.36 -0.00	0.16+0.82 -0.16	1.47 ± 0.69	85.55+3.90 -2.57	9.8+2.5 -0.5	0.089 ± 0.002	1304 ± 182	145 ± 9	6.0	0.7	0.147	0.812
K01929.02	10136549	133.0093	3.29274	+0.00008 -0.00008	0.68+0.15 -0.15	0.009+0.001 -0.001	0.04+0.37 -0.00	0.45+0.31 -0.00	2.20 ± 0.35	79.37+3.24 -3.45	4.0+0.5 -0.6	0.044 ± 0.001	2037 ± 166	83 ± 5	5.1	0.3	0.145	0.809
K01930.01	5511081	138.7478	13.72686	+0.00010 -0.00011	0.00+0.38 -0.00	0.013+0.001 -0.000	0.00+0.07 -0.00	0.00+0.14 -0.00	2.25 ± 0.21	90.00+0.00 -1.47	15.5+1.2 -1.2	0.115 ± 0.003	1006 ± 50	200 ± 12	7.0	1.5	0.170	0.911
K01930.02	5511081	137.0438	24.31058	+0.00024 -0.00028	0.00+0.45 -0.00	0.013+0.001 -0.000	0.00+0.05 -0.00	0.00+0.12 -0.00	2.19 ± 0.22	90.00+0.00 -1.12	22.9+1.9 -1.8	0.168 ± 0.004	821 ± 43	180 ± 15	8.3	1.8	0.104	0.852
K01930.03	5511081	143.5344	44.43150	+0.00028 -0.00020	0.00+0.26 -0.00	0.015+0.001 -0.001	0.17+0.17 -0.00	0.00+0.00 -0.00	2.57 ± 0.26	90.00+0.00 -0.44	34.7+2.4 -2.4	0.252 ± 0.006	663 ± 35	248 ± 21	9.7	1.6	0.116	0.867
K01930.04	5511081	132.3931	9.34131	+0.00038 -0.00032	0.17+0.30 -0.17	0.008+0.001 -0.001	0.50+0.15 -0.47	3.56+1.11 -3.00	1.32 ± 0.18	89.21+1.42 -1.62	12.5+1.0 -1.2	0.089 ± 0.002	1105 ± 70	79 ± 9	6.1	1.6	0.057	0.752
K01932.01	5202905	144.4640	22.82485	+0.00007 -0.00004	0.71+0.13 -0.34	0.017+0.003 -0.004	0.00+0.37 -0.00	0.44+3.13 -0.44	6.05 ± 1.96	87.21+1.63 -1.36	13.4+4.0 -3.1	0.203 ± 0.007	1429 ± 236	317 ± 69	8.7	0.6	0.019	0.328
K01932.02	5202905	143.5855	14.84440	+0.00185 -0.00204	0.79+1.06 -0.03	0.012+0.028 -0.002	0.26+0.15 -0.02	2.16+2.62 -1.15	3.05 ± 4.04	85.54+0.18 -2.82	11.3+3.2 -2.6	0.123 ± 0.021	1715 ± 359	200 ± 54	7.2	0.5	0.088	0.707
K01955.01	9892816	132.6668	15.17019	+0.00021 -0.00035	0.94+0.02 -0.03	0.016+0.002 -0.001	0.00+0.06 -0.00	0.00+0.19 -0.00	4.40 ± 1.23	85.02+1.14 -2.2	12.7+2.3 -2.2	0.146 ± 0.009	1309 ± 128	230 ± 12	4.3	1.1	0.175	0.914
K01955.02	9892816	136.4553	39.45988	+0.00008 -0.00014	0.00+0.00 -0.00	0.012+0.001 -0.001	0.22+0.22 -0.22	3.56+3.55 -3.55	1.88 ± 0.65	90.00+0.00 -1.49	36.7+8.1 -8.5	0.251 ± 0.013	728 ± 107	231 ± 21	9.4	0.5	0.172	0.912
K01955.03	9892816	131.7567	1.64420	+0.00003 -0.00003	0.20+0.45 -0.20	0.004+0.002 -0.000	0.79+0.08 -0.53	4.03+0.25 -2.14	2.54 ± 0.24	87.71+1.29 -7.24	4.9+1.6 -1.1	0.028 ± 0.002	1900 ± 398	31 ± 4	7.4	0.6	0.016	0.443
K01955.04	9892816	141.9958	26.23420	+0.00069 -0.00105	0.68+0.19 -0.19	0.019+0.009 -0.009	0.38+0.38 -0.38	4.72+4.72 -4.72	0.53 ± 0.70	88.82+0.52 -0.65	31.3+6.8 -5.8	0.178 ± 0.012	747 ± 104	170 ± 17	3.6	1.2	0.068	0.784
K02004.01	12154526	146.3714	56.18945	+0.00058 -0.00086	0.64+0.24 -0.62	0.017+0.003 -0.001	0.00+0.46 -0.00	0.00+1.54 -0.00	2.38 ± 0.66	89.21+0.77 -0.71	49.3+11.7 -11.7	0.291 ± 0.013	560 ± 92	368 ± 31	7.2	0.9	0.326	0.960
K02004.02	12154526	133.5255	3.18899	+0.00017 -0.00005	0.90+0.09 -0.09	0.008+0.001 -0.001	0.07+0.16 -0.00	1.83+0.69 -1.83	1.73 ± 0.32	79.74+1.09 -3.22	5.3+0.6 -0.6	0.044 ± 0.003	1700 ± 130	69 ± 7	2.6	0.5	0.083	0.819
K02004.03	12154526	132.7764	1.72107	+0.00002 -0.00002	0.99+0.01 -0.01	0.008+0.001 -0.001	0.00+0.03 -0.00	0.00+0.05 -0.00	0.83 ± 0.12	39.70+0.00 -9.40	1.3+0.2 -0.2	0.027 ± 0.003	1250 ± 300	37 ± 7	1.9	1.5	0.083	0.819
K02011.01	5384079	132.5342	7.05670	+0.00014 -0.00014	0.91+0.04 -0.05	0.015+0.001 -0.00												

Table 3—Continued

KOI	KIC	T_0 (BKJD)	Period (d)	Impact Parameter	R_{PL}/R_*	e	ω (radian)	R_{PL} (R_{\oplus})	Inclination (deg)	a/ R_*	a (AU)	T_{PL} (K)	Depth (ppm)	Dur (hr)	Sig (σ)	p1	p2
K02148.01	6021193	142.1019	11.93223 ^{+0.00021} _{-0.00025}	0.00 ^{+0.71} _{-0.35}	0.011 ^{+0.003} _{-0.000}	0.19 ^{+0.41} _{-0.19}	1.38 ^{+2.92} _{-1.38}	2.68 ± 0.83	90.00 ^{+0.00} _{-3.60}	10.1 ^{+3.0} _{-2.5}	0.104 ± 0.004	1128 ± 159	194 ± 17	7.0	0.2	0.138	0.889
K02148.02	6021193	132.9564	7.54236 ^{+0.00029} _{-0.00029}	0.50 ^{+0.60} _{-0.50}	0.009 ^{+0.002} _{-0.001}	0.42 ^{+0.26} _{-0.42}	0.28 ^{+2.31} _{-0.28}	2.14 ± 0.65	86.40 ^{+3.60} _{-3.88}	7.5 ^{+1.9} _{-1.9}	0.077 ± 0.003	1315 ± 193	123 ± 14	5.5	0.4	0.138	0.889
K02148.03	6021193	134.7000	3.61461 ^{+0.00011} _{-0.00010}	1.13 ^{+0.60} _{-0.74}	0.008 ^{+0.009} _{-0.001}	0.73 ^{+0.07} _{-0.32}	2.40 ^{+1.96} _{-1.56}	2.00 ± 1.36	75.75 ^{+9.85} _{-5.98}	4.3 ^{+1.2} _{-0.9}	0.047 ± 0.002	1734 ± 269	72 ± 9	12.1	0.8	0.083	0.819
K02158.01	5211199	132.6314	4.56215 ^{+0.00014} _{-0.00014}	0.77 ^{+0.27} _{-0.27}	0.009 ^{+0.001} _{-0.001}	0.11 ^{+0.11} _{-0.11}	0.96 ^{+0.96} _{-0.96}	1.64 ± 0.37	83.35 ^{+1.72} _{-1.72}	6.3 ^{+0.9} _{-0.9}	0.052 ± 0.001	1390 ± 138	81 ± 7	3.5	1.0	0.023	0.370
K02158.02	5211199	132.1895	6.68232 ^{+0.00020} _{-0.00033}	0.72 ^{+0.17} _{-0.25}	0.007 ^{+0.001} _{-0.002}	0.00 ^{+0.14} _{-0.00}	0.00 ^{+0.41} _{-0.00}	1.39 ± 0.49	85.37 ^{+1.66} _{-1.31}	8.2 ^{+2.1} _{-1.7}	0.072 ± 0.006	1205 ± 161	50 ± 8	4.1	1.1	0.005	0.104
K02169.01	9006186	134.1486	5.45300 ^{+0.00009} _{-0.00011}	0.71 ^{+0.13} _{-0.25}	0.008 ^{+0.002} _{-0.001}	0.32 ^{+0.16} _{-0.32}	0.27 ^{+1.37} _{-0.27}	1.01 ± 0.23	86.53 ^{+1.58} _{-1.22}	11.4 ^{+2.3} _{-1.7}	0.058 ± 0.002	1056 ± 105	94 ± 4	2.5	1.0	0.105	0.854
K02169.02	9006186	136.0883	3.26661 ^{+0.00006} _{-0.00005}	0.66 ^{+0.14} _{-0.36}	0.007 ^{+0.000} _{-0.001}	0.00 ^{+0.30} _{-0.00}	0.00 ^{+0.71} _{-0.00}	0.86 ± 0.21	85.27 ^{+2.92} _{-1.59}	7.9 ^{+1.5} _{-1.4}	0.042 ± 0.001	1275 ± 135	58 ± 3	2.4	0.1	0.077	0.808
K02169.03	9006186	133.2112	4.27235 ^{+0.00011} _{-0.00009}	0.59 ^{+0.21} _{-0.46}	0.006 ^{+0.001} _{-0.001}	0.29 ^{+0.16} _{-0.29}	0.00 ^{+0.39} _{-0.00}	0.69 ± 0.18	86.57 ^{+2.72} _{-1.77}	9.5 ^{+2.1} _{-1.5}	0.050 ± 0.001	1150 ± 138	48 ± 4	2.7	1.2	0.057	0.751
K02169.04	9006186	132.2252	2.19259 ^{+0.00003} _{-0.00005}	1.44 ^{+1.39} _{-1.13}	0.004 ^{+0.000} _{-0.001}	0.73 ^{+0.40} _{-0.40}	1.50 ^{+1.17} _{-1.32}	0.51 ± 0.18	76.83 ^{+10.21} _{-10.57}	6.3 ^{+1.8} _{-1.6}	0.032 ± 0.001	1435 ± 269	18 ± 3	1.0	0.6	0.040	0.677
K02173.01	11774991	141.1054	37.81526 ^{+0.00098} _{-0.00103}	0.39 ^{+0.38} _{-0.39}	0.013 ^{+0.003} _{-0.000}	0.00 ^{+0.42} _{-0.00}	0.00 ^{+1.13} _{-0.00}	1.16 ± 0.29	89.58 ^{+0.42} _{-0.60}	52.3 ^{+11.0} _{-9.8}	0.200 ± 0.006	434 ± 58	272 ± 21	5.1	0.8	0.020	0.333
K02173.02	11774991	171.1865	53.57820 ^{+0.00170} _{-0.00251}	0.07 ^{+0.72} _{-0.07}	0.012 ^{+0.001} _{-0.001}	0.90 ^{+0.01} _{-0.71}	3.82 ^{+0.52} _{-0.52}	1.04 ± 0.35	89.94 ^{+0.76} _{-0.76}	68.7 ^{+10.6} _{-13.8}	0.253 ± 0.007	389 ± 57	280 ± 26	6.3	0.9	0.015	0.277
K02175.01	9022166	142.1752	26.84734 ^{+0.00034} _{-0.00035}	0.00 ^{+0.60} _{-0.00}	0.016 ^{+0.001} _{-0.001}	0.00 ^{+0.45} _{-0.00}	0.00 ^{+1.25} _{-0.00}	1.79 ± 0.59	90.00 ^{+0.00} _{-1.03}	33.9 ^{+12.9} _{-7.0}	0.167 ± 0.009	614 ± 117	259 ± 26	6.3	0.6	0.086	0.702
K02175.02	9022166	179.5122	72.38130 ^{+0.00071} _{-0.00134}	0.25 ^{+0.28} _{-0.34}	0.018 ^{+0.001} _{-0.001}	0.00 ^{+0.11} _{-0.00}	0.00 ^{+0.13} _{-0.00}	1.87 ± 0.50	89.79 ^{+0.21} _{-0.32}	71.0 ^{+19.0} _{-12.7}	0.320 ± 0.016	423 ± 60	364 ± 42	7.7	0.3	0.087	0.703
K02289.01	3867615	157.3033	62.78500 ^{+0.00180} _{-0.00121}	0.76 ^{+0.12} _{-0.64}	0.018 ^{+0.001} _{-0.005}	0.00 ^{+0.49} _{-0.00}	0.00 ^{+0.71} _{-0.00}	2.65 ± 0.82	89.21 ^{+0.69} _{-0.37}	53.7 ^{+11.1} _{-12.5}	0.335 ± 0.015	558 ± 80	358 ± 43	5.9	0.6	0.038	0.497
K02289.02	3867615	147.2808	20.09846 ^{+0.00061} _{-0.00076}	0.14 ^{+0.45} _{-0.14}	0.012 ^{+0.001} _{-0.003}	0.17 ^{+0.17} _{-0.17}	0.58 ^{+0.07} _{-0.58}	1.63 ± 0.43	89.69 ^{+0.31} _{-0.13}	25.5 ^{+6.2} _{-4.4}	0.148 ± 0.009	811 ± 110	157 ± 22	5.3	0.4	0.024	0.380
K02311.01	4247991	294.4400	191.88569 ^{+0.01091} _{-0.03101}	0.00 ^{+0.90} _{-0.00}	0.024 ^{+0.002} _{-0.022}	0.00 ^{+0.02} _{-0.00}	0.09 ^{+0.24} _{-0.09}	3.22 ± 2.86	90.00 ^{+0.00} _{-1.60}	120.6 ^{+84.8} _{-52.3}	0.691 ± 0.079	239 ± 42	200 ± 39	4.8	0.5	0.024	0.379
K02311.02	4247991	145.0410	13.72535 ^{+0.00072} _{-0.00069}	0.91 ^{+0.09} _{-0.91}	0.010 ^{+0.016} _{-0.008}	0.02 ^{+0.00} _{-0.02}	0.17 ^{+0.03} _{-0.17}	1.38 ± 1.90	81.52 ^{+0.68} _{-0.58}	20.0 ^{+13.5} _{-8.3}	0.119 ± 0.013	514 ± 75	51 ± 15	7.5	0.3	0.006	0.133
K02352.01	8013439	133.0583	13.39140 ^{+0.00054} _{-0.00034}	0.68 ^{+0.05} _{-0.05}	0.010 ^{+0.002} _{-0.002}	0.53 ^{+0.14} _{-0.14}	4.43 ^{+0.66} _{-0.66}	3.37 ± 5.00	85.30 ^{+1.00} _{-1.00}	8.2 ^{+0.7} _{-0.7}	0.119 ± 0.018	1522 ± 215	50 ± 4	4.3	0.8	0.049	0.720
K02352.02	8013439	134.7477	5.62903 ^{+0.00012} _{-0.00010}	0.32 ^{+0.29} _{-0.32}	0.005 ^{+0.001} _{-0.000}	0.01 ^{+0.22} _{-0.01}	0.01 ^{+0.91} _{-0.01}	0.84 ± 0.27	87.98 ^{+2.02} _{-2.45}	8.7 ^{+2.4} _{-2.2}	0.065 ± 0.005	1467 ± 229	38 ± 2	4.5	0.4	0.060	0.761
K02352.03	8013439	137.9280	8.25621 ^{+0.00023} _{-0.00028}	0.87 ^{+0.06} _{-0.10}	0.008 ^{+0.000} _{-0.000}	0.00 ^{+0.12} _{-0.00}	3.83 ^{+1.69} _{-3.88}	1.27 ± 0.30	85.87 ^{+0.77} _{-0.88}	11.7 ^{+1.9} _{-2.0}	0.083 ± 0.007	1261 ± 147	37 ± 3	2.6	1.9	0.050	0.724
K02541.01	12306058	137.9603	7.14682 ^{+0.00030} _{-0.00026}	0.41 ^{+0.26} _{-0.34}	0.007 ^{+0.001} _{-0.001}	0.00 ^{+0.16} _{-0.00}	0.01 ^{+0.36} _{-0.01}	2.40 ± 0.53	86.31 ^{+0.36} _{-1.20}	5.6 ^{+1.5} _{-0.3}	0.079 ± 0.002	1376 ± 174	78 ± 12	8.3	0.4	0.188	0.853
K02541.02	12306058	146.9230	20.48565 ^{+0.00148} _{-0.00123}	0.23 ^{+0.46} _{-0.23}	0.009 ^{+0.001} _{-0.002}	0.43 ^{+0.02} _{-0.43}	0.00 ^{+0.26} _{-0.00}	2.84 ± 0.97	88.97 ^{+2.02} _{-2.05}	11.3 ^{+3.5} _{-2.4}	0.160 ± 0.028	973 ± 133	93 ± 20	11.1	0.3	0.188	0.853
K02585.01	7673841	136.3069	5.34189 ^{+0.00018} _{-0.00017}	0.92 ^{+0.07} _{-0.07}	0.009 ^{+0.002} _{-0.002}	0.03 ^{+0.07} _{-0.03}	0.33 ^{+0.33} _{-0.33}	2.25 ± 1.68	81.02 ^{+0.16} _{-1.70}	6.2 ^{+1.1} _{-0.6}	0.066 ± 0.003	1778 ± 405	67 ± 8	3.1	0.7	0.073	0.797
K02585.02	7673841	135.1572	10.42305 ^{+0.00027} _{-0.00032}	0.73 ^{+0.18} _{-0.27}	0.008 ^{+0.003} _{-0.003}	0.00 ^{+0.26} _{-0.00}	0.00 ^{+0.88} _{-0.00}	1.30 ± 0.51	87.22 ^{+1.15} _{-0.95}	14.1 ^{+3.1} _{-2.9}	0.096 ± 0.006	1106 ± 158	73 ± 11	3.6	0.5	0.066	0.779
K02585.03	7673841	138.5965	7.87811 ^{+0.00025} _{-0.00025}	0.88 ^{+0.52} _{-0.52}	0.008 ^{+0.002} _{-0.003}	0.66 ^{+0.15} _{-0.66}	3.93 ^{+0.59} _{-0.89}	1.27 ± 1.95	85.72 ^{+2.23} _{-2.82}	11.0 ^{+2.9} _{-3.4}	0.080 ± 0.006	1255 ± 205	47 ± 10	2.7	0.2	0.017	0.463
K02595.01	8883329	134.0478	9.18252 ^{+0.00029} _{-0.00033}	1.00 ^{+0.03} _{-0.34}	0.009 ^{+0.001} _{-0.001}	0.33 ^{+0.32} _{-0.33}	0.65 ^{+0.65} _{-0.65}	2.50 ± 0.60	83.05 ^{+2.94} _{-0.60}	8.3 ^{+1.7} _{-1.2}	0.098 ± 0.003	1558 ± 167	85 ± 10	4.6	0.1	0.111	0.758
K02595.02	8883329	140.4080	14.61360 ^{+0.00076} _{-0.00084}	0.88 ^{+0.57} _{-0.57}	0.010 ^{+0.004} _{-0.001}	0.17 ^{+0.04} _{-0.17}	0.00 ^{+0.43} _{-0.00}	2.55 ± 1.05	85.73 ^{+0.46} _{-1.13}	12.1 ^{+4.2} _{-2.4}	0.134 ± 0.004	1299 ± 223	81 ± 13	5.0	0.8	0.159	0.826
K02672.01	11253827	182.6526	88.51658 ^{+0.00020} _{-0.00016}	0.52 ^{+0.28} _{-0.52}	0.044 ^{+0.008} _{-0.001}	0.00 ^{+0.41} _{-0.00}	0.00 ^{+0.69} _{-0.00}	5.34 ± 1.48	89.61 ^{+0.39} _{-0.37}	71.9 ^{+18.1} _{-16.5}	0.374 ± 0.010	425 ± 60	2611 ± 35	8.1	0.3	0.847	0.993
K02672.02	11253827	162.5118	42.99066 ^{+0.00009} _{-0.00014}	0.65 ^{+0.25} _{-0.65}	0.032 ^{+0.002} _{-0.003}	0.01 ^{+0.62} _{-0.01}	0.00 ^{+1.01} _{-0.00}	3.89 ± 1.03	89.22 ^{+0.78} _{-0.69}	43.6 ^{+11.8} _{-9.1}	0.231 ± 0.006	536 ± 78	1162 ± 17	5.5	0.3	0.895	0.995
K02674.01	8022489	272.3869	197.51031 ^{+0.00035} _{-0.00032}	0.82 ^{+0.32} _{-0.32}	0.052 ^{+0.006} _{-0.006}	0.00 ^{+0.00} _{-0.00}	0.00 ^{+0.00} _{-0.00}	10.05 ± 3.96	89.46 ^{+0.81} _{-0.81}	83.8 ^{+30.0} _{-27.5}	0.671 ± 0.021	422 ± 77	2643 ± 58	10.9	0.8	0.369	0.967
K02674.02	8022489	140.0090	11.17265 ^{+0.00061} _{-0.00066}	1.08 ^{+4.19} _{-0.42}	0.009 ^{+0.036} _{-0.000}	0.24 ^{+0.17} _{-0.23}	1.58 ^{+1.16} _{-1.50}	1.57 ± 3.22	81.42 ^{+0.07} _{-1.48}	13.4 ^{+7.5} _{-4.4}	0.099 ± 0.003	1473 ± 1376	80 ± 13	5.5	0.4	0.079	0.810
K02674.03	8022489	133.0107	2.53574 ^{+0.00006} _{-0.00006}	0.91 ^{+0.34} _{-0.34}	0.008 ^{+0.000} _{-0.001}	0.51 ^{+0.35} _{-0.46}	0.72 ^{+1.44} _{-0.63}	2.15 ± 0.60	73.54 ^{+16.44} _{-7.31}	3.4 ^{+1.3} _{-0.7}	0.037 ± 0.001	2216 ± 385	73 ± 6	15.7	0.7	0.038	0.664
K02675.01	5794570	132.4894	5.44833 ^{+0.00002} _{-0.00002}	0.59 ^{+0.23} _{-0.23}	0.021 ^{+0.006} _{-0.002}	0.00 ^{+0.39} _{-0.00}	0.00 ^{+1.86} _{-0.00}	2.21 ± 0.68	87.45 ^{+1.89} _{-2.32}	13.4 ^{+2.2} _{-3.0}	0.061 ± 0.003	1037 ± 130	554 ± 6	2.6	1.7	0.796	0.990
K02675.02	5794570	131.8464	1.11613 ^{+0.00001} _{-0.00001}	0.57 ^{+0.37} _{-0.49}	0.009 ^{+0.001} _{-0.001}	0.10 ^{+0.58} _{-0.10}	0.00 ^{+2.48} _{-0.00}	1.05 ± 0.29	82.17 ^{+6.90} _{-10.33}	4.2 ^{+0.9} _{-0.8}	0.021 ± 0.001	1856 ± 235	106 ± 2	1.7	1.8	0.112	0.760
K02687.01	7202957	132.0299	1.71684 ^{+0.00001} _{-0.00001}	0.99 ^{+0.12} _{-0.12}	0.010 ^{+0.001} _{-0.002}	0.05 ^{+0.05} _{-0.05}	1.19 ^{+1.19} _{-1.19}	3.31 ± 0.92	62.19 ^{+11.62} _{-0.76}	2.1 ^{+0.1} _{-0.1}	0.029 ± 0.001	2648 ± 363	62 ± 1	2.5	4.3	0.470	0.957
K02687.02	7202957	136.2009	8.16739 ^{+0.00007} _{-0.00007}	0.94 ^{+0.02} _{-0.05}	0.012 ^{+0.001} _{-0.001}	0.00 ^{+0.06} _{-0.00}	0.00 ^{+0.57} _{-0.00}	3.69 ± 0.73	82.00 ^{+2.06} _{-1.53}	6.3 ^{+1.9} _{-0.6}	0.082 ± 0.003	1485 ± 152	104 ± 3</				

Table 3—Continued

KOI	KIC	T_0 (BKJD)	Period (d)	Impact Parameter	R_{PL}/R_*	e	ω (radian)	R_{PL} (R_{\oplus})	Inclination (deg)	a/ R_*	a (AU)	T_{PL} (K)	Depth (ppm)	Dur (hr)	Sig (σ)	p1	p2
K02732.03	9886361	140.7182	54.28085 ^{+0.00238} _{-0.00179}	0.66 ^{+0.22} _{-0.52}	0.011 ^{+0.002} _{-0.001}	0.00 ^{+0.51} _{-0.56}	0.00 ^{+0.63} _{-0.00}	1.93 ± 1.15	89.20 ^{+0.69} _{-0.56}	42.6 ^{+18.9} _{-15.3}	0.318 ± 0.034	610 ± 155	157 ± 21	6.7	0.5	0.113	0.864
K02732.04	9886361	146.8040	24.56084 ^{+0.00009} _{-0.00181}	0.12 ^{+0.77} _{-0.12}	0.007 ^{+0.001} _{-0.002}	0.01 ^{+0.56} _{-0.01}	0.00 ^{+3.81} _{-0.00}	1.16 ± 0.57	89.76 ^{+0.24} _{-1.56}	25.9 ^{+12.4} _{-8.5}	0.171 ± 0.014	779 ± 220	60 ± 13	6.5	1.0	0.035	0.643
K02949.01	6026737	132.3611	10.17444 ^{+0.00045} _{-0.00056}	0.70 ^{+1.07} _{-0.01}	0.013 ^{+0.016} _{-0.007}	0.35 ^{+0.21} _{-0.30}	4.48 ^{+0.20} _{-3.49}	3.08 ± 2.83	83.82 ^{+1.40} _{-1.63}	9.8 ^{+3.4} _{-2.2}	0.096 ± 0.003	1600 ± 614	74 ± 12	6.6	0.6	0.076	0.673
K02949.02	6026737	134.8168	3.75017 ^{+0.00000} _{-0.00000}	0.63 ^{+0.28} _{-0.23}	0.005 ^{+0.001} _{-0.001}	0.00 ^{+0.15} _{-0.00}	0.04 ^{+0.53} _{-0.04}	1.13 ± 0.41	83.41 ^{+2.39} _{-2.76}	5.2 ^{+1.4} _{-1.1}	0.049 ± 0.005	1747 ± 274	32 ± 7	4.1	1.4	0.023	0.368
K03083.01	7106173	133.2040	10.18329 ^{+0.00044} _{-0.00043}	0.98 ^{+1.51} _{-0.08}	0.007 ^{+0.025} _{-0.002}	0.21 ^{+0.15} _{-0.21}	0.40 ^{+0.09} _{-0.40}	0.82 ± 1.58	85.63 ^{+0.38} _{-1.30}	19.3 ^{+5.6} _{-5.5}	0.096 ± 0.004	1095 ± 353	50 ± 9	2.8	0.7	0.014	0.409
K03083.02	7106173	135.2410	6.23203 ^{+0.00023} _{-0.00025}	0.89 ^{+1.32} _{-0.05}	0.006 ^{+0.025} _{-0.003}	0.05 ^{+0.00} _{-0.05}	6.21 ^{+0.07} _{-6.20}	0.64 ± 1.61	84.34 ^{+0.46} _{-1.06}	14.0 ^{+3.9} _{-3.4}	0.069 ± 0.003	1307 ± 436	29 ± 7	2.4	0.6	0.014	0.408
K03083.03	7106173	134.8440	8.29442 ^{+0.00047} _{-0.00033}	0.46 ^{+0.42} _{-0.46}	0.006 ^{+0.000} _{-0.002}	0.00 ^{+0.12} _{-0.00}	0.00 ^{+0.32} _{-0.00}	0.65 ± 0.20	88.51 ^{+1.49} _{-1.31}	16.8 ^{+4.5} _{-3.3}	0.084 ± 0.004	931 ± 150	34 ± 8	3.2	0.3	0.013	0.399
K03097.01	7582689	137.4610	11.92196 ^{+0.00069} _{-0.00060}	0.77 ^{+1.13} _{-0.12}	0.007 ^{+0.018} _{-0.001}	0.00 ^{+0.16} _{-0.00}	0.00 ^{+0.51} _{-0.00}	1.81 ± 2.53	85.86 ^{+1.79} _{-3.30}	9.9 ^{+4.0} _{-2.5}	0.108 ± 0.003	1281 ± 249	51 ± 8	5.5	0.4	0.092	0.835
K03097.02	7582689	138.0420	6.80273 ^{+0.00027} _{-0.00029}	0.04 ^{+0.50} _{-0.50}	0.005 ^{+0.034} _{-0.001}	0.38 ^{+0.00} _{-0.12}	0.22 ^{+4.53} _{-3.52}	1.10 ± 3.81	89.74 ^{+0.26} _{-8.58}	8.0 ^{+2.5} _{-2.1}	0.074 ± 0.002	1352 ± 231	31 ± 6	4.7	0.4	0.028	0.589
K03097.03	7582689	140.1620	8.70295 ^{+0.00036} _{-0.00039}	0.81 ^{+0.45} _{-0.19}	0.005 ^{+0.006} _{-0.002}	0.00 ^{+0.07} _{-0.00}	2.67 ^{+0.20} _{-2.66}	1.27 ± 0.98	85.10 ^{+0.58} _{-1.26}	8.8 ^{+2.4} _{-1.7}	0.088 ± 0.003	1358 ± 215	26 ± 7	4.2	0.6	0.028	0.589
K03111.01	8581240	138.5101	10.76792 ^{+0.00044} _{-0.00054}	0.90 ^{+0.44} _{-0.18}	0.009 ^{+0.003} _{-0.002}	0.13 ^{+0.36} _{-0.13}	1.84 ^{+1.83} _{-1.83}	2.17 ± 0.79	84.61 ^{+0.88} _{-1.09}	9.4 ^{+1.9} _{-1.9}	0.101 ± 0.004	1297 ± 159	67 ± 9	4.8	0.6	0.056	0.597
K03111.02	8581240	132.5113	4.32854 ^{+0.00010} _{-0.00014}	1.00 ^{+0.00} _{-1.00}	0.006 ^{+0.000} _{-0.001}	0.90 ^{+0.00} _{-0.08}	1.20 ^{+0.27} _{-0.40}	1.54 ± 0.45	62.05 ^{+27.57} _{-2.59}	4.9 ^{+1.7} _{-1.1}	0.055 ± 0.002	1757 ± 295	40 ± 6	2.2	0.8	0.011	0.217
K03158.01	6278762	133.2591	3.60011 ^{+0.00003} _{-0.00003}	0.21 ^{+0.33} _{-0.33}	0.004 ^{+0.000} _{-0.000}	0.00 ^{+0.17} _{-0.00}	0.00 ^{+0.31} _{-0.00}	0.38 ± 0.04	88.97 ^{+1.03} _{-1.91}	11.7 ^{+0.8} _{-1.0}	0.044 ± 0.001	997 ± 57	27 ± 1	2.3	2.6	0.126	0.878
K03158.02	6278762	131.5239	4.54586 ^{+0.00003} _{-0.00004}	0.37 ^{+0.27} _{-0.30}	0.006 ^{+0.000} _{-0.001}	0.00 ^{+0.31} _{-0.00}	0.00 ^{+0.31} _{-0.00}	0.49 ± 0.06	88.44 ^{+1.26} _{-1.19}	13.7 ^{+1.0} _{-0.7}	0.051 ± 0.001	917 ± 47	47 ± 1	2.4	8.5	0.243	0.941
K03158.03	6278762	134.7885	6.18936 ^{+0.00007} _{-0.00008}	0.40 ^{+0.27} _{-0.40}	0.006 ^{+0.001} _{-0.000}	0.00 ^{+0.17} _{-0.00}	0.00 ^{+0.32} _{-0.00}	0.49 ± 0.07	88.63 ^{+1.37} _{-1.0}	16.9 ^{+0.9} _{-1.0}	0.063 ± 0.001	827 ± 56	45 ± 1	2.6	0.7	0.227	0.936
K03158.04	6278762	135.0872	7.74359 ^{+0.00011} _{-0.00011}	0.91 ^{+0.07} _{-0.05}	0.008 ^{+0.001} _{-0.001}	0.05 ^{+0.00} _{-0.05}	0.07 ^{+0.07} _{-0.07}	1.84 ± 0.32	83.71 ^{+0.86} _{-0.92}	8.1 ^{+1.2} _{-1.0}	0.080 ± 0.004	1173 ± 86	51 ± 1	3.1	2.1	0.190	0.921
K03158.05	6278762	134.8777	9.74050 ^{+0.00004} _{-0.00005}	0.77 ^{+0.07} _{-0.15}	0.009 ^{+0.000} _{-0.002}	0.00 ^{+0.43} _{-0.00}	0.06 ^{+1.53} _{-0.06}	0.76 ± 0.11	88.11 ^{+0.46} _{-0.36}	20.7 ^{+1.7} _{-1.2}	0.084 ± 0.002	699 ± 39	74 ± 1	2.1	1.1	0.287	0.953
K03196.01	9002538	135.3143	4.96067 ^{+0.00016} _{-0.00013}	0.43 ^{+0.26} _{-0.40}	0.004 ^{+0.001} _{-0.001}	0.00 ^{+0.00} _{-0.00}	0.27 ^{+0.27} _{-0.27}	0.51 ± 0.10	87.67 ^{+1.58} _{-1.14}	13.0 ^{+1.0} _{-1.0}	0.058 ± 0.003	1316 ± 126	23 ± 3	3.2	0.8	0.029	0.426
K03196.02	9002538	134.1634	6.88299 ^{+0.00021} _{-0.00018}	0.96 ^{+1.19} _{-0.39}	0.009 ^{+0.025} _{-0.007}	0.00 ^{+0.06} _{-0.01}	0.48 ^{+0.02} _{-0.42}	1.14 ± 2.03	80.65 ^{+1.86} _{-0.47}	13.2 ^{+0.8} _{-1.7}	0.072 ± 0.004	1773 ± 898	29 ± 3	2.8	1.5	0.034	0.471
K03384.01	8644365	139.0648	10.54837 ^{+0.00018} _{-0.00013}	0.79 ^{+0.15} _{-0.16}	0.009 ^{+0.006} _{-0.006}	0.10 ^{+0.37} _{-0.00}	0.06 ^{+4.61} _{-0.04}	1.10 ± 0.51	87.61 ^{+0.64} _{-1.04}	18.4 ^{+2.8} _{-2.2}	0.094 ± 0.004	930 ± 125	82 ± 11	2.7	1.3	0.086	0.701
K03384.02	8644365	139.3678	19.91594 ^{+0.00017} _{-0.04764}	0.00 ^{+0.50} _{-0.00}	0.011 ^{+0.000} _{-0.002}	0.00 ^{+0.16} _{-0.00}	0.00 ^{+0.82} _{-0.00}	1.41 ± 0.25	90.00 ^{+0.00} _{-1.15}	27.2 ^{+2.3} _{-3.5}	0.145 ± 0.008	781 ± 97	150 ± 16	5.6	0.9	0.086	0.701
K03398.01	3561464	137.2253	7.31947 ^{+0.00017} _{-0.00027}	0.00 ^{+0.47} _{-0.00}	0.012 ^{+0.000} _{-0.002}	0.00 ^{+0.08} _{-0.00}	0.00 ^{+0.01} _{-0.00}	1.51 ± 0.28	90.00 ^{+0.00} _{-1.22}	13.8 ^{+1.1} _{-2.1}	0.074 ± 0.004	1197 ± 138	149 ± 19	4.2	0.1	0.051	0.731
K03398.02	3561464	144.9642	35.79896 ^{+0.00004} _{-0.00004}	0.00 ^{+0.00} _{-0.00}	0.022 ^{+0.003} _{-0.003}	0.00 ^{+0.00} _{-0.00}	0.00 ^{+0.00} _{-0.00}	2.79 ± 0.55	90.00 ^{+0.00} _{-0.82}	39.7 ^{+2.2} _{-5.7}	0.213 ± 0.013	688 ± 86	561 ± 50	7.0	0.3	0.078	0.809
K03398.03	3561464	131.6023	4.32702 ^{+0.00014} _{-0.00015}	0.00 ^{+0.30} _{-0.00}	0.010 ^{+0.000} _{-0.002}	0.00 ^{+0.04} _{-0.00}	0.00 ^{+0.23} _{-0.00}	1.23 ± 0.25	90.00 ^{+0.00} _{-1.94}	9.8 ^{+0.9} _{-1.3}	0.052 ± 0.003	1417 ± 171	98 ± 14	3.5	0.7	0.015	0.434
K03403.01	11754430	166.6626	39.81811 ^{+0.00058} _{-0.00064}	0.00 ^{+0.48} _{-0.39}	0.014 ^{+0.001} _{-0.002}	0.00 ^{+0.06} _{-0.00}	0.00 ^{+0.12} _{-0.15}	1.73 ± 0.36	90.00 ^{+0.00} _{-0.95}	43.4 ^{+5.7} _{-7.2}	0.229 ± 0.012	635 ± 97	237 ± 28	7.4	0.4	0.105	0.745
K03403.02	11754430	135.4936	6.15844 ^{+0.00000} _{-0.00000}	0.00 ^{+0.39} _{-0.00}	0.007 ^{+0.001} _{-0.001}	0.00 ^{+0.09} _{-0.00}	0.00 ^{+0.15} _{-0.00}	0.89 ± 0.19	90.00 ^{+0.00} _{-1.89}	12.5 ^{+1.6} _{-1.6}	0.066 ± 0.003	1151 ± 169	51 ± 10	3.8	0.1	0.032	0.449
K03425.01	9117416	145.4378	20.03515 ^{+0.00078} _{-0.00063}	0.26 ^{+0.43} _{-0.43}	0.012 ^{+0.000} _{-0.002}	0.00 ^{+0.25} _{-0.00}	0.00 ^{+0.46} _{-0.00}	1.12 ± 0.45	89.52 ^{+0.48} _{-1.22}	34.8 ^{+5.6} _{-12.1}	0.139 ± 0.008	625 ± 137	121 ± 18	4.8	0.1	0.011	0.211
K03425.02	9117416	131.6995	3.15720 ^{+0.00008} _{-0.00009}	0.22 ^{+0.44} _{-0.22}	0.007 ^{+0.001} _{-0.002}	0.00 ^{+0.11} _{-0.00}	0.02 ^{+0.26} _{-0.02}	0.63 ± 0.27	88.55 ^{+1.45} _{-3.43}	10.2 ^{+1.6} _{-3.4}	0.040 ± 0.002	1168 ± 249	59 ± 7	2.7	0.5	0.011	0.211
K03500.01	6058816	188.5180	73.75110 ^{+0.00106} _{-0.00028}	0.00 ^{+0.65} _{-0.00}	0.015 ^{+0.001} _{-0.002}	0.00 ^{+0.13} _{-0.00}	0.00 ^{+0.06} _{-0.00}	1.98 ± 0.50	90.00 ^{+0.00} _{-0.70}	64.1 ^{+6.6} _{-15.9}	0.348 ± 0.018	557 ± 101	251 ± 34	10.4	0.2	0.082	0.690
K03500.02	6058816	135.8111	4.74823 ^{+0.00005} _{-0.00005}	0.91 ^{+0.09} _{-0.45}	0.006 ^{+0.003} _{-0.003}	0.00 ^{+0.05} _{-0.01}	0.10 ^{+0.05} _{-0.05}	0.68 ± 0.30	72.49 ^{+1.70} _{-0.29}	10.6 ^{+1.6} _{-1.0}	0.055 ± 0.003	1507 ± 364	36 ± 8	5.2	0.3	0.025	0.387
K03681.01	2581316	238.8192	217.83189 ^{+0.00009} _{-0.00009}	0.34 ^{+0.37} _{-0.05}	0.089 ^{+0.003} _{-0.000}	0.46 ^{+0.31} _{-0.46}	0.00 ^{+1.63} _{-0.00}	13.29 ± 5.85	89.73 ^{+0.09} _{-0.35}	114.6 ^{+13.5} _{-43.8}	0.736 ± 0.062	489 ± 36	9267 ± 36	21.2	0.8	0.911	0.986
K03681.02	2581316	134.5660	10.51420 ^{+0.00034} _{-0.00035}	0.08 ^{+0.55} _{-0.08}	0.008 ^{+0.000} _{-0.002}	0.33 ^{+0.24} _{-0.30}	2.09 ^{+1.88} _{-1.88}	1.18 ± 0.21	89.73 ^{+0.27} _{-2.11}	16.1 ^{+1.2} _{-1.8}	0.096 ± 0.005	1036 ± 76	80 ± 6	3.7	0.5	0.009	0.181
K03864.01	4164922	132.3795	1.21073 ^{+0.00001} _{-0.00001}	0.88 ^{+0.04} _{-0.11}	0.012 ^{+0.014} _{-0.001}	0.08 ^{+0.53} _{-0.08}	0.01 ^{+4.62} _{-0.01}	2.98 ± 1.90	69.47 ^{+4.30} _{-3.39}	2.3 ^{+0.5} _{-0.3}	0.023 ± 0.001	2169 ± 235	102 ± 3	2.0	1.2	0.182	0.847
K03864.02	4164922	134.4413	18.25734 ^{+0.00093} _{-0.00089}	0.09 ^{+0.52} _{-0.09}	0.011 ^{+0.002} _{-0.011}	0.03 ^{+0.21} _{-0.03}	0.00 ^{+2.01} _{-0.00}	0.82 ± 0.18	89.86 ^{+0.14} _{-0.52}	37.6 ^{+4.0} _{-5.2}	0.125 ± 0.006	549 ± 69	159 ± 15	3.8	0.6	0.053	0.582
K04021.01	11967788	133.1229	7.23530 ^{+0.00039} _{-0.00017}	0.47 ^{+0.11} _{-0.47}	0.009 ^{+0.001} _{-0.001}	0.00 ^{+0.00} _{-0.00}	0.00 ^{+0.00} _{-0.00}	1.22 ± 0.23	87.89 ^{+2.11} _{-0.65}	12.6 ^{+0.9} _{-1.1}	0.074 ± 0.004	1198 ± 91	113 ± 8	3.8	1.8	0.199	0.861
K04021.02	11967788	132.4524	4.93209 ^{+0.00000} _{-0.00000}	0.22 ^{+0.24} _{-0.22}	0.007 ^{+0.001} _{-0.001}	0.00 ^{+0.13} _{-0.00}	0.08 ^{+0.22} _{-0.08}	1.02 ± 0.16	88.71 ^{+1.29} _{-1.44}	9.8 ^{+0.6} _{-1.0}	0.057 ± 0.003	1365 ± 87	67 ± 7	3.8	1.8	0.114	0.

Table 4. Visual companion detections with UKIRT images.

KOI	ΔK_P (mag)	Separation (arcsec)	Significance (σ)	PA (deg)
K00005
K00041
K00070	4.7	7.7	57.7	51.4
K00072
K00082	7.3	12.3	5.1	135.9
K00085	7.5	19.3	6.6	304.8
K00089	7.5	12.1	5.1	43.8
K00089	6.3	8.8	10.3	207.4
K00094	5.1	19.9	41.4	130.4
K00094	4.4	19.6	77.1	34.6
K00094	6.9	17.9	6.4	238.3
K00094	2.2	14.7	654.0	108.0
K00102	6.3	21.0	12.7	161.4
K00102	3.0	5.8	258.8	232.9
K00108	4.1	19.0	124.4	349.6
K00108	6.0	17.7	20.0	20.0
K00108	6.8	10.0	7.7	113.7
K00111	7.2	19.8	5.0	96.7
K00111	6.5	18.0	9.8	176.3
K00111	6.4	13.8	10.8	118.7
K00112
K00115	2.8	18.1	183.0	212.8
K00115	5.4	8.2	13.9	157.9
K00116	3.6	17.0	133.0	350.4
K00116	6.8	16.0	6.4	103.7
K00117	3.3	16.2	232.1	5.9
K00119	0.1	20.4	2253.8	161.0
K00119	3.7	18.7	82.6	214.7
K00119	6.0	17.0	8.7	273.4
K00123	5.7	20.4	20.3	96.2
K00123	4.5	19.1	67.8	199.3

Table 4—Continued

KOI	ΔK_P (mag)	Separation (arcsec)	Significance (σ)	PA (deg)
K00123	7.4	16.3	5.4	184.7
K00124	6.0	17.3	6.1	5.3
K00139	6.4	14.8	5.4	133.3
K00148	4.7	16.3	34.4	245.1
K00148	4.8	5.0	24.9	243.5
K00153
K00159	4.9	19.9	21.7	311.4
K00159	6.6	15.5	5.1	124.6
K00168
K00244	5.8	16.7	35.1	102.0
K00244	0.7	16.6	3379.6	290.0
K00245	3.2	16.8	217.0	199.5
K00246	3.9	21.6	165.4	145.5
K00246	7.0	14.7	7.5	29.6
K00260
K00262
K00270	0.2	21.7	3226.7	237.7
K00270	7.0	11.5	5.2	134.0
K00271
K00274
K00274	7.1	8.5	5.1	176.7
K00275	5.3	17.8	45.0	354.7
K00277
K00279	6.0	8.5	11.9	197.7
K00282	7.8	13.8	5.5	110.2
K00282	4.1	8.4	117.2	209.6
K00283	5.8	17.4	28.9	219.8
K00283	7.2	12.0	6.4	271.2
K00284
K00285	7.5	20.0	5.9	236.4
K00289

Table 4—Continued

KOI	ΔK_P (mag)	Separation (arcsec)	Significance (σ)	PA (deg)
K00291	6.6	20.3	9.3	20.3
K00295
K00298	6.6	15.3	5.3	64.6
K00298	6.6	14.7	5.5	54.3
K00298	6.6	12.7	5.6	56.5
K00298	0.6	2.2	56.6	273.9
K00301	6.7	18.7	9.5	302.6
K00304	7.0	18.8	6.2	139.7
K00307	2.1	21.9	595.3	265.4
K00307	7.0	18.7	6.1	118.1
K00307	3.9	17.1	110.7	317.5
K00307	3.9	16.8	130.3	244.9
K00307	4.7	11.1	65.9	282.6
K00307	6.4	9.6	11.1	275.8
K00312	6.2	18.8	16.7	51.4
K00312	3.6	17.8	180.2	1.5
K00312	5.7	13.8	22.2	234.1
K00312	7.1	12.4	6.4	148.7
K00312	5.5	9.8	23.8	121.0
K00312	6.4	7.9	7.7	87.6
K00312	6.3	5.7	7.1	99.9
K00313	4.8	14.9	41.2	203.1
K00314
K00316	6.4	19.5	11.0	202.1
K00316	1.9	17.1	804.3	190.8
K00316	6.9	10.2	7.5	8.7
K00321
K00326	5.2	21.0	27.2	312.6
K00326	2.9	7.6	292.5	89.3
K00327	2.4	11.4	217.6	286.0
K00332	6.3	18.2	5.7	330.5

Table 4—Continued

KOI	ΔK_P (mag)	Separation (arcsec)	Significance (σ)	PA (deg)
K00332	3.8	16.9	57.6	168.1
K00338	5.9	14.1	7.2	351.4
K00338	5.8	11.0	6.0	218.0
K00341	6.8	15.5	5.2	262.4
K00343	4.6	10.2	29.0	145.1
K00353	6.2	19.9	17.6	32.1
K00353	4.9	15.1	48.1	168.7
K00354	4.8	19.7	17.5	71.0
K00354	2.3	15.7	158.3	327.9
K00354	2.5	13.5	130.3	110.5
K00354	2.6	10.1	82.7	151.4
K00354	4.9	7.4	12.1	209.6
K00369
K00370
K00623	2.5	10.2	346.5	204.5
K00626	6.5	18.5	7.5	195.3
K00626	4.0	16.4	58.3	300.7
K00626	6.7	14.1	5.3	24.7
K00626	6.5	14.0	6.0	263.6
K00626	5.1	5.5	20.5	347.4
K00627	5.4	21.3	37.2	253.9
K00627	5.5	19.8	38.7	206.6
K00627	6.7	19.6	12.6	263.6
K00627	7.2	11.8	7.9	209.8
K00655	6.9	15.8	5.3	15.7
K00655	6.0	14.4	14.3	61.3
K00664
K00665
K00678
K00679
K00710

Table 4—Continued

KOI	ΔK_P (mag)	Separation (arcsec)	Significance (σ)	PA (deg)
K00717	4.8	20.1	18.4	136.1
K00719	6.9	16.0	11.9	199.2
K00719	7.7	14.2	5.2	0.6
K00972	7.6	18.2	6.1	250.6
K00972	7.1	15.2	6.7	203.1
K01001	7.0	19.2	5.3	34.7
K01001	6.9	14.9	5.8	222.4
K01151	5.9	19.5	15.5	91.3
K01175
K01215	1.9	17.6	533.0	68.2
K01221	8.2	15.0	5.0	136.4
K01241	7.2	16.5	6.1	22.9
K01316	5.3	19.7	40.5	15.0
K01316	5.9	14.5	21.3	354.4
K01316	5.6	5.5	14.8	106.3
K01445
K01525	5.9	20.6	21.6	16.6
K01534	5.1	17.2	18.3	298.0
K01534	5.7	14.3	10.0	36.3
K01534	5.2	11.4	16.7	245.2
K01613	6.8	20.6	14.2	290.9
K01613	5.5	19.9	52.1	89.9
K01628	5.2	15.4	30.2	136.0
K01692	6.6	14.5	12.4	188.7
K01692	6.5	6.2	8.4	340.1
K01779	6.5	14.8	5.4	65.9
K01781	3.0	7.3	264.1	326.1
K01806	7.0	19.3	12.4	49.5
K01809
K01824	6.8	12.9	8.8	17.6
K01909	7.1	16.8	5.1	120.3

Table 4—Continued

KOI	ΔK_P (mag)	Separation (arcsec)	Significance (σ)	PA (deg)
K01929	4.6	19.0	54.0	152.3
K01929	3.1	15.4	174.4	282.5
K01929	4.1	13.9	87.3	274.1
K01930
K01932	6.3	19.7	9.5	245.5
K01932	3.7	16.2	96.2	257.6
K01932	4.3	9.2	57.4	312.4
K01955	6.9	18.3	11.0	241.3
K01955	7.5	10.6	5.4	101.3
K02004	5.8	18.6	5.1	26.8
K02011	6.7	16.8	9.0	345.1
K02011	7.0	16.7	6.9	54.1
K02011	2.0	16.7	647.4	315.2
K02011	5.8	13.2	20.3	133.1
K02011	6.8	13.1	7.0	6.9
K02011	2.7	9.9	287.2	293.5
K02029	4.8	18.8	37.2	68.1
K02053
K02059
K02148
K02158	7.2	16.2	6.8	329.2
K02158	4.6	13.3	64.5	335.1
K02158	4.7	4.3	30.5	12.7
K02169	4.2	21.8	74.7	220.3
K02169	3.4	7.2	115.4	66.6
K02173	5.3	20.2	31.3	299.3
K02175	5.1	20.6	34.7	162.7
K02289	5.9	10.5	8.1	32.4
K02311	7.1	20.2	10.1	310.9
K02311	6.4	17.5	16.3	326.8
K02311	7.3	17.2	8.5	311.0

Table 4—Continued

KOI	ΔK_P (mag)	Separation (arcsec)	Significance (σ)	PA (deg)
K02352
K02541
K02585	5.7	13.6	16.5	251.4
K02595	5.1	20.6	35.8	308.0
K02595	3.6	19.4	134.7	79.3
K02672	6.0	9.2	19.2	309.1
K02674	5.5	19.2	17.3	346.4
K02674	6.7	15.2	6.3	223.9
K02675
K02687
K02693	6.5	19.1	9.5	283.5
K02693	5.2	9.7	25.3	120.0
K02696
K02714	3.7	19.2	37.9	326.1
K02722	5.2	16.6	61.2	169.1
K02722	6.3	14.6	20.1	115.0
K02722	5.9	6.5	22.7	282.3
K02732
K02949	6.7	10.1	5.1	313.6
K02949	4.0	4.7	59.2	310.6
K03083	7.3	17.7	8.2	253.2
K03097
K03111	5.5	11.4	15.5	151.8
K03111	5.6	6.8	9.4	235.5
K03158
K03196	3.8	19.6	123.2	122.6
K03196	6.7	17.0	5.6	138.2
K03384	4.8	17.8	23.5	151.5
K03384	5.5	16.8	15.7	79.6
K03398	5.1	18.7	19.0	230.1
K03398	5.2	17.3	13.6	3.4

Table 4—Continued

KOI	ΔK_P (mag)	Separation (arcsec)	Significance (σ)	PA (deg)
K03398	5.7	16.5	8.9	333.4
K03398	5.2	15.9	14.3	43.4
K03398	6.4	14.8	7.3	278.0
K03403	6.2	16.4	9.2	136.9
K03425	6.9	9.2	6.0	222.7
K03500	3.3	20.2	74.8	332.9
K03500	4.2	12.6	31.0	96.2
K03500	3.7	4.9	47.6	138.9
K03681	7.1	16.4	7.8	339.8
K03864
K04021	5.8	14.1	5.8	154.2
K04032	6.8	19.0	9.3	176.7
K04097	5.6	19.6	23.3	170.6
K04269	3.7	18.1	121.5	135.6
K04288	6.0	15.3	25.3	179.0
K04288	6.7	10.4	13.4	223.0
K04288	6.5	5.3	6.0	279.2

Table 5. RV measurement results for 23 KOIs.

KOI	t_{start} (MJD)	t_{end} (MJD)	n_{obs}	RMS ($\text{m}\cdot\text{s}^{-1}$)	δv ($\text{m}\cdot\text{s}^{-1}$)
00005 [†]	54983.515714	55843.325819	18	98.2	6.3
00041	54988.510954	55814.257203	41	5.7	3.6
00070	55073.385713	55723.555721	30	7.0	2.6
00072	55074.377797	55414.302550	40	3.5	3.1
00082	55311.578536	55814.275163	22	3.5	2.3
00085	55696.490478	55738.515810	6	10.1	2.8
00102	55107.034592	55381.183923	5	40.0	7.4
00108	55134.287135	55809.400772	13	4.1	2.9
00111	55372.555316	55795.410792	6	5.0	2.8
00116	55133.397351	55759.492485	10	5.4	3.0
00123	55074.492468	55378.370526	14	7.3	7.0
00148*	55311.606882	55814.365587	18	40.5	2.9
00153	55313.591538	55811.316797	20	10.0	3.1
00244	55366.602834	55814.427264	64	8.5	3.7
00245	55312.586400	55798.251068	25	4.1	2.4
00246*	55312.581849	55814.235957	50	18.4	2.4
00274	55403.446880	55413.344080	6	2.7	2.6
00283	55433.368391	55795.441507	12	4.6	2.4
00321	55378.533747	55843.311883	18	4.0	2.5
01781	55777.097702	55846.197558	10	150.6	50.0
02311	55777.432523	55827.322805	4	154.6	50.0
02672	56082.381916	56231.214294	3	49.5	35.4
02687	56193.286594	56225.133901	3	44.2	50.0

Note. — [†] marks the star with linear trend indicating a stellar companions. * indicates the stars with a non-transiting planet companion (KOI 148, Howard Isaacson, private communication; KOI 246, Gilliland et al. 2013).